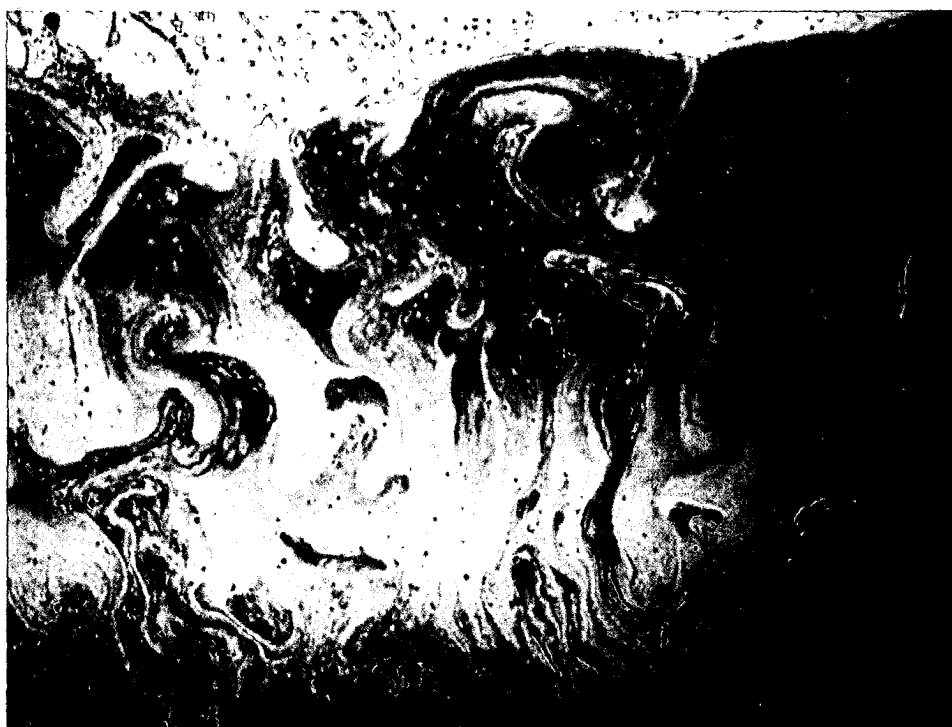


REACTIONS OF NITROGEN OXIDES IN POWER-PLANT PLUMES

models and measurements



LEON JANSSEN

**TR diss
1630**

66.665
317 1600
TR diss 1630

Reactions of nitrogen oxides in power-plant plumes

- models and measurements -

Reacties van stikstofoxiden
in de rookpluimen van elektriciteitscentrales

PROEFSCHRIFT



ter verkrijging van
de graad van doctor aan de Technische Universiteit Delft,
op gezag van de Rector Magnificus,
Prof. Dr. J.M. Dirken,
in het openbaar te verdedigen
ten overstaan van een commissie
door het College van Dekanen daartoe aangewezen,
op dinsdag 17 mei 1988
te 14.00 uur

door

Leonardus Henricus Josephus Maria Janssen
geboren te Tilburg,
doctorandus

TR diss
1630

Dit proefschrift is goedgekeurd door de promotores

Prof. Dr. M. Donze

en

Prof. Dr. F.T.M. Nieuwstadt

*"Hé ik wou dat jij was de lucht
dat ik je ademen kon"*

Herman Gorter
(Individualistische Verzen, 1903)

CIP-GEGEVENS KONINKLIJKE BIBLIOTHEEK, DEN HAAG

Janssen, L. H. J. M.

Reactions of nitrogen oxides in power-plant plumes : models and measurements / L.H.J.M. Janssen.

- Arnhem : KEMA, - Ill.

Thesis Delft. - With ref.

ISBN 90-353-1010-1

SISO 614.623 UDC[621.311:661.98];504.3.054(043.3)

Subject heading: nitrogen oxides ; emission ; power plants.

Voorwoord

Het in dit proefschrift beschreven onderzoek is uitgevoerd bij de Afdeling Milieu Onderzoek van de Divisie Onderzoek en Ontwikkeling van de N.V. KEMA.

Veel mensen zijn mij bij het doen van dit onderzoek behulpzaam geweest. In het bijzonder wil ik mijn promotoren Prof. Dr. Marcel Donze en Prof. Dr. Ir. Frans Nieuwstadt bedanken voor het vertrouwen dat zij beiden al in een vroeg stadium van mijn onderzoek hebben getoond en voor hun constructieve commentaar bij de totstandkoming van dit proefschrift. Dr. Han van Wakeren dank ik voor zijn stimulerende hulp tijdens het onderzoek; Ir. Hans Visser en Drs. Frank van Haren (K.U. Nijmegen) dank ik voor hun hulp bij het maken van de computer programma's. Ir. Albert Elshout zette mij op dit spoor; Dr. Jan van der Kooij liet mij het spoor ook volgen.

Ing. Han van Duuren dank ik voor zijn bijdrage in de opzet van de metingen; Bertus van den Belt, Wim de Bruin, Peter Gamelkoorn, Ing. Hans Jaspers, André van Leeuwen, Harrie Slangewal, Alfons Veldkamp en medewerkers van Geosens B.V. voor hun bijdragen aan de uitvoering daarvan; Ing. Jens Vaessen voor zijn vele hulp bij de verwerking van de meetgegevens en de data-analyse.

Drs. Peter van Slingerland dank ik voor zijn hulp bij de vertalingen; de medewerksters van het secretariaat van de Afdeling Milieu Onderzoek - Joke Banga, Karin Derks, Jeanette van Wijngaarden en Ali Rommers - evenals de medewerkers van de grafische tekenkamer - de heren Buiskool, Gorter, le Fevre, Lagerweij en Zegveld - dank ik voor de verzorging van mijn teksten en figuren. Dr. Tom van Loon en Janette Rietbergen zijn verantwoordelijk voor de bureaureactie en vormgeving van dit proefschrift en ik dank hen graag voor deze bijdrage.

Dr. Dirk Onderdelinden (RIVM, Laboratorium voor Luchtonderzoek) bedank ik omdat hij mij niet alleen milieu-onderzoek maar ook fysisch experimenteren heeft willen leren.

Dank aan Lite.

Contents

| | |
|--|----|
| Scope of this thesis | 11 |
| Previously published parts | 13 |
| | |
| Chapter 1: Nitrogen oxides and air pollution; chemical reactions in a plume | 15 |
| Abstract | 15 |
| Introduction | 15 |
| Emissions and concentrations of nitrogen oxides | 16 |
| Dispersion of air pollutants from a point source | 18 |
| Chemical reactions of nitrogen oxides in the atmosphere | 19 |
| Modelling dispersion and chemical reactions in a plume | 21 |
| | |
| Chapter 2: Dispersion and chemistry in relation to measurements and models | 23 |
| Abstract | 23 |
| Introduction | 23 |
| Time scales of NO-O ₃ reactions in a plume | 24 |
| The time scale of the chemical reactions | 24 |
| The time scale of the dispersion process | 25 |
| Mixing, modelling and measuring | 26 |
| Measurements | 26 |
| Models | 27 |
| Box models | 28 |
| Models with non-uniform concentration distributions | 29 |
| Models assuming local chemical equilibrium ($t_p/t_c > 1$) | 29 |
| Models assuming fast dispersion ($t_p/t_c < 1$) | 29 |
| Models dealing explicitly with mixing of O ₃ into the plume | 30 |
| Modelling micromixing | 31 |
| | |
| Chapter 3: Experimental methods | 35 |
| Monitoring | 35 |
| Measuring strategy | 36 |
| Remote detection of the plume | 37 |

| | |
|--|----|
| Chapter 4: Modelling the oxidation of NO on the basis of Gaussian dispersion and chemical equilibrium in the plume | 39 |
| Abstract | 39 |
| Introduction | 39 |
| Description of the model | 40 |
| Measurements | 41 |
| Results and analysis | 43 |
| Chapter 5: Conversion processes of nitrogen oxides in the daytime and at night - measurements and modelling of reactions in the plumes of power plants- | 47 |
| Abstract | 47 |
| Introduction | 48 |
| Chemical reactions of nitrogen oxides in the atmosphere | 49 |
| Results and analysis | 50 |
| Measurements | 50 |
| Modelling | 54 |
| Modelling daytime conditions | 57 |
| Modelling night-time conditions | 59 |
| Conclusions | 61 |
| Chapter 6: Mixing of ambient air in a plume and its effects on the oxidation of NO | 63 |
| Abstract | 63 |
| Introduction | 63 |
| Representation of the plume | 64 |
| Description of the model | 65 |
| Reaction equations in the exhaust plume | 66 |
| Results and analysis | 67 |
| Fitting procedure | 67 |
| Atmospheric conditions | 70 |
| Deviation from photostationary equilibrium | 72 |
| Width of the mixed plume | 74 |
| Contribution of oxygen in the oxidation process | 77 |
| Measurements at ground level | 78 |
| Conclusions | 79 |

| | |
|--|-----|
| Chapter 7: A classification of NO-oxidation rates in power-plant plumes based on atmospheric conditions | 81 |
| Abstract | 81 |
| Introduction | 81 |
| Results and analysis | 82 |
| The NO ₂ /NO _x ratio as a function of distance from the source | 82 |
| Selection of atmospheric parameters | 84 |
| The classification of NO-oxidation rates | 85 |
| Uncertainty limits of measurements and model calculations | 87 |
| Measurements | 87 |
| Model calculations | 90 |
| The ozone parameter A | 91 |
| The wind parameter α | 91 |
| Measurements of α | 93 |
| Discussion | 93 |
| Seasonal dependence of the NO-oxidation rates | 94 |
| Homogeneous and inhomogeneous mixing | 94 |
| Application of the classification to the calculation of ground-level NO ₂ concentrations | 95 |
| Conclusions | 97 |
| Chapter 8: Summary and conclusions | 99 |
| Introduction | 99 |
| Reactive-plume models | 99 |
| Results from four models compared with results from measurements | 100 |
| Plume profiles | 102 |
| Conclusions | 102 |
| References | 105 |
| Appendix: nomenclature | 109 |
| Samenvatting | 111 |



Scope of the thesis

The competition between the processes of dispersion and mixing (t_p) on the one hand, and chemical reactions (t_c) on the other hand, in the oxidation of NO in power-plant plumes will be discussed in subsequent chapters. The mixing process is studied by comparing results of time-averaged dispersion modelling with results from a model that treats dispersion from a momentary aspect. The NO and NO₂ concentrations measured in a plume are taken as basis and are compared with the concentrations calculated by means of four different models.

The thesis is structured as follows.

Chapter 1 concerns the contribution of nitrogen oxides to air pollution. The concentrations of nitrogen dioxide which occur in Dutch outdoor air are shown together with air quality standards. Mixing and chemical reactions of nitrogen oxides in a plume in the atmosphere are discussed.

In Chapter 2, the time scales of dispersion and of chemical reactions in a plume are calculated. These time scales are related to those used in the measurements and models presented in this thesis. Concepts which are used in reactive-plume models are reviewed and the literature is surveyed.

Chapter 3 describes the experimental methods used during the plume measurements.

Chapter 4 compares the results obtained with a reactive-plume model with data obtained from measurements. The dispersion of the plume is described in this model by an ordinary Gaussian concentration profile, which means that time-averaged dispersion is assumed. The chemical kinetics are assumed to be fast ($t_p/t_c > 1$), implying that chemical equilibrium exists locally in the plume. The NO₂ concentrations calculated with this model are usually too high, as compared with the measured values. Moreover, this model is only applicable to daytime conditions because chemical (photostationary) equilibrium must be assumed in this model to obtain a closed set of equations.

Chapter 5 describes a reactive-plume model in which Gaussian dispersion of the plume is assumed, but without the assumption of chemical equilibrium. Model calculations are compared with the same set of measurements as used in the model presented in Chapter 4. This second model is based on a solution of the diffusion equation. A solution is chosen which describes the concentration distributions of NO, NO₂ and O₃ as Gaussian profiles with the same relations for the growth of the plume widths σ_y and σ_z as used in the first model. Dispersion is therefore described in the same way by model 1 and model 2. However, the assumption of chemical equilibrium is not needed in the second

model. Deviations from chemical equilibrium in the plume were calculated. These are found to be important until about 500 s after emission from the stack. The reason for these deviations from equilibrium is the fact that the dispersion near the stack is fast with respect to chemical reactions. The assumption of fast chemical kinetics, as made in the first model, is obviously not valid in this region (distance from the stack < 5 km). It was found that NO₂ concentrations near the stack, calculated by the second model, are lower than those calculated with the first model. This means that the NO₂ concentrations were in better agreement with the measurements. But the concentrations at larger distances from the stack (> 5 km) in daytime, nevertheless often exceeded measured values. The model has also been applied to night-time conditions. In this case the results of model calculations agreed well with the measurements.

Chapter 6 presents a reactive-plume model in which neither Gaussian dispersion nor chemical equilibrium are assumed. This model is used to study inhomogeneous mixing in a momentary plume. The results of model calculations are compared with the same measurements as dealt with in the previous chapters. The cause of the discrepancy between measured concentrations of NO₂ and those calculated with the first and second model for daytime conditions, was investigated by means of this third model. In this model, dispersion in a momentary plume is described. Chemical equilibrium need not to be assumed and deviations from chemical equilibrium are calculated. Calculations with this model at larger distances from the stack gave the same results as those previously obtained by means of the second model for distances not too far from the stack. As mentioned above, chemical equilibrium does not occur because the dispersion process is faster than the chemical reactions ($\tau_p/\tau_c < 1$). Calculations showed that this effect lasts up to about 5 km from the stack. However, large deviations from chemical equilibrium were also found in the third model at distances larger than 5 km from the stack, which agrees with measurements. These deviations can be explained by taking inhomogeneous mixing in the plume into account: an inhomogeneously mixed plume can contain parcels of mixed plume, unmixed flue gas and unmixed ambient air, even at a relatively large distance from the stack. The mean plume is an average over all these different parcels and therefore chemical equilibrium is generally not obtained for the mean plume. Nevertheless, chemical equilibrium will exist in the individual plume parcels because dispersion in this phase is slower than the chemical reactions. The oxidation rate of NO is then determined by the mixing rate of the plume, i.e. limited by diffusion. Models that assume complete mixing of the plume with the air will therefore overestimate NO₂ concentrations in the plume. It can thus be concluded that the τ_p/τ_c ratio is less than one in the first phase of dispersion of a plume in the atmosphere (due to rapid dispersion), whereas this ratio is greater than one in the second phase, due to limited diffusion.

Chapter 7 describes an empirical reactive-plume model which is based on statistical analysis of a large database of plume measurements. This model

serves to circumvent problems in analytical modelling of inhomogeneous mixing. It is used to order the field data according to meteorological conditions. A classification of NO-oxidation rates is presented, based on measurements which were carried out under a wide range of atmospheric conditions during winter, spring, summer and autumn. The ozone concentration in the air, wind velocity and season appeared the most important factors determining the oxidation rate of NO. In this analysis the 'season' functions as an aggregated variable incorporating physical factors such as temperature and light intensity. It is deduced from the measurements that inhomogeneous mixing can retard NO₂ formation in a plume by a factor of about 10-20 compared to NO₂ formation in a homogeneously mixed gas.

Chapter 8 summarizes the results obtained with the reactive-plume models which were described in Chapters 4-7. Conclusions concerning the modelling of reactions of NO in a smoke plume are drawn in this chapter.

Previously published parts

The following chapters or parts thereof either have been published or have been submitted for publication.

Chapters 1 and 2 form part of a paper by L.H.J.M. Janssen & A.J. Elshout: 'Formation of NO₂ in power-plant plumes: measurements and modelling', published in 'KEMA Scientific and Technical Reports' 5: 259-297 (1987); other parts of these chapters are derived from a paper by L.H.J.M. Janssen & A.J. Elshout: 'Modelling of chemical reactions in power plant plumes', to be published by Gulf Publishing in 'Library of Environmental Control Technology' (in press).

Chapter 3, describing the various experimental methods applied, is based on all publications that have been used for the other chapters.

Chapter 4 is based on a conference contribution by P.J.H. Builtjes, L.H.J.M. Janssen, G.L.H. Beugeling & A.J. Elshout: 'Chemical reactive plumes; field experiments and modelling', published in 'Proceedings of the 7th World Clean Air Congress (Sydney)': 540-548 (1986); the chapter is also based on a paper by L.H.J.M. Janssen, A.J. Elshout, H. van Duuren & F. van Haren: 'Modelling reactions of nitrogen oxides in power plant plumes', published in 'Proceedings of the International Conference on Acid Rain: Scientific and Technical Advances (Lisbon)': 137-143 (1987).

Chapter 5 is based on a paper by L.H.J.M. Janssen, F. van Haren, H. van Duuren & J.H.A. van Wakeren: 'Conversion processes of nitrogen oxides in daytime and at night. Measurements and modelling in the plumes of power plants', which was submitted to 'Atmospheric Environment'.

Chapter 6 is based on a paper by L.H.J.M. Janssen: 'Mixing of ambient air in a plume and its effects on the oxidation of NO', published in 'Atmospheric Environment' 20: 2347-2357 (1986).

Chapter 7 is based on L.H.J.M. Janssen, J.H.A. van Wakeren, H. van Duuren & A.J. Elshout: 'A classification of NO-oxidation rates in power plant plumes based on atmospheric conditions', published in 'Atmospheric Environment' 22: 43-53 (1988).

Chapter 1

Nitrogen oxides and air pollution; chemical reactions in a plume

Abstract

Data on emissions of NO_x and concentrations of NO_x at ground level in The Netherlands are presented together with the relevant standards. Aspects concerning modelling of chemical reactions in stack plumes, especially reactions of nitrogen oxides, are discussed. These aspects are: the effects of simultaneity of turbulent dispersion and chemical reactions, and the influence of the mixing process on the reaction rates of nitrogen oxides.

Introduction

The world energy consumption was low until the beginning of the nineteenth century and demand could mostly be met by supply. Man used his muscle power, that of animals and the speed of wind and water as sources of mechanical energy. Burning of wood and fossil fuels such as coal or peat produced heat. The situation changed in the second half of the nineteenth century: an increase of the world population and the emerging industrialization of Western Europe increased the consumption of energy.

Production became concentrated in factories and human labour was replaced or supplemented by mechanical labour. Energy consumption started to increase by about 5% per year. The fast economic growth, especially that occurring after World War II, for a large part of the world population, caused a more than threefold increase of world energy consumption in the years between 1950 and 1980 (Anonymous, 1980).

Energy from primary sources such as the fossil fuels (wood, peat, coal, natural gas and oil) was more and more transformed into secondary energy carriers such as coke, petrol and electricity. Electricity evolved into a very important energy carrier without which our present-day society would be hardly imaginable (Fig. 1). Some 25% of the fossil-fuel consumption in The Netherlands is now used for generation of electricity. This process causes environmental problems but the final use of electricity is very clean. Electricity

is therefore well suited as an energy source for domestic purposes or for industrial applications in densely populated areas.

Environmental problems related to the generation of electricity depend primarily on the fuel used. When natural gas is burned, the problems are mainly due to the emission of nitrogen oxides (NO_x) and carbon dioxide (CO_2); when coal and oil are burned emissions of sulphur dioxide (SO_2) and dust (fly-ash) also contribute to the concentrations of air pollutants in the atmosphere.

The problems related to NO_x emissions by power plants are those which are especially considered in this thesis.

Emissions and concentrations of nitrogen oxides

Some general aspects of nitrogen oxides (NO and NO_2) as air pollutants are dealt with first. Nitrogen oxides are formed in power plants during the high-temperature combustion process through oxidation of nitrogen in the combustion air. Nitrogen bound in the fuel is also an important contribution to formation of nitrogen oxides in coal- or oil-fired power plants (Van der Kooij & Elshout, 1975). Most of the nitrogen oxides (~ 95%) are released as nitrogen monoxide (NO).

NO is rapidly converted in the atmosphere into nitrogen dioxide (NO_2). NO_2 is more toxic than NO for man and animals and it is known that NO_2 , even in relatively low concentrations, can suppress the growth of vegetation and cause corrosion of metals (Lanting, 1983; Anonymus, 1984, 1987). Apart from having direct effects, nitrogen oxides are pollutants which are also involved in many chemical processes in the atmosphere. Conversion products of NO_2 , i.e. nitrates

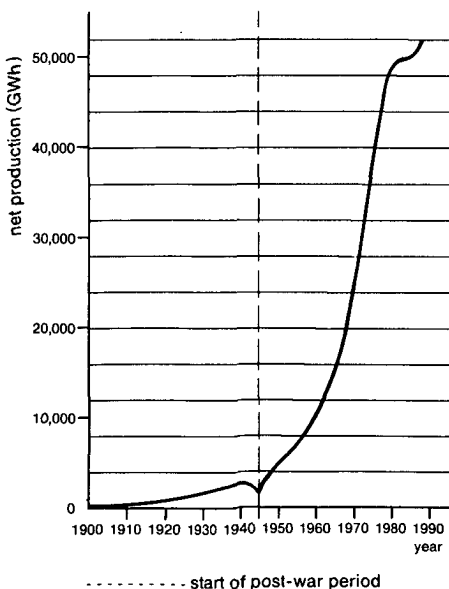


Fig. 1

Production of electricity (in GWh) via the public network in The Netherlands between 1900 and 1987.

Table 1

NO_2 air-quality standards in the framework of the Air Pollution Act as laid down in the General Administrative Order published in The Netherlands' 'Staatsblad' 1987 no. 33, 24 February 1987.

| P1 | limit value ($10^{-9} \text{ kg}\cdot\text{m}^{-3}$) | guide value ($10^{-9} \text{ kg}\cdot\text{m}^{-3}$) |
|------|---|---|
| 50 | - | 25 |
| 98 | 135 ² | 80 |
| 99.5 | 175 | - |

¹ P (percentile) is defined as the concentration for which P per cent of the 1-hour averaged NO_2 concentrations measured in one year, is lower than the limit value.

² A less stringent standard of $160 \cdot 10^{-9} \text{ kg}\cdot\text{m}^{-3}$ has been set for street canyons. This standard will be lowered to $150 \cdot 10^{-9} \text{ kg}\cdot\text{m}^{-3}$ by 92-01-01.

such as peroxy acetyl nitrate (PAN) and nitric acid (HNO_3), contribute to the concentration of inhalable toxic matter in the air and to acid deposition (Richards, 1983; Brodzinsky et al., 1984; Russell et al., 1985; Schneider & Bresser, 1987). Moreover, nitrogen oxides are pollutants which are involved in the formation of photochemical smog and the production of ozone (Eschenroeder & Martinez, 1972). NO_2 at concentrations over about 100 $\text{ppm}\cdot\text{m}$ may cause visibility degradation by colouring a plume brown (Melo et al., 1981).

In order to protect and improve air quality, emission standards and the standards of maximum allowed concentrations of air pollutants at ground level have been set by the Dutch government. Annual NO_x emissions in The Netherlands are about $500 \cdot 10^6 \text{ kg}\cdot\text{a}^{-1}$ (Anonymous, 1984). More than half of this NO_x emission is caused by traffic. Electricity generation contributes about 15% of the total NO_x emission. The maximum permissible NO_x emission set by the Dutch government is now $500 \cdot 10^6 \text{ kg}\cdot\text{a}^{-1}$ but is to be reduced considerably, viz. to $350 \cdot 10^6 \text{ kg}\cdot\text{a}^{-1}$ in the year 2000 to avoid further acidification of the environment (Anonymous, 1984, 1986; Schneider & Bresser, 1987).

In the air, nitrogen oxides are able to reach all parts of the respiratory system because of their low solubility in water. Concentrations of $300 \cdot 10^{-9} \text{ kg}(\text{NO}_2)\cdot\text{m}^{-3}$ present high risks and could very well lead to permanent health effects (Anonymous, 1983). The NO_2 ground-level concentrations in The Netherlands often exceed the Dutch guide values (Table 1; Fig. 2).

It is most important, in view of the adverse effects of NO_2 , that the NO_2 concentrations found at ground level as a result of emissions from a stack, are known. Measurements and models describing the dispersion of a plume,

together with the chemical reactions of air pollutants, are needed for this purpose. This thesis addresses this problem by developing and discussing models and measurements that describe the dispersion and conversion of nitrogen oxides in power-plant plumes.

Dispersion of air pollutants from a point source

Flue gases of power plants, after their emission from the stack into the atmosphere, are transported by the wind and dispersed by turbulence. Turbulence in the atmosphere can be interpreted as three-dimensional irregular variations of the wind speed and wind direction. This turbulence leads to spreading of the plume by dilution with ambient air. As a consequence, the plume reaches the ground at a certain distance from the stack. Depending on the concentration level, the pollutants may then harm human and animal health or the vegetation.

A so-called dispersion model, given the characteristics of the point source (in this case the stack of a power plant involved), is needed to estimate the concentrations. A well known example in the case of inert or slowly reacting pollutants is the Gaussian plume model to be discussed in more detail in Chapter 4. The main characteristic of this model is the assumption that the average concentration distribution of pollutants in a plume is Gaussian, in both the horizontal and the vertical plane (Fig. 3). As mentioned above, application of the Gaussian plume model is in principle restricted to inert or slowly reacting

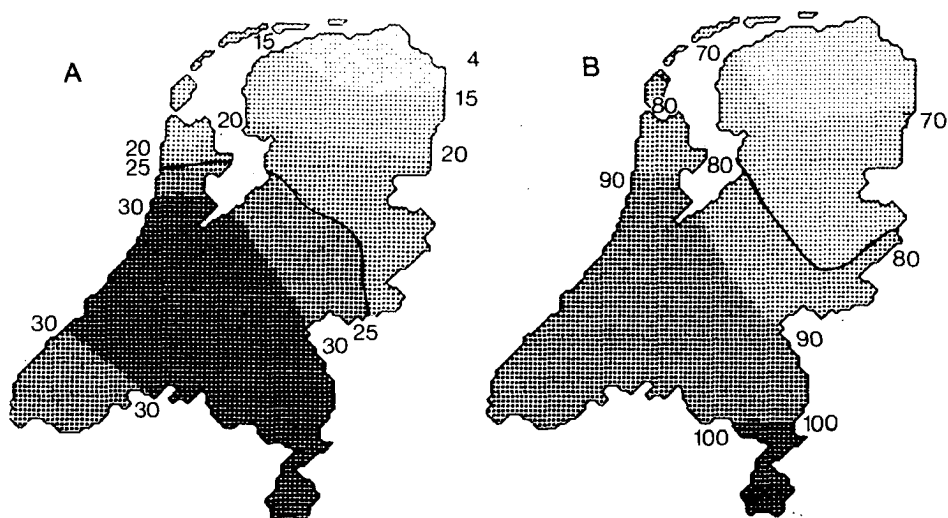


Fig. 2
The 50 (A) and 98 (B) percentiles of NO₂ concentrations averaged over one hour in The Netherlands in 1985, together with their guide values.

gasses such as SO₂. The present case however, concerns the emission of NO and this compound can undergo a fast chemical reaction i.e. conversion to NO₂. Because this conversion is a fast non-linear reaction which cannot be decoupled from the dispersion process, simple models such as the Gaussian plume model cannot be used. A dispersion model in which turbulent diffusion and chemical reactions can be treated simultaneously is therefore needed to calculate the NO and NO₂ concentrations at ground level.

Chemical reactions of nitrogen oxides in the atmosphere

Various chemical reactions of nitrogen oxides will be discussed in this thesis. The oxidation reaction of NO in the plume with ozone (O₃) in the ambient air is one of these reactions:



where the reaction rate given by $k_1 = 1400 \exp(-1200/T) \text{ ppm}^{-1} \cdot \text{min}^{-1}$ (Finlayson-Pitts & Pitts, 1986). Based on (1), the reaction-rate equations read:

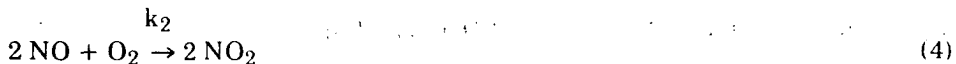
$$d[\text{NO}]/dt = -k_1 [\text{NO}][\text{O}_3] \quad (2)$$

and

$$d[\text{NO}_2]/dt = +k_1 [\text{NO}][\text{O}_3] \quad (3)$$

Equation (2) indicates that the conversion rate of NO depends on the product of the concentration of NO and that of O₃. In other words: Equations (1)-(3) describe a non-linear reaction of second order.

In the vicinity of the stack, where NO concentrations are still high, the third-order reaction of NO with O₂ may contribute to NO₂ formation. This reaction reads:



where $k_2 = [3.3 \cdot 10^{-12}] \exp(1780/T) \text{ ppm}^{-2} \cdot \text{min}^{-1}$ (Finlayson-Pitts & Pitts, 1986). In differential form, the reaction-rate equations read:

$$d[\text{NO}_2]/dt = +k_2 [\text{NO}]^2[\text{O}_2] \quad (5)$$

and

$$d[\text{NO}]/dt = -k_2 [\text{NO}]^2[\text{O}_2] \quad (6)$$

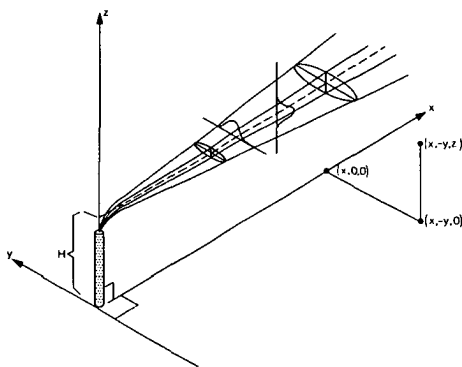
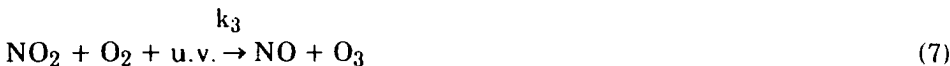


Fig. 3

Scheme of a stack plume as described by the Gaussian plume model.

Photodissociation of NO_2 through absorbtion of ultra-violet radiation during the daytime leads to the formation of NO and O_3 :



The value of k_3 varies with the intensity of solar radiation from 0 in the dark to about 0.5 min^{-1} in full sunlight (Becker & Schurath, 1975; Parrish et al., 1983). The differential form of (7) reads:

$$d[\text{NO}_2]/dt = -k_3 [\text{NO}_2] \quad (8)$$

and

$$d[\text{NO}]/dt = +k_3 [\text{NO}_2] \quad (9)$$

The total change of NO_2 as a function of time is found by summation of the three reactions (3), (5) and (8). The result reads:

$$d[\text{NO}_2]/dt = +k_1[\text{NO}][\text{O}_3] + k_2[\text{NO}]^2[\text{O}_2] - k_3[\text{NO}_2] \quad (10)$$

For chemical equilibrium during the daytime holds:

$$d[\text{NO}_2]/dt = 0 \quad (11)$$

It is clear that equilibrium is only possible when $k_3 \neq 0$. Chemical equilibrium can therefore only exist during the daytime.

The third-order reaction (5) can be neglected because it is only of importance when NO concentrations are high, i.e. in or near the stack. Chemical (photostationary) equilibrium can therefore be written as:

$$\Psi = \frac{k_1 [NO][O_3]}{k_3 [NO_2]} = 1 \quad (12)$$

Modelling dispersion and chemical reactions in a plume

A plume is dispersed in the atmosphere by turbulence. An important property of turbulent flow is mixing, a process which lessens the differences between a plume and the ambient air with respect to temperature and concentrations of water vapour or air pollutants. As a result of mixing, reactive species such as nitrogen monoxide (NO) and ozone (O_3), which are initially separated into flue gas and atmospheric air respectively, can meet on a molecular scale: this is the beginning of chemical reactions and the formation of NO_2 (Fig. 4).

When chemical reactions are important, the model should include the combined transport and chemistry in a plume (Fig. 5). This is difficult because the scales of turbulent mixing and molecular mixing differ greatly. Turbulent mixing, which determines the dispersion of the plume, takes place on a large spatial scale in the atmosphere. Large eddies in the atmosphere are in the order of tens to several hundreds of metres in size or even greater. The smallest eddies (e.g. Kolmogorov micro-scale), on the other hand, are of the order of millimetres only. These micro-scale eddies are dominant in molecular diffusion. They are therefore important for chemical reactions because, for a reaction to occur, mixing must take place on a molecular scale. Seen from another perspective, it may also be argued that times scales of the physical dispersion process and the time scale of chemical processes may also differ greatly.

Carmichael & Peters (1981) classified atmospheric reactions according to time scales of physical (t_p) and chemical (τ_c) processes, following Donaldson & Hilst (1972). A commonly used dimensionless quantity in this respect is the Damköhler number: the t_p/τ_c ratio. Carmichael & Peters (1981) distinguished between:

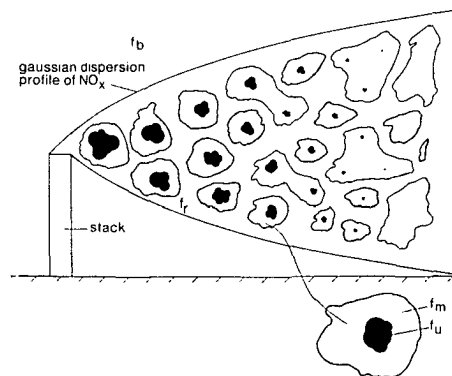


Fig. 4

Representation of a momentary plume. Parcels of unmixed flue gas (f_u), mixed plume (f_m) and ambient air (f_r) are enclosed by the Gaussian dispersion profile.

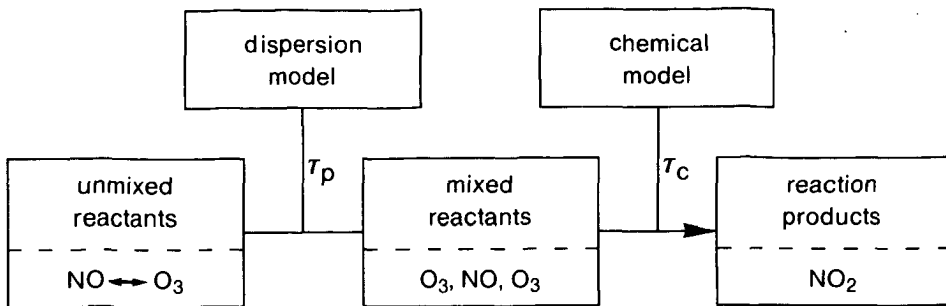


Fig. 5

Simplified reaction scheme illustrating the processes of dispersion (τ_p) and chemical reactions (τ_c) in a plume.

- (1) Slow chemical reactions ($\tau_p/\tau_c < 1$). Turbulent mixing is complete before any chemical reaction occurs. Average concentrations can therefore be used in the reaction equations.
- (2) Very fast chemical reactions ($\tau_p/\tau_c > 1$). Chemical-reaction rates are faster than the rate of mixing. It then becomes a good approximation to assume that the reaction proceeds locally at an infinite speed. This means that the reaction is completely finished, or - in case an equilibrium such as expressed in (12) is possible - that chemical equilibrium can be taken to exist locally. The concentration distribution of all reactive species then depends on the mixing rate at a molecular scale and on the initial distribution of the reactants, i.e. whether they were mixed or segregated.
- (3) Moderate reactions ($\tau_p/\tau_c \sim 1$). The rate for these reactions depends in a complex way on both the chemical-reaction rate and the mixing rate.

Chapter 2

Dispersion and chemistry in relation to measurements and models

Abstract

The rates of the NO-O₃ reaction are considered in relation to the rate of dispersion for a reactive plume. Dispersion near the source acts on a shorter time scale than the chemical reactions. Because the reactions are non-linear, both the measuring instruments and the models must have a high resolution to allow a sufficiently detailed study of the fast processes concerning nitrogen oxides in a plume. In practice, the resolution appears to be insufficiently high. Modelling the formation of NO₂ in a plume therefore requires approximations to be made.

Reactive-plume models which differ in their approach to dispersion and to chemical reactions are discussed in this chapter.

Introduction

The first three sections of this chapter deal with the chemical and physical times scales of NO-O₃ reactions in a plume and with aspects of the mixing process. Because a fast non-linear chemical reaction (such as the oxidation of NO in a power-plant plume) cannot be measured and modelled down to the finest details, assumptions must be made concerning the relative importance of the various processes involved. Furthermore, how to average concentrations of the various species in space and time must be decided.

Several plume models are available at the moment. They describe turbulent mixing and chemical reactions in a plume. These models differ greatly in complexity.

The concept of a well-mixed box is often used in models with emphasis on chemistry and in these models chemical reaction rates are based on mean, i.e. spatially averaged, concentrations in the plume. Chemical equilibrium is assumed to exist in the plume.

A plume cannot be considered as a well mixed box, because concentration gradients have to be taken into account. These can be calculated by mean, i.e. time-averaged, plume-dispersion equations such as used in, e.g. the Gaussian

plume model (Eq. 16). An interaction between physical and chemical processes can be expected in this case. Models using this approach may differ in that they assume either chemical equilibrium (Damköhler number greater than 1) or no chemical equilibrium (Damköhler number smaller than 1). In the latter case, the time scale of chemical reactions is larger than the diffusion time scale. As a result, the reaction can be expressed in terms of mean concentrations.

However, the conversion rate in the case of fast non-linear chemical reactions (like the oxidation of NO) is not determined by averaged but by actual local concentrations. In other words: chemical equilibrium can exist locally and instantaneously.

Because NO_2 is formed when O_3 in the ambient air is entrained in the plume containing NO, models have been developed which describe mixing processes in the plume in more detail.

Models using the above concepts and described in the literature are discussed in subsequent sections.

Time scales of NO-O_3 reactions in a plume

The time scales of both the physical processes of turbulent mixing on one hand, and the chemical processes of molecular reactions on the other hand must be taken into account if the NO-NO_2 conversion in the atmosphere is to be modelled. The ranking of both contributions in the NO-NO_2 oxidation process is achieved by estimating their time scales as follows.

The time scale of the chemical reactions

The time scales of the chemical reactions can be deduced from reactions (3) and (8). The time scale of reaction (3) is:

$$\tau_c(3) \sim 1/(k_1 \cdot [\text{O}_3]) \quad (13)$$

The concentration of NO in the middle of the plume is high and that of O_3 is very low because almost all the O_3 is used for the oxidation reaction (3). As a result, this reaction will almost stop and the time scale will consequently be long. On the other hand, the O_3 concentration at the edge of the plume is relatively high and NO is available for reaction (3) so that much NO_2 can be formed; this means that the reaction rate is fast and the chemical time scale is short. For O_3 concentrations in the range of 0.5 ppb in the middle of the plume and 50 ppb in the background air, the time scale for reaction (3) varies between one hour and half a minute.

The time scale for the photo-dissociation reaction of NO_2 can be estimated from Equation (8):

$$\tau_c(8) \sim 1/k_3 \quad (14)$$

The time scale for this reaction is about three to six minutes for normal atmospheric conditions (Parrish et al., 1983; Janssen et al., 1988).

The production of NO₂ through reaction (3) equals the destruction of NO₂ through reaction (8) if a state of chemical equilibrium exists. If equilibrium is affected because of rapidly changing of concentrations of the reactants, as happens in a dispersing plume, the slowest reaction determines whether equilibrium can be maintained. The time scale of both reactions (3) and (8) is obviously of the same order of magnitude. The following value for τ_c is here taken to be representative for rapid conversion at the edge of the plume:

$$\tau_c[\text{NO}_2] \sim 5 \text{ minutes} \quad (15)$$

(which corresponds with an O₃ concentration of 10 ppb).

The time scale of the dispersion process

The time scale of dilution due to turbulent dispersion of the plume in the atmosphere will now be dealt with. This time scale of dispersion can be estimated from the growth rate of the plume. If it is assumed that the shape of the plume is described by a Gaussian profile (see Eq. 16 and Fig. 3), the growth rate of the plume can be derived from the growth of the plume width in the vertical plane described by σ_z .

$$C_{\text{NO}_x}(x, y, z, H) = \frac{Q e^{-\frac{1}{2}(\frac{y}{\sigma_y})^2}}{2\pi u \sigma_y \sigma_z} \left[\exp\left(-\frac{1}{2} \frac{H-z}{\sigma_z}\right)^2 + \exp\left(-\frac{1}{2} \frac{H+z}{\sigma_z}\right)^2 \right] \quad (16)$$

The growth of the plume width in the vertical plane (σ_z) is:

$$\tau_p^{-1} \sim (1/\sigma_z^2) \cdot (d\sigma_z^2/dt) \quad (17)$$

If σ_z is taken to be ax^b with $a = 0.2$ and $b = 0.76$ (KNMI, 1979), then it is found that $\tau_p \sim 0.7 t$. If this expression for τ_p is compared with the chemical time scale τ_c derived in the previous paragraph, it can be deduced that the dispersion process of the plume is faster than the chemical reactions ($\tau_p/\tau_c < 1$) in the first five to ten minutes after emission from the stack whereas afterwards chemical reactions will be faster than dispersion ($\tau_p/\tau_c > 1$). In other words, the dispersion process is that fast in the first phase of plume dispersion ($t < 5$ minutes) that chemical equilibrium cannot be established.

In the second phase ($t > 10$ minutes), the chemical reaction rate can be considered fast, so that chemical equilibrium exists locally in the plume. Whether this equilibrium can be measured depends on the state of the plume

(i.e. homogeneously or inhomogeneously mixed) and the characteristics of the measuring instruments. This will be discussed in more detail in the next section.

Mixing, modelling and measuring

Oxidation of NO by O₃ as described by Equation (3) is a non-linear reaction. This means that the oxidation rate depends on both the concentration of NO and the concentration of O₃. The reaction is non-linear, so that the reaction rate and consequently the rate of NO₂ formation also can only be described by average concentrations of NO and O₃ if both reactants are mixed homogeneously within the plume. In this case an average is defined by some space or time average, whereas 'homogeneously mixed' means: (1): there are no concentration gradients in the plume ($\partial C / \partial x$, $\partial C / \partial y$ and $\partial C / \partial z$ are all zero) and (2) changes in concentration of NO and O₃ in time are exactly correlated. It is known, however, that concentration gradients do exist in a dispersing plume and because NO and O₃ have different origins (flue gas and ambient air respectively), it is not to be expected that changes of concentrations in time will correlate exactly.

Formation of NO₂ therefore takes place in an inhomogeneously mixed plume and cannot be described by average concentrations of NO and O₃ but only by local instantaneous concentrations (Fig. 4). However, averaging always takes place, both with measuring and modelling. Measuring instruments are not infinitesimally fast and always have a limited spatial resolution. The same holds for models. Processes are described by averages and are not described down to the finest spatial details.

NO₂ formation in a plume can however be studied by using average concentrations of NO and O₃, if the resolution in space and time of measurements and models is well below the order of variations in space and time of concentrations of NO and O₃ in the plume. Because both dispersion and chemistry of nitrogen oxides are fast processes which occur on small spatial scales, these prerequisites are therefore almost never met when formation of NO₂ in a power-plant plume is studied.

Measurements

The response times and the spatial resolution of the measuring instruments are shown in Table 2. With this spatial resolution large scale concentration variations in a plume averaged over a few seconds can be followed, see Figures 7, 10, 20 and 29. These macroscopic concentration variations are caused by eddies in the atmosphere which are of the order of the plume cross-section. They cause the plume to break up in parcels which may survive in the atmosphere for some time, and are responsible for the dispersion, see also Figure 4. In this

Table 2

Response times and spatial resolution of the chemoluminescence monitors used in the measurements.

| | R-C time (s) | measuring speed (m·s ⁻¹) | spatial resolution (m) |
|---------------|-----------------|---|---------------------------|
| measuring van | 10 | 5 | > 50 |
| aircraft | 1 | 70 | > 70 |

process O₃ from outside the plume is mixed in at the edges and this is called macromixing. The measuring instruments are fast enough to register NO, NO₂ and O₃ concentration variations on this scale rather accurately.

Micromixing is mixing within the plume parcels on much smaller scales than macromixing (< 50 m). On this scale the spatial resolution of the measuring instruments will distort the concentration profiles in the plume, see Figures 7 and 20.

Models

It was already mentioned that formation of NO₂ is a non-linear reaction. If the concentrations of NO₂ measured, which are averages over time and space, are compared with the calculated values, momentary local concentrations of NO and O₃ are needed in the model. There is a procedure, common in modelling, that is used to evaluate the effect of local and momentary variations in the concentration of NO and O₃ upon the rate of NO₂ formation in an inhomogeneously mixed plume. This procedure consists in subdivision of the concentrations into a mean and a fluctuating part, e.g. subdivision of the NO concentration into NO + NO' concentrations and subdivision of the O₃ concentration into O₃ + O₃' concentrations. If this procedure is applied here, Equation (10) becomes:

$$\overline{d(\text{NO}_2)/dt} = k_1 \overline{[\text{NO}]} \cdot \overline{[\text{O}_3]} - k_3 \overline{[\text{NO}_2]} + k_1 \overline{[\text{NO}']} \overline{[\text{O}_3']} \quad (18)$$

The bars above the terms in Equation (18) refer to ensemble averages which may be connected to spatial averaging, averaging in time or both, depending on the application.

Table 3
Characteristics of the various models.

| dispersion | concentration |
|------------------|----------------------|
| 1. time-averaged | 1. averaged in space |
| 2. momentary | 2. locally |

Formation of NO_2 can thus be expressed in terms of mean concentrations plus a contribution due to fluctuations. The average NO and O_3 concentrations measured can often be brought into agreement with the average NO and O_3 concentrations needed in the model. However, the fluctuating term in Equation (18) must also be taken into account if the NO_2 concentration calculated on the basis of average NO and O_3 concentrations in the plume does not agree with the measurements.

Concentration fluctuations occur in time and space. Models that describe the momentary and local formation of NO_2 in a plume do not exist and therefore averaging always takes place. Models can then be differentiated according to Table 3.

Dispersion in the reactive-plume models presented in Chapters 4 and 5 is described by Gaussian profiles. This means that the equations for the growth of the plume widths σ_y and σ_z represent time averages. However, concentrations are treated locally in these models because concentration gradients in the plume can be calculated. The model in Chapter 6 describes a momentary plume by subdivision of the plume into parcels, thus treating dispersion as momentary. This model allows no concentration gradients in the mixed plume, so the concentrations used are averages over a parcel. The model presented in Chapter 7 assumes a Gaussian profile of the plume and time-averaged dispersion. The ratio of the NO_2 and NO_x concentrations is considered to be constant at a fixed distance from the source and represents an average over the plume.

The following section deals with the models described in the literature.

Box models

Uniform, homogeneous mixing, i.e. a flat concentration profile in the plume is assumed in models that apply the concept of a single well-mixed box. The dimension of the box may vary as a function of time according to the Gaussian plume profile (Liu, 1977) or to other profiles as described in models developed by Isaksen et al. (1978), Forney & Giz (1981) and Schurath & Ruffing (1981). The

assumption of homogeneous mixing allows these models to be applied at greater distances from the source (> 50 km) where concentration gradients in the plume have almost disappeared. The emphasis in these models is on chemistry rather than on dispersion and the models involved can incorporate relatively many chemical reactions.

Models with non-uniform concentration distributions

This category includes two types of models, those assuming local chemical equilibrium and those assuming fast dispersion.

Models assuming local chemical equilibrium ($t_p/t_c > 1$) — A model which incorporates mean concentration profiles of chemical reactants in a plume was described by Peters & Richards (1977). Dispersion is modelled by calculating the concentration distribution of the conserved quantity NO_x ($\equiv \text{NO} + \text{NO}_2$) in the plume using the Gaussian plume model (Eq. 16).

As concerns the chemistry, only those reactions are considered which are sufficiently fast ($t_p/t_c > 1$). In other words, it is assumed that chemical equilibrium exists locally between the reactants in the plume. This chemical equilibrium is applied to mean concentrations, so the effect of inhomogeneous mixing is neglected. The assumption of photostationary equilibrium in the plume makes it obvious that this model is only applicable for the description of daytime chemistry.

The results of calculations with this model will be compared with the results obtained from field measurements and calculations with other models in Chapter 4.

Models assuming fast dispersion ($t_p/t_c < 1$) — A model proposed by Varey et al. (1978) uses a diffusion equation in a Langrangian coordinate system which moves along with the mean wind. Reactions (3), (5) and (8) are added to the diffusion equation.

In polar coördinates the equation for $[\text{NO}_2]$ becomes

$$\delta \left[\text{NO}_2 \right] / \delta t = D \left(\frac{\delta^2 \left[\text{NO}_2 \right]}{\delta r^2} + \frac{1}{R} \frac{\delta \left[\text{NO}_2 \right]}{\delta r} \right) + k_1 \left[\text{NO} \right] \left[\text{O}_3 \right] + k_2 \left[\text{NO} \right]^2 \left[\text{O}_2 \right] - k_3 \left[\text{NO}_2 \right] \quad (19)$$

where the first term on the right-hand side describes the radially symmetrical dispersion of the plume; D is a turbulent diffusion coefficient and, in this model, represents a constant which depends only on atmospheric conditions. The next terms on the right-hand side are the chemical reactions added to the diffusion equation. Equation (19) describes chemical reactions in a model in which time-averaged dispersion equations are used. Concentration fluctuations of reacting

compounds in a momentary plume which could - if they are correlated - add terms to the right-hand side of Equation (19), are neglected.

Equation (19) can be solved numerically. It should be noted that the assumption of photostationary equilibrium is not needed in this model and that NO, NO₂ and O₃ concentrations in a plume at night can be calculated in principle by omitting the photodissociation reaction (8). The results of calculations with an adapted version of this model will be compared with those of field measurements and calculations with other models in Chapter 5.

Richard et al. (1985) also used the diffusion equation, but in a Eulerian coordinate system. These authors used the Gaussian parameters σ_y and σ_z in deriving diffusion coefficients for the y and z directions, respectively. Llewelyn (1983) also solved the transport diffusion equation numerically but modelled NO oxidation as a simple first-order reaction term.

A problem with the use of numerical solutions for the diffusion equation combined with fast chemistry, such as Equation (19), is stability of the numerical procedure. The optimum step size in the calculations must be chosen for each phase of oxidation process. Step size should not be too small because of increasing computing time and should not be too large so as to avoid instability or inaccurate solutions.

Models dealing explicitly with mixing of O₃ into the plume

The effect of the entrainment of O₃ into the plume is not explicitly taken into account in the models described above. Models with emphasis on the process of entrainment were developed by Melo et al. (1978), Hov & Isaksen (1981), Stewart & Liu (1981), Persson (1984) and Persson & Funkquist (1984).

Melo et al. (1978), Hov & Isaksen (1981) and Stewart & Liu (1981) modelled atmospheric diffusion by subdivision of the plume into concentric elliptical rings or cells (Fig. 6). These authors took into account the turbulent exchange of material between adjacent rings. Mixing of O₃ into the plume, also called macro-scale mixing, can be modelled in this way. The diffusion coefficients used to calculate the mass transfer across the rings correspond to the diffusion coefficients used in Gaussian dispersion models, and these models can be considered as a discretisation of a Gaussian plume. Average concentrations within each ring are calculated and the effect of concentration fluctuations on the oxidation rate is neglected. When the results of calculations with these models were compared with measurements, the agreement between measured and calculated values was fairly good but the measurements were carried out at very large distances (from forty to over a hundred kilometres from the source) where small concentration gradients can be expected and chemical reactions will be faster than dispersion ($t_p/t_c > 1$). The mixing process will no longer be very important. However, the accuracy of results obtained by means of these types of models can be expected to improve at shorter distances from the stack,

where dispersion is still important. The adaptions in these models thus remain difficult to evaluate.

Persson & Funkquist (1984) and Persson (1986) modelled the oxidation of NO emitted from a point source and took mixing of O₃ into the plume into account by calculating mass fluxes of NO and O₃ in the plume during dispersion. They separated the dispersion of the plume into two domains: near the source (where the buoyancy of the hot exhaust gases determined the turbulence within the plume) and at greater distances (where dispersion was controlled by atmospheric turbulence depending on atmospheric conditions). The radius (R) of the plume near the source expands according to $R = \beta \cdot \Delta h$, β depending on atmospheric conditions ($\beta \sim 5$) and Δh being the plume rise, on the basis of equations derived from Briggs (1976) and Hogström (1978). Ordinary Gaussian values of σ_y and σ_z are used to describe plume dispersion at greater distances.

Modelling micromixing

The rate of NO₂ formation is calculated in the reactive-plume models just discussed, by use of mean concentration profiles equivalent to spatial averaging and mean plume dispersion equations equivalent to temporal averaging, respectively. The effect of small-scale in-plume fluctuations of NO, NO₂ and O₃ concentrations, also called micro-scale mixing, on the oxidation rate of NO is not included. However, in the case of fast non-linear chemical reactions (such as

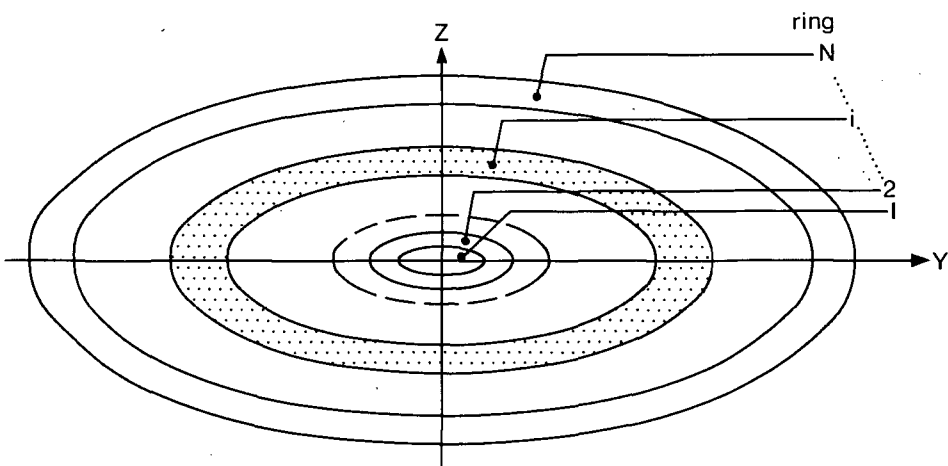


Fig. 6

Cross section of a plume showing a division of the plume into elliptic rings, as presented by Lusis (1976). The exchange of material between the rings is modelled.

Concentrations of reactants in a plume may fluctuate on different spatial scales. Builtjes & Talmon (1987) discuss measurements reported by Hanna (1984) which show the differences between relatively small in-plume fluctuations and the turbulent meandering which leads to different plume parcels. Areas with clean air, the 'intermittency', exist between the plume parcels. This macroscopic structure of a momentary plume leads to large-scale concentration variations on this spatial scale (Figs. 4, 7, 10, 20 and 29). It is difficult to incorporate these fluctuations in the model of a momentary plume.

Donaldson & Hilst (1972) were the first to discuss the effect of correlation between fluctuating concentrations of reactants on chemical reaction rates in the atmosphere. If it is assumed that the reactive components NO_2 and O_3 are inhomogeneously mixed in a plume, the reaction equation for NO_2 formation will be:

$$\begin{aligned} \frac{d[\overline{\text{NO}}_2]}{dt} = & \frac{d(\overline{[\text{NO}_2]} + [\text{NO}_2]')}{dt} = k_1(\overline{[\text{NO}]} + [\text{NO}'])(\overline{[\text{O}_3]} + [\text{O}_3']) \\ & + k_2(\overline{[\text{NO}]} + [\text{NO}'])(\overline{[\text{NO}]} + [\text{NO}'])(\overline{[\text{O}_2]} + [\text{O}_2']) + \\ & - k_3(\overline{[\text{NO}_2]} + [\text{NO}_2']) \end{aligned} \quad (20)$$

Formation of mean NO_2 can thus be described on the basis of mean concentrations plus a contribution due to the correlation of fluctuations:

$$\begin{aligned} \frac{d[\overline{\text{NO}}_2]}{dt} = & k_1 \overline{[\text{NO}]} \overline{[\text{O}_3]} + k_2 \overline{[\text{NO}]}^2 \overline{[\text{O}_2]} - k_3 \overline{[\text{NO}_2]} + \\ & + k_1 \overline{[\text{NO}']} \overline{[\text{O}_3']} + k_2 (\overline{[\text{NO}']}^2 \overline{[\text{O}_2]}) \end{aligned} \quad (21)$$

If the plume is inhomogeneously mixed and consists of different plume parcels, large differences between in-plume and out-plume NO and O_3 concentrations exist on a relatively small spatial scale, in particular near the stack (Figs. 4, 7 and 20a). In a Eulerian frame of reference, these concentrations will also fluctuate rapidly in time. A negatively correlated term $[\text{NO}'][\text{O}_3']'$ exists if NO and O_3 concentrations are described in a mean (i.e. averaged over several plume

parcels) and a fluctuating part. Builtjes & Talmon (1987) reported averaged values of $([NO]/[O_3])/(([NO]/[O_3])$ of about -0.3 to -0.4 for distances between 200 and 700 m from the stack, based on wind-tunnel measurements and a value of -0.45 at distances up to 2 km, based on field experiments.

The magnitude of the fluctuating terms will decrease through molecular diffusion. Donaldson & Hilst (1972) derived an expression for the decrease of the $[NO]/[O_3]$ term. If the $[NO]/[O_3]$ terms vanishes rapidly by intensive mixing, the product $[NO]/[O_3]$ will be close to zero and NO₂ formation can be described on the basis of mean concentrations. If the reaction rate of NO and O₃ is faster than the mixing rate, the product $[NO]/[O_3]$ will be negative and NO₂ formation will be suppressed, i.e. diffusion-limited, as is the case with NO₂ formation in power-plant plumes at greater distance from the stack (> 5 km).

It was argued in the first part of this chapter that the mixing rate near the stack (< 5 km) is faster than the chemical reaction rates. The effect of fast concentration fluctuations on the rate of NO₂ formation is therefore damped by the relatively slow chemical reaction rates.

Kewley (1978) proposed a model in which the influence of concentration fluctuations on the NO-oxidation rate can be calculated by introduction of the probability density function (p.d.f.) in the model described by Peters & Richards (1977). Results of calculations carried out by Kewley indicate that fluctuations in the concentration of NO, NO₂, and O₃ cause a retardation of NO₂ formation in a plume. Since this is a modified Gaussian dispersion model which also assumes photostationary equilibrium of the mean concentrations in the plume, it cannot be used to study the night-time chemistry of NO_x.

Lamb & Shu (1978) and Shu et al. (1978) developed a complicated model which takes concentration fluctuations of the reacting species into account to describe second-order chemical reactions in a turbulent flow. According to this model, the time before 50% of the available NO will be converted increases from three to twenty minutes due to negative correlation of NO and O₃ concentration fluctuations in a power plant plume. In their approach, the mixing was

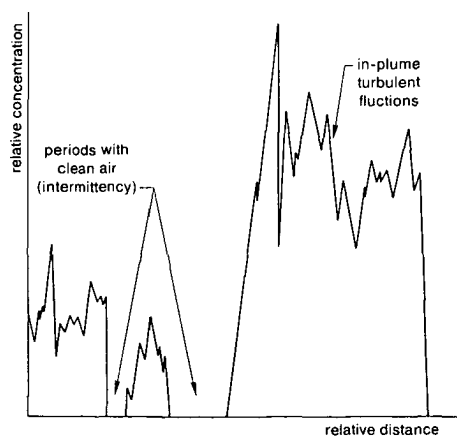


Fig. 7
Example of a time-resolved recording of concentration fluctuations in a plume, as described by Hanna (1984).

separated from the chemical reactions by deriving the mixing parameters from the dispersion of inert species.

Georgopoulos & Seinfeld (1986a,b) recently published two papers in which a detailed model is described to handle the complex coupling between transport and chemistry and which also takes macromixing and micromixing into account. Macromixing is modelled by defining 'instantaneous' plume widths based on a separation of the dispersion into relative diffusion and meandering. Microscale mixing is modelled by taking concentration fluctuations into account.

The complex models described by Lamb & Shu (1978), Shu et al. (1978) and Georgopoulos & Seinfeld (1986a,b) which try to describe all relevant processes in detail, present the problem of obtaining the required reliable input values for all parameters in the model and also of obtaining the required detailed measurements to test them. Sufficiently detailed information is generally lacking. The model of Lamb & Shu (1978) and Shu et al. (1978) was tested during only one measuring campaign in the plume of a power station and the model of Georgopoulos & Seinfeld (1986a,b) was tested against wind-tunnel experiments only, which means no effect of photodissociation ($k_3 = 0$) and in a regular flow field.

It is obvious from the above considerations that there now exist several reactive-plume models of increasing complexity. However, reliable plume measurements in the atmosphere to test them are almost absent. It is therefore difficult to evaluate the relative importance of the assumptions made in the various models concerning, for instance, the time scales of physical and chemical processes, the contribution of macromixing and micromixing and of concentration fluctuations to the rate of the chemical conversion processes.

Reactive-plume models are described in Chapters 4, 5 and 6 and they are tested against the same set of plume measurements. The results of calculations with these models are evaluated. As a result, it is possible to evaluate the assumptions concerning the time scales of physical and chemical processes in modelling fast chemical reactions in power-plant plumes.

A very large number of plume measurements carried out under widely varying atmospheric conditions is systematically dealt with in an empirical model presented in Chapter 7.

Chapter 3

Experimental methods

Three experimental aspects will be dealt with here in detail: the monitoring procedure, the measuring strategy and the technique used for remote detection of plumes.

Monitoring

The aircraft used for measuring flights, a Piper Navajo Chieftain, was equipped with a TECO 14D NO, NO_x chemoluminescence monitor and a Bendix 8002 chemoluminescence ozone analyser. R-C times of both instruments were set at one second. The SO₂ concentrations were measured with a TECO 43 SO₂-pulsed fluorescence analyser with an R-C time of four seconds. The aircraft was also equipped with a Rosemount Total Temperature Sensor, model 102 BE, with an R-C time of 0.1 s. The data were sampled by a Monitor Labs datalogger using a sample frequency of 2 Hz, and stored on cartridges.

For two measuring flights which were made at night, the aircraft was also equipped with filter packets to measure aerosol concentrations in the plume and to investigate the possibility of nitric acid formation in the plume. The filter packets consisted of a teflon filter to measure nitrate and sulphate concentrations in the aerosol and a nylon back-up filter to measure gaseous nitric acid concentrations in the plume. The total air volume sampled at a specific distance from the source was about 0.5-2 m³, depending on the distance from the source. After the flights, the loaded filters were kept in the dark in a refrigerator. They were extracted the next morning and analysed together with unloaded blanks by ionchromatography (Dionex Model 10).

Measurements on the ground were carried out by a KEMA measuring van. The speed of the van during plume measurements on the ground depended on the measuring distance from the source and ranged from about 5 m·s⁻¹ at a distance of 5 km to about 10 m·s⁻¹ at a distance of 10 km. SO₂ was measured by a Beckman 953 fluorescence monitor. NO, NO_x and O₃ were measured by the same methods as used in the aircraft. Because of the slower speed of the measuring van, the R-C times of the monitors were set at 10 s. The sample frequency of the data logger was 4 Hz.

The data obtained during the measurements were processed by computer and concentration profiles were plotted in a fixed co-ordinate system. The NO, NO₂, O₃ and SO₂ concentrations integrated over the plume (ppm·m) and the plume widths (m) were determined from the concentration profiles measured. Average NO, NO₂ and O₃ concentrations in the plume were calculated from the integrated concentrations divided by the overall plume width. NO₂/NO_x ratios were correlated to plume travelling time, using the estimated wind speed at plume height.

The wind speed at plume height (several hundreds of metres) was calculated by means of the power law $u(z_2)/u(z_1) = (z_2/z_1)^p$ based on measurements of the wind speed at an altitude of 10 m ($u(z_1)$), and z_2 being the average altitude of a number of crossings at one distance. The value for p depends on atmospheric stability.

For each measuring day atmospheric stability was determined on the basis of meteorological information from nearby weather stations. Values for p , as recommended by the Royal Dutch Meteorological Institute (KNMI) for atmospheric conditions in the Netherlands were taken as: Pasquill classes A and B: $p = 0.10$; Pasquill classes C and D: $p = 0.16$, and Pasquill classes E and F: $p = 0.30$ (KNMI, 1979).

Measuring strategy

NO-oxidation rates are inferred from NO₂/NO_x ratios measured as a function of distance from the source. The measurements were carried out by means of an aircraft at distances between 0.5 and 30 km downwind of a limited number of oil-, gas- and coal-fired power plants in The Netherlands. Measurements started and ended with spiral flights outside the plume to measure NO, NO₂, O₃ and SO₂ background concentrations and to establish the height of the inversion from temperature data (Fig. 8). Sampling of the plume took place during several horizontal crossings at different altitudes perpendicular to the plume axis. Commonly four to ten crossings were made at each selected distance from the source, which took fifteen to thirty minutes. The flight speed of the aircraft during the measurements was 70 m·s⁻¹.

Plume crossings at daytime were carried out between 11h00 and 16h00 at altitudes between 200 and 700 m. The plume heights were between 200 and 500 m. Because the mixing heights during these measurements were at least 500 m (KNMI, 1979), the entire plume was considered to be in the mixing layer of the atmosphere. No temperature inversions were recorded below 600 m during the plume flights. Plume crossings at night were carried out at least three hours after sunset, i.e. between 21h00 and 02h00 in winter and between 00h00 and 03h00 in spring. The depth of the mixing layer, characterized by the height of the temperature inversion, decreases at night. The plumes of the power plant could therefore be located above or below the temperature inversion.

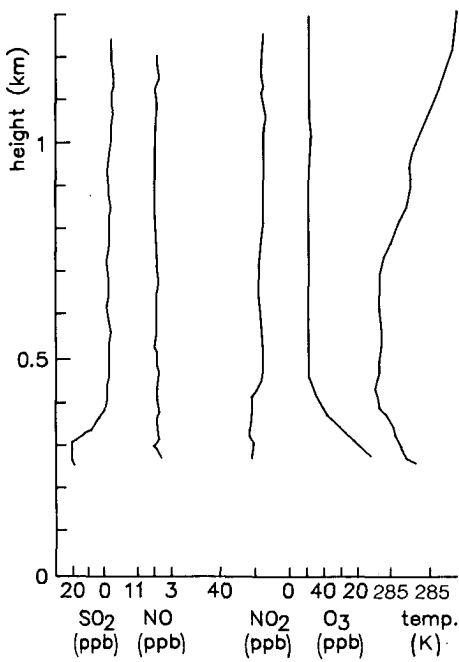


Fig. 8
 SO_2 , NO , NO_2 , O_3 and temperature gradient as functions of height, as measured in a spiral flight during flight 9.

Remote detection of the plume

All night-time measuring flights were carried out in the plumes of the 2000 MWe Amer power station near Geertruidenberg. Carrying out successful night-time measuring flights appeared to be rather difficult. The plume was not easy to detect because of its relatively small dimensions and because of uncertainty about the position of the plume, i.e. below or above the nocturnal temperature inversion. If the plume stayed too low (i.e. below the inversion), it was often impossible to monitor the plume in situ by the aircraft because of Dutch flight legislations: flying below 1000 ft (~ 305 m) is not allowed. When only two coal-fired units of 200 MWe had been in operation, the plumes stayed too low to be measured. It appeared that night-time measuring flights could only be carried out successfully when the 650 MWe unit was in operation, because of its larger heat output and the consequently higher plume rise.

An electric (E-)field meter was installed in the aircraft for remote detection of the plume at night. This meter was mounted in the wingtips of the aircraft (Fig. 9). It detects disturbances of the natural electric field of the earth caused by local space charge, such as present in the exhaust plumes of coal-fired power plants. The position of the aircraft (above, below or in the plume) could thus be established, which was very helpful under night-time conditions (Fig. 10). It is a newly developed instrument to function also under humid conditions, e.g. in fog and rain, and has been described by Van Wakeren et al. (1984).

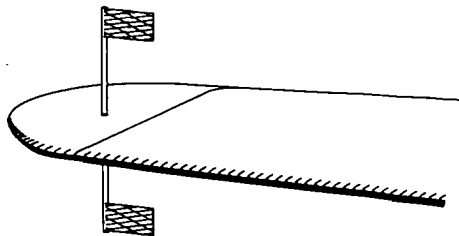
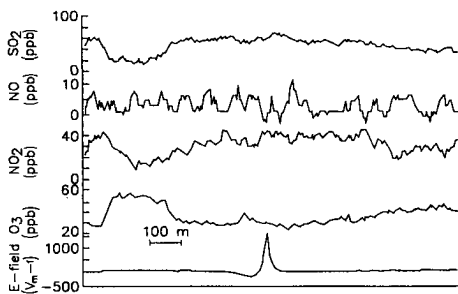
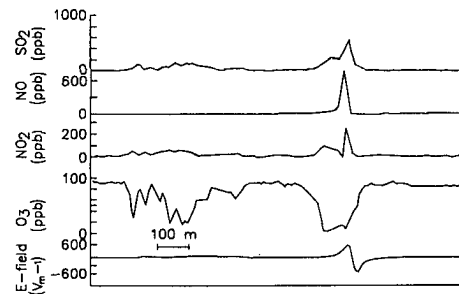


Fig. 9

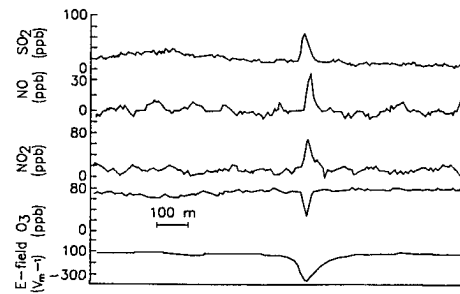
Detailed view of the right wing tip of the aircraft. The sources of the E-field meter are mounted on both sides of the wing tip. The wing tip contains the measuring circuit.



A



B



C

Fig. 10

Characteristic traverse records for SO_2 , NO , NO_2 , O_3 and electric field.

A: a strong positive E-field is detected; the aircraft is above the plume. The monitor signals cannot detect the power-plant plume. Distance from the source: 1 km.

B: the aircraft is in the middle of the plume (distance from the source: 7 km). The E-field changes its sign during the plume crossing. Very high concentrations of the gaseous components SO_2 and NO_x are recorded.

C: a negative E-field is recorded; the aircraft is at the lower edge of the plume (distance from the source: 7 km). Low SO_2 and NO_x concentrations are recorded.

Chapter 4

Modelling the oxidation of NO on the basis of Gaussian dispersion and chemical equilibrium in the plume

Abstract

The reactive-plume model developed by Peters & Richards (1977) is used to calculate concentrations and concentration gradients of the reactants, NO, NO₂ and O₃ in power-plant plumes. Local chemical equilibrium in the plume is assumed, i.e. $t_p/t_c > 1$. The results of these calculations are compared with results obtained from measurements in the plumes of Dutch and German power plants.

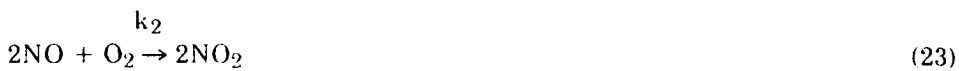
It appears that the calculated NO₂/NO_x ratios are generally too high. This is explained by the fact that dispersion and mixing near the source are faster than the chemical reactions i.e. the assumption that $t_p/t_c > 1$ is not valid in the model. It is also assumed in the model that the plume is homogeneously mixed at larger distances from the source or, stated differently, that the effect of concentration fluctuations on the reaction rate is neglected. Measurements indicate that this is not the case. This means that the oxidation of NO is limited by diffusion. This is not taken into account in the model and the NO₂/NO_x ratios are therefore also too high at greater distances from the source.

Introduction

Conversion of NO to NO₂ in the plume from a tall stack is illustrated in Figure 4. NO₂ is formed when ambient air containing O₃ mixes on a molecular scale with the plume containing NO, according to:



Near the source, where the concentration of NO is still high, a contribution from the reaction with O₂ can be expected:



Absorbtion of ultraviolet radiation by NO_2 leads, during the daytime, to the photodissociation reaction:



If it is assumed that reactions (22), (23) and (24) describe the relevant chemical processes in the plume, NO_x ($= \text{NO} + \text{NO}_2$) will be conserved because NO_x does not take part in other chemical reactions in the first 10-25 km downwind of a stack (Buitjes et al., 1985). The distribution of the NO_x concentration in a stationary homogeneous turbulent layer with a continuous source can then be calculated with the ordinary Gaussian dispersion equation for an inert material.

Besides conversion and dispersion, also dry deposition of NO and NO_2 must be taken into account if the plume reaches the ground. It can be shown with the dry-deposition model of Horst (1982), however, that for tall stacks such as those of power stations dry deposition of NO and NO_2 is negligible upto about 50 km downwind from the stack (Buitjes et al. 1985). The formation of HNO_3 , as discussed by Richards (1983) and Russell et al. (1985), also plays a role in the processes of removal of NO_2 from the atmosphere. This process will not be very important during the daytime at relatively short distances from the source and is therefore neglected in this model.

Results of calculations with this reactive-plume model will be compared with results of calculations with other reactive-plume models which use the same database and are described in Chapters 5 and 6.

Description of the model

As mentioned above, the Gaussian plume model was used to describe the dispersion of the plume. The effect of concentration fluctuations on the oxidation rate of NO is neglected. Furthermore, it is assumed that chemical equilibrium in terms of mean concentrations exists everywhere. The rate constant of the reaction of NO with O_2 is so small that a significant contribution of this reaction to the formation of NO_2 can only be expected if high concentrations of NO (of the order of several ppms) are present. Because such high NO concentrations occur only at a very small distance ($x < 1 \text{ km}$) from the source, the reaction of NO with O_2 is neglected in this model (Buitjes et al., 1986; Janssen, 1986).

The concentration distribution of NO_x in a stationary, homogeneously turbulent mixed layer with a continuous source can then be calculated with the ordinary Gaussian dispersion equation:

$$c_{NO_x}(x,y,z,H) = \frac{Q e^{-\frac{(y/\sigma_y)^2}{2}}}{2\pi u \sigma_y \sigma_z} \left| \exp\left(-\frac{1}{2} \frac{H-z}{\sigma_z}\right)^2 + \exp\left(-\frac{1}{2} \frac{H+z}{\sigma_z}\right)^2 \right| \quad (25)$$

where Q is the source strength of NO_x calculated as NO_2 ($kg \cdot s^{-1}$), H is the effective stack height (m), U is the wind velocity at height H ($m \cdot s^{-1}$), and σ_y and σ_z are dispersion parameters that depend on stability.

The following definitions for nitrogen and oxidants were used:

$$[NO_x] = [NO] + [NO_2] \quad (26)$$

and

$$[O_x] = [NO_2] + [O_3] \quad (27)$$

Assuming that $[O_x]$ inside the plume is equal to $[O_x]$ outside the plume, this results in:

$$[O_x] = ([NO_2] + [O_3]) \text{ background} + p \cdot [NO_x] \quad (28)$$

where p is the fraction of NO_x emitted as NO_2 . A fraction of NO_2 in NO_x of 5% has been assumed in these calculations (cf. Mey et al., 1986).

It follows further from equating the reactions (22) and (24) that photostationary equilibrium exists locally between the (time-averaged) concentrations of NO, NO_2 and O_3 in the plume and can be defined by:

$$\Psi = \frac{k_1 \begin{bmatrix} NO \\ O_3 \end{bmatrix}}{k_3 \begin{bmatrix} NO_2 \end{bmatrix}} \quad (29)$$

The NO_x concentrations in the plume are calculated from equation (25). The NO, NO_2 and O_3 concentrations in the plume are then calculated with equations (26)-(29).

Measurements

The experimental methods used for the measurements are described in Chapter 3. The database used for the model calculations is given in Table 4. NO_2/NO_x ratios derived from measurements are averages of several plume crossings. The

Table 4
Emission and atmospheric data from daytime measuring flights.

| flight/ ride no. | date | unit | load (MWe) | fuel | flue gas volume (10 ⁻³ m ³ ·h ⁻¹) | NO _x (kg·h ⁻¹) | SO ₂ (kg·h ⁻¹) | stability class (Pasquill) | ozone (ppb) | wind speed at plume height (m·s ⁻¹) |
|------------------------|------------|---------------|---------------|------|---|--|--|----------------------------------|----------------|---|
| 1 | 1981-03-19 | Waalhaven 4 | 320 | oil | 720 | 325 | 1245 | D | 35 | 15 |
| 2 | 1982-03-18 | Flevo 1 | 150 | oil | 350 | 255 | 1200 | D | 50 | 10 |
| 3 | 1979-08-30 | Wilhelmshaven | 500-700 | coal | 1800-2500 | 1500-2000 | 1200-1700 | D | 40 | 10 |
| 4 | 1978-08-30 | Maasvlakte 1 | 450 | oil | 1100 | 615 | 1800 | D | 30 | 10 |
| 5 | 1975-11-04 | Maasvlakte 1 | 400 | gas | 1100 | 250 | | D | 35 | 5 |

NO_2/NO_x ratio of one crossing is calculated by dividing the NO_x and NO_2 concentrations integrated over their plume profiles.

Results and analysis

The NO_2/NO_x ratios were calculated on the basis of this reactive-plume model and with the database given in Table 4. The results of measurements and model calculations are presented in Figure 11.

It appears that NO_2/NO_x ratios calculated with this model are generally too high in comparison with the measurements. This can be explained for data from near the source by the different time-scales of the physical processes of dispersion and mixing and the chemical processes of molecular reactions. Equations (28) and (29) will be exact only if complete mixing takes place and if reactions (22) and (24) occur at an infinite rate or, stated differently: if the time-scales of the chemical reactions are much smaller than those for turbulent diffusion ($\tau_p/\tau_c > 1$). The chemical time-scales of reactions (22) and (24) were discussed in Chapter 2. It was shown that they are about five minutes for rapid conversion at the edge of the plume.

The time-scale for turbulent mixing can be estimated as (also see Chapter 2):

$$\tau_p \sim 0.7 t \quad (30)$$

It can be concluded on the basis of these estimates that, in the first five to ten minutes after emission (which means up to a distance of at least 3 km from the stack if the wind speed is about $10 \text{ m}\cdot\text{s}^{-1}$), the time-scales of the turbulences (τ_p) are of the same magnitude or even smaller than the chemical time-scales (τ_c). The condition $\tau_p/\tau_c > 1$ is therefore no longer valid and photostationary equilibrium will not exist in the plume. NO and O₃ will occur side by side in the plume because they have not had sufficient time to react. The NO_2 concentration in the real plume will be lower than the calculated value. As a consequence, the ratio Ψ will be > 1 . The NO_2/NO_x ratio or the oxidation rate, as calculated on the basis of photostationary equilibrium, will be too high.

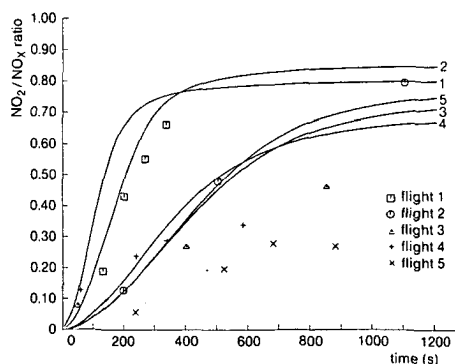


Fig. 11

NO_2/NO_x ratios measured and calculated by the first reactive-plume model by means of the database shown in Table 4.

Despite the fact that this model cannot predict the NO₂/NO_x ratios observed, it is very useful to calculate NO, NO₂ and O₃ concentration profiles for showing what happens in the NO plume.

Figure 12 shows the calculated NO, NO₂ and O₃ concentration profiles obtained at distances of 500 (A), 1000 (B), 2000 (C) and 5000 m (D) and (E) from the stack based on emission data from measuring flight 2. It appears that the plume was very narrow ($o_y \sim 50$ m) at a distance of 500 m. The NO concentration in the middle of the plume was high, ~ 400 ppb, which is much higher than the NO₂ concentration, which was about 80 ppb. The O₃ concentration in the centre of the plume was near zero (~ 2 ppb). Much NO₂ had already been formed at a distance of 1000 m. The NO concentration was higher only in the centre of the plume. The NO₂ plume was wider than the NO plume. The O₃ concentration in the plume was already more than 10 ppb.

At a distance of 2000 m, the plume width had increased to about 800 m ($o_y \sim 200$ m). O₃ had been mixed in and a large amount of NO was oxidized to NO₂. The NO₂ concentration in the plume was already more than double the NO concentration. The O₃ concentration in the plume calculated with this model was more than 20 ppb. At 5000 m from the stack, the plume width was about 2000 m (o_y is more than 400 m) and the plume was largely diluted with air. The NO₂ and NO concentrations were low: less than 10 ppb. O₃ concentrations calculated with this model are only slightly reduced in the plume and everywhere more than 40 ppb.

The NO, NO₂ and O₃ concentrations in the plume calculated with this reactive-plume model which applies time-averaged dispersion equations and assumes chemical equilibrium (model 1), can be compared with the NO, NO₂ and O₃ concentrations calculated with a model which is assumed to describe the dispersion of a momentary plume and in which the assumption of equilibrium is not needed (model 2). This second model is described in Chapter 6.

The results obtained with both models are compared with those of measurements (Fig. 12D-12E, Table 5). It can be concluded from this table that the NO and NO₂ concentrations as measured during one plume crossing in a momentary plume were much higher than the NO and NO₂ concentrations calculated on the basis of time-averaged dispersion equations (model 1). The O₃ concentrations in a momentary plume were much lower than the O₃ concentrations calculated by means of model 1. The NO, NO₂ and O₃ concentrations calculated with the momentary plume model (model 2) agree reasonably well with the values measured in the momentary plume.

At distances not too far from the stack (< 5 km), fast dispersion causes deviations from photostationary equilibrium. Measurements indicate that large deviations from photostationary equilibrium also occur at greater distances from the stack, although the chemical reactions can be assumed to be fast enough to create chemical equilibrium in the plume at distances larger than about 10 km. For larger distances from the source, model 1 assumes complete mixing of the plume containing NO and the ambient air containing O₃.

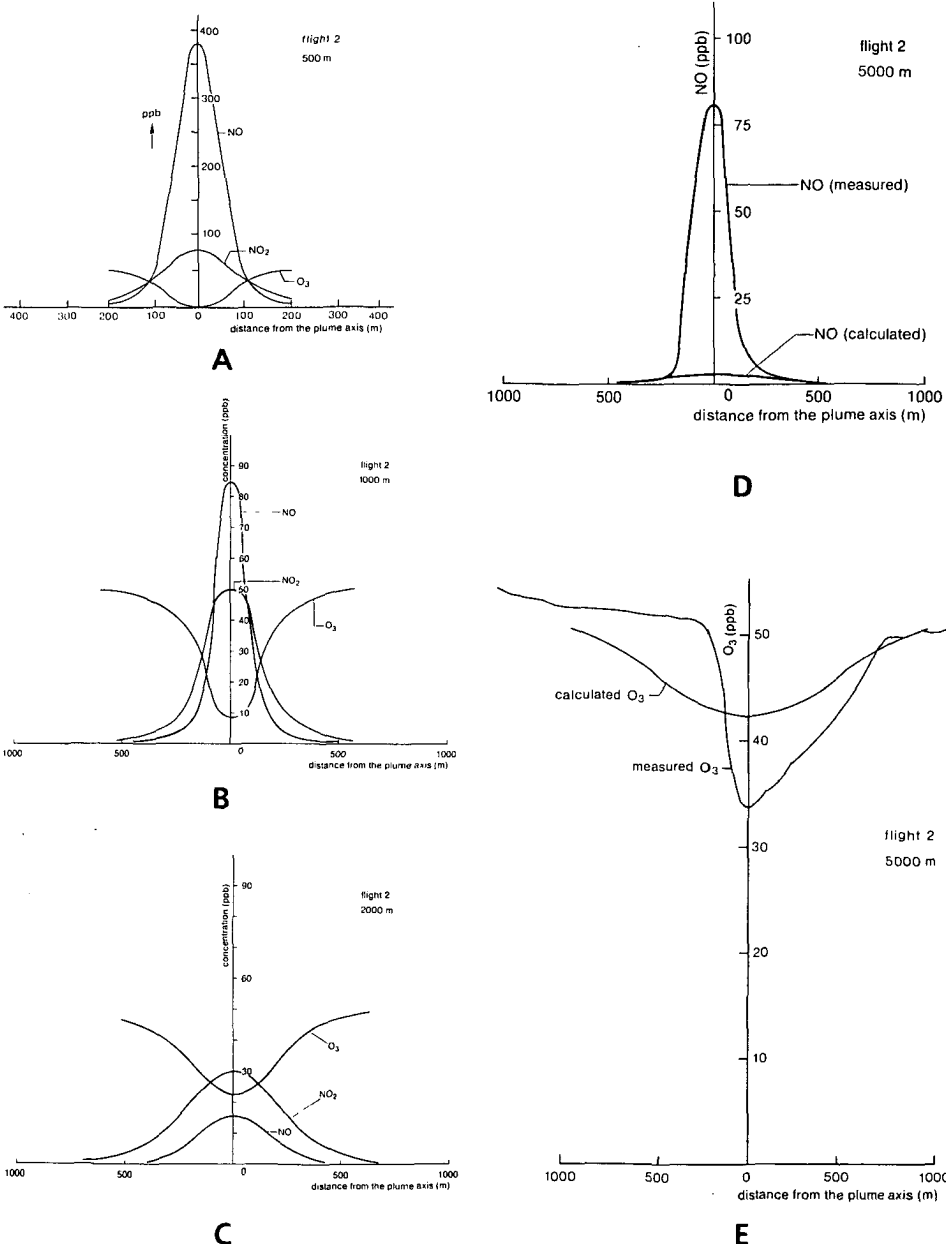


Fig. 12

Measured and calculated NO, NO₂ and O₃ concentration profiles for measuring flight 2.

A: distance 500 m from the stack.

B: distance 1000 m from the stack.

C: distance 2000 m from the stack.

D: NO profiles measured and calculated at a distance of 5000 m from the stack.

E: O₃ profiles measured and calculated at a distance of 5000 m from the stack.

Table 5

Calculated and measured concentrations (in ppb) of NO, NO₂ and O₃ in the centre of the plume.

| distance (m) | | 500 | 1000 | 2000 | 5000 |
|-----------------|-------------------------|-----|------|------|------|
| NO | calculated with model 1 | 400 | 85 | 15 | 2 |
| NO | calculated with model 2 | - | 440 | 300 | 50 |
| NO | measured | - | - | >200 | 80 |
| NO ₂ | calculated with model 1 | 80 | 50 | 30 | 8 |
| NO ₂ | calculated with model 2 | - | 35 | 45 | 40 |
| NO ₂ | measured | - | - | > 50 | 30 |
| O ₃ | calculated with model 1 | 2 | 7 | 22 | 42 |
| O ₃ | calculated with model 2 | - | 2 | 3 | 10 |
| O ₃ | measured | - | - | - | 30 |

Measurements indicate that this is not the case and that the plume remains inhomogeneously mixed, even at distances of more than 10 km, and consists of parcels of diluted flue gas separated by air parcels (Fig. 4). Although chemical equilibrium may exist in the plume parcels, it will not be recorded if plume parcels and ambient air are measured together.

The effect of inhomogeneous mixing on the oxidation rate of NO will be discussed in more detail in Chapter 6.

Chapter 5

Conversion processes of nitrogen oxides in the daytime and at night – measurements and modelling of reactions in the plumes of power plants –

Abstract

The oxidation of NO in power-plant plumes both during the daytime and at night was studied on the basis of aircraft measurements and modelling. NO in the plume mixes much faster with O₃ in the ambient air during the day than during the night. Dispersion is limited at night and the plume remains narrow. If the plume is located above the inversion layer at night, the O₃ concentrations that are needed for the oxidation reaction with NO can be rather high and NO₂ can therefore be formed. However, in this case the plume will not reach the ground and will not cause NO₂ concentrations at ground level. If, on the other hand, the plume is below the inversion in the mixing layer, O₃ concentrations will be low and oxidation of NO will therefore be slow and not much NO₂ will be formed in the mixing layer.

An electric field meter was installed in an aircraft to facilitate detection of the plume at night. This made remote detection of the plume possible.

Measurements carried out during the daytime are compared with the results from two reactive-plume models. In the first model, developed by Peters & Richards (1977), Gaussian dispersion of the plume and photostationary equilibrium are assumed. The second model is based on a numerical solution of the diffusion equation in which chemical reactions have been added. Intrusion of O₃ into the plume is taken into account in this model and photostationary equilibrium need not be assumed.

Results of measurements and model calculations indicate that, in the first phase of the dispersion of the plume, the dispersion process is faster than the chemical reactions. This causes deviations of photostationary equilibrium in the plume and the NO-oxidation rates calculated using the first model are too high. The chemical reactions at a somewhat larger distance from the stack are faster than dispersion and photochemical equilibrium can be established. Intrusion of O₃ into the plume must then be taken into account in modelling the

mixing process. This causes retardation of the formation of NO_2 . Results of calculations using the second model are in better agreement with field observations than those of the first model.

Because the first model requires the assumption of photostationary equilibrium, it cannot be applied to night-time conditions. The diffusion model is thus used to model night-time oxidation rates of NO in power-plant plumes. Measurements and model calculations are in good agreement. Calculations with the diffusion model regarding the formation of HNO_3 in power-plant plumes indicate that only little HNO_3 is formed, which is in agreement with the measurements.

Introduction

Little work has been done up to now on modelling night-time oxidation of NO in power-plant plumes. Peters & Richards (1977) and Forney & Giz (1980, 1981) proposed dispersion models which incorporate the reaction of NO with O_3 , assuming photochemical equilibrium in the plume. This means equilibrium between the production of NO_2 through the reaction of NO with O_3 , and the destruction of NO_2 by means of ultraviolet solar radiation. There is no photodissociation of NO_2 at night, so that equilibrium between NO, NO_2 and O_3 is absent. These models therefore cannot be applied. Moreover, models assuming photostationary equilibrium cannot incorporate side reactions for which no equilibrium conditions exist, such as the reaction of NO with O_2 .

Solving the diffusion equation after the addition of chemical reactions makes the assumption of chemical equilibrium superfluous and other chemical reactions can be introduced. Models describing the oxidation of NO on the basis of the diffusion equation were proposed by Llewelyn (1983) and Varey et al. (1984). Llewelyn (1983) solved the transport-diffusion equation by treating the oxidation of NO as a first-order reaction, which is incorrect (Buitjes, 1981). Varey et al. (1984) treated the oxidation reaction of NO correctly as a second-order reaction. These authors solved the equations for NO, NO_2 and O_3 simultaneously but assumed a constant diffusion coefficient. The diffusion equations for NO, NO_2 and O_3 are solved here simultaneously but the approach followed allows the along-wind diffusivity to vary according to Gaussian dispersion of the plume (Pasquill; 1974, Brubaker & Rote, 1978).

Firstly, results of calculations with the diffusion model will be compared with results obtained with the reactive-plume model described by Peters & Richards (1977). The results will also be compared with those from aircraft measurements carried out during the daytime (see also Janssen, 1986).

Secondly, the diffusion model is applied to the modelling of five measuring flights carried out at night near a 2000 MWe power station in The Netherlands. Carrying out night-time measuring flights successfully appeared to be rather difficult because of the very small dimensions of the plume and because it was not known whether the plume was located above or below the night-time

temperature inversion. A specially designed instrument had been installed in the aircraft to detect the plume remotely at night: an electric field (E-field) meter, the use of which was discussed in Chapter 3.

Chemical reactions of nitrogen oxides in the atmosphere

NO_2 is formed when a plume containing NO mixes on a molecular scale with ambient air containing O_3 :



where $k_1 = 29 \text{ ppm}^{-1} \cdot \text{min}^{-1}$ (Finlayson-Pitts & Pitts, 1986).

NO_2 is also formed by the reaction of NO with both O_2 in the ambient air (20%) and O_2 in the flue gases (5%), (Janssen, 1986):



where $k_2 = 1.45 \cdot 10^{-9} \text{ ppm}^{-2} \cdot \text{min}^{-1}$ (Finlayson-Pitts & Pitts, 1986).

Photodissociation of NO_2 by absorption of ultra-violet radiation during the daytime leads to the formation of NO and O_3 :



The value of k_3 depends on solar radiation and is between zero in the dark and 0.5 min^{-1} in full sunlight (Parrish et al., 1983). Russell et al. (1985) discussed oxidation reactions of NO_2 which may occur both during the daytime and at night.

Nitric acid (HNO_3) is produced by the following reaction, which is supposed to occur mainly during the daytime:



where $k_4 = 1.52 \cdot 10^4 \text{ ppm}^{-1} \cdot \text{min}^{-1}$.

Reactions involving the NO_3 radical, which are not operative during daylight hours due to photolytic breakdown of NO_3 , become important at night (Platt et al., 1984). This radical is formed as follows:



where k_5 is $0.05 \text{ ppm}^{-1} \cdot \text{min}^{-1}$.

This may be followed by two subsequent reactions (36) and (37):



where $k_6 = 2510 \text{ ppm}^{-1} \cdot \text{min}^{-1}$, followed by the homogeneous hydrolysis:



where $k_7 = 1.9 \cdot 10^{-6} \text{ ppm}^{-1} \cdot \text{min}^{-1}$.

Reactions (34)-(37) may lead to the disappearance of NO_2 from the plume and to production of nitric acid. However, the fast back reactions:



(where $k_8 = 29560 \text{ ppm}^{-1} \cdot \text{min}^{-1}$),



(where $k_9 = 2.9 \text{ ppm}^{-1} \cdot \text{min}^{-1}$) and



(where $k_{10} = 0.59 \text{ ppm}^{-1} \cdot \text{min}^{-1}$) will limit the production of nitric acid at night.

Other reactions include gas-phase reactions with hydrocarbons or heterogeneous reactions with aerosols. These reactions will not be discussed here.

Results and analysis

This section concerns the results obtained from measurements and modelling applied under various conditions.

Measurements

Five daytime measuring flights in the plumes of oil- and gas-fired Dutch power plants and one German coal-fired power plant, were selected from a database of

plume measurements (see Janssen et al., 1988). Emission data for the power plants and atmospheric conditions are given in Table 4. All flights were carried out in a neutral atmosphere (Pasquill D) but differed in wind speed and ozone concentration. The data from the same measuring flights were used by Janssen (1986) to test a box model which incorporated inhomogeneous mixing and is described in Chapter 6.

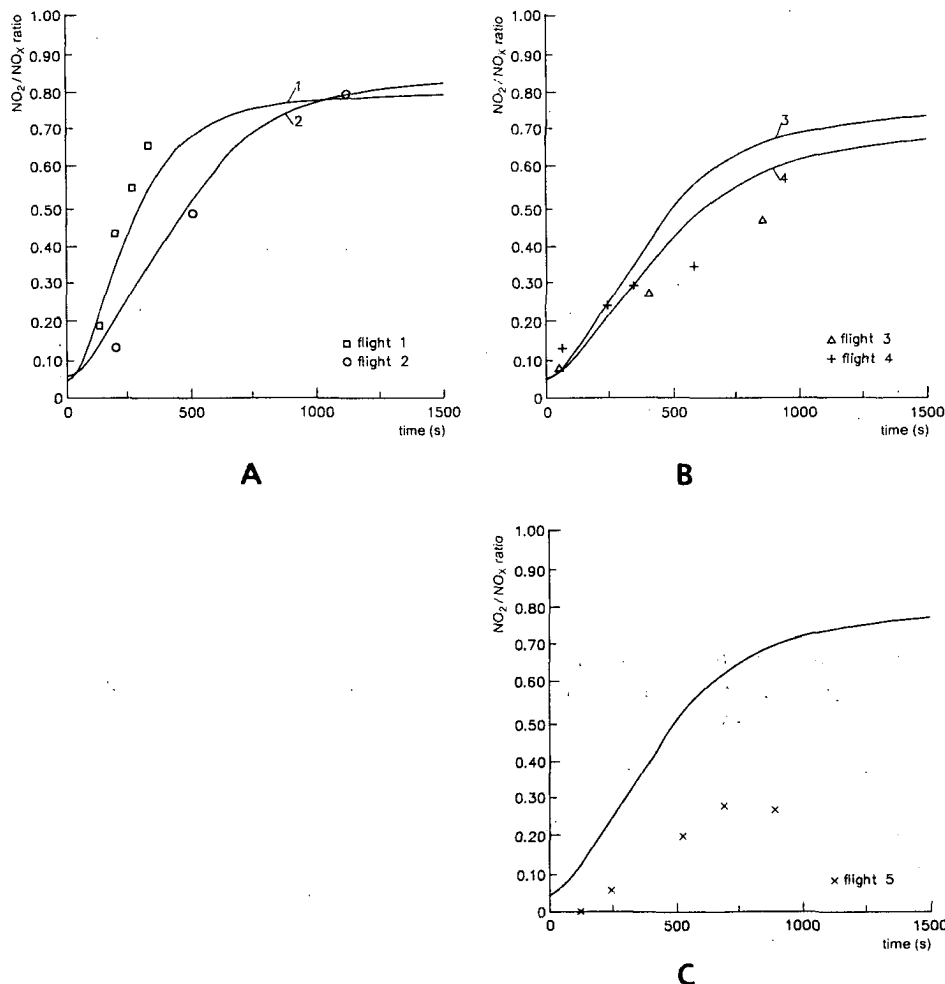


Fig. 13

NO-oxidation rates measured and calculated in the plumes of power plants during the daytime, using the diffusion model.

A: flights 1 and 2.

B: flights 3 and 4.

C: flight 5.

NO-oxidation rates, as measured during the flights, were calculated as NO₂/NO_x ratios as a function of distance from the source. These rates are shown in Figures 11 and 13 together with the modelling results.

Emission data and atmospheric conditions during the night-time flights are given in Table 6. During flight 6, the plume was below the strong temperature inversion ($\Delta T \sim 3.5$ K) in the ground layer. The ozone concentration in the ground layer was almost zero. During flights 7, 8 and 10, the plume had penetrated the temperature inversion and stayed in the transport layer where the ozone concentrations were relatively high compared with the ozone concentrations in the ground layer (Fig. 8). During flight 9, the plume was located near or at inversion height. Ozone concentrations at plume level were about 25 ppb: they varied between 0 ppb in the ground layer below the inversion and 50 ppb in the transport layer above the inversion.

The operators reported very stable atmospheric conditions during the flights at night. No turbulence was noticed at plume height, even for flights 6 and 9, which were wholly or partly carried out in the ground layer. Only the turbulence of the plume itself was noticeable at short distances from the stack. It was mentioned that turbulence increased considerably when the aircraft descended from the transport layer to the ground layer during flights 7 and 8.

NO-oxidation rates at night, as measured during the flights, are given as NO₂/NO_x ratios as a function of distance from the source and are shown in Figures 16A-16C, together with the modelling results.

Table 6a

Emission data from measuring flights at night. All flights were carried out in the plume of coal-fired unit Amer 8 of the Amer power station. The load during the flights was 625 MWe.

| flight no. | date | flue gas volume ($10^{-3} \cdot m_0^3 \cdot h^{-1}$) | NO _x emission (kg·h ⁻¹) | SO ₂ emission (kg·h ⁻¹) |
|------------|------------|---|---|---|
| 6 | 1986-02-12 | 2000 | 1750 | 2300 |
| 7 | 1986-05-02 | 2000 | 1750 | 1900 |
| 8 | 1986-11-20 | 1950 | 1750 | 3000 |
| 9 | 1986-12-04 | 2050 | 1890 | 3000 |
| 10 | 1986-12-10 | 2000 | 1750 | 3000 |

Table 6b

Atmospheric and plume data from measuring flights at night. Plume heights measured above temperature inversion (+) and below temperature inversion (—) are indicated in column 4.

| flight no. | plume height measured (m) | height of temperature inversion measured (m) | position of the plume | plume height calculated (KNMI, 1979) (m) | temperature at a height of 10 m (K) | ozone concentration at plume height (ppb) | wind speed (m·s ⁻¹) | stability class (Pasquill) |
|------------|---------------------------|--|-----------------------|--|-------------------------------------|---|---------------------------------|----------------------------|
| 6 | 275 | 330 | — | 575 | 271 | 1 | 4 | F |
| 7 | 300 | 270 | + | 510 | 290 | 70 | 4 | F |
| 8 | 600 | 250 | + | 552 | 277.5 | 35 | 3 | F |
| 9 | 400 | 400 | ± | 475 | 283 | 25 | 6 | F |
| 10 | 680 | 250 | + | 602 | 276.5 | 30 | 3 | F |

Modelling

The Gaussian plume model of Peters & Richards (1977), which describes chemical reactions and dispersion of a plume, is used in our model to describe dispersion. The chemical reactions considered are the oxidation of NO with O₃ (Eq. 22) and the photodissociation of NO₂ (Eq. 24). The assumption of chemical equilibrium between the reactants is essential to obtain a closed set of equations. The scalars NO_x and O_x are defined as:

$$[\text{NO}_x] = [\text{NO}] + [\text{NO}_2] \quad (41)$$

[NO_x] is inert in this definition and the NO_x concentration can be calculated by means of Gaussian dispersion equations. Moreover:

$$[\text{O}_x] = [\text{NO}_2] + [\text{O}_3] \quad (42)$$

It is assumed that [O_x] inside the plume is equal to [O_x] outside the plume. If chemical equilibrium is assumed, Equations (22) and (24) can be equated and the expression for photostationary equilibrium in the plume then becomes:

$$\Psi = \frac{k_1 \left[\text{NO} \right] \left[\text{O}_3 \right]}{k_3 \left[\text{NO}_2 \right]} = 1 \quad (43)$$

The NO, NO₂ and O₃ concentrations in the plume can be calculated using Equations (41)-(43) and Gaussian dispersion of NO_x. The results of measurements and model calculations for daytime conditions are shown in Figure 11. These results show that, for high wind speed and maximal oxidation of NO (flights 1 and 2), the calculated and the measured NO₂/NO_x ratios agree fairly well although the calculated NO₂/NO_x ratios are generally too high.

This model has three important limitations. In the first place, only the reaction of NO with O₃ (22) and the photodissociation reaction of NO₂ (24) can be taken into account. Secondly, it is assumed that O₃ is mixed instantaneously and homogeneously over the plume. The process of intrusion of O₃ from the ambient air into the plume is not modelled. In the third place, the assumption of photostationary equilibrium in the plume is essential in the model. For this reason the model of Peters & Richards (1977) cannot be applied in night-time situations when there is no photodissociation of NO₂ and therefore no chemical equilibrium between NO, NO₂ and O₃.

These limitations are avoided in a new model incorporating the diffusion equation, to which chemical reactions are added. This model is an extension of the work by Varey et al. (1984). Varey et al. (1984) described the dispersion of a radially symmetric plume in a Langrangian co-ordinate system. NO, NO₂ and

O_3 concentration in the plume can be calculated by solving the diffusion equations for NO, NO_2 and O_3 simultaneously. Varey et al. (1984) used a constant diffusion coefficient in their model and a Gaussian distribution of the concentration in the plume as a starting condition.

The equations for NO, NO_2 and O_3 in the diffusion model presented here will be solved in a way that allows the diffusion coefficient to vary as a function of distance from the source. The dispersion of the plume is described by means of a relation between the turbulent diffusion coefficient D and the often used empirical dispersion parameter σ (Brubaker & Rote, 1978). Block-shaped NO, NO_2 and O_3 concentration profiles corresponding to the diameter of the stack are taken as starting conditions. To reduce computer time in evaluating fast chemical reactions, such as the reaction of NO with O_3 , a radially symmetric plume is also assumed in the present model. The assumption of a radially symmetric plume need not be a serious limitation in the study of chemical reactions in the plume because the investigations are aimed primarily at concentrations and less at the shape of the plume.

The model was applied first to the same daytime measuring flights as used previously in the model of Peters & Richards to compare both results, and subsequently to the five night-time measuring flights.

The diffusion equations for NO, NO_2 and O_3 in the model presented here are:

$$\frac{\partial [NO_2]}{\partial t} = D_r(t) \left(\frac{\partial^2 [NO_2]}{\partial r^2} + \frac{1}{r} \frac{\partial [NO_2]}{\partial r} \right) + k_1 [NO] [O_3] + k_2 [NO]^2 [O_2] - k_3 [NO_2] \quad (44)$$

$$\frac{\partial [NO]}{\partial t} = D_r(t) \left(\frac{\partial^2 [NO]}{\partial r^2} + \frac{1}{r} \frac{\partial [NO]}{\partial r} \right) - k_1 [NO] [O_3] - k_2 [NO]^2 [O_2] + k_3 [NO_2] \quad (45)$$

$$\frac{\partial [O_3]}{\partial t} = D_r(t) \left(\frac{\partial^2 [O_3]}{\partial r^2} + \frac{1}{r} \frac{\partial [O_3]}{\partial r} \right) - k_1 [NO] [O_3] + k_3 [NO_2] \quad (46)$$

where $D_r(t)$ is a turbulent diffusion coefficient.

The solution of the diffusion equations (44)-(46) is a radially symmetric Gaussian plume. A dispersion parameter σ_r is therefore defined, its value being the goniometric average of the ordinary dispersion parameters σ_y and σ_z :

$$\sigma_r = (\sigma_y \sigma_z)^{\frac{1}{2}} \quad (47)$$

Because σ_y takes the form:

$$\sigma_y = a_y x (b_y) \quad (48)$$

and σ_z takes the form:

$$\sigma_z = a_z x (b_z) \quad (49)$$

where a and b are empirically derived coefficients (Pasquill, 1974; Singer & Smith, 1966), the relation for $\sigma_r = (\sigma_y \sigma_z)^{1/2}$ holds:

$$\sigma_r = a_r x (b_r) = (a_y \cdot a_z)^{1/2} x^{(b_y + b_z)^{1/2}} \quad (50)$$

The values for a_r and b_r used in the calculations are given in Table 7 for daytime and night-time measurements.

If the dispersion coefficients D_y and D_z are related to the eddy diffusivities by:

$$\sigma_y^2 = (2D_y x)/u \quad (51)$$

and

$$\sigma_z^2 = (2D_z x)/u \quad (52)$$

where x is the distance from the source and u the wind speed (Brubaker & Rote, 1978), the following relation for the diffusion coefficient $D_r(t)$ can be derived:

$$D_r(t) = u^{2b} b a^2 t^{2b-1} \quad (53)$$

where $x = ut$ and a and b for each flight are given in Table 7.

Table 7

Atmospheric stability and coefficients a_r and b_r of the dispersion parameter σ (Equation 50).

| flight no. | 1 | 2 | 4 | 4 | 5 | 6 | 7 | 8 | 9 | 10 |
|-----------------|------|------|------|------|------|------|------|------|------|------|
| stability class | D | D | D | D | D | F | F | F | F | F |
| a_r | 0.2 | 0.2 | 0.2 | 0.2 | 0.2 | 0.15 | 0.15 | 0.15 | 0.15 | 0.15 |
| b_r | 0.83 | 0.83 | 0.83 | 0.83 | 0.83 | 0.69 | 0.69 | 0.69 | 0.69 | 0.69 |

Equation (53) gives the time-dependent diffusion coefficient needed in the diffusion equations (44)-(46) that were solved simultaneously using an implicit finite difference method (Crank - Nicolson). This method is stable for each choice of Δt and Δr (Ames, 1965). However, this does not mean that each choice of Δt and Δr will yield accurate results. The time step (Δt) must be small (in the order of 0.01 s), especially near the stack, where dispersion is very fast ($\Delta r/\Delta t$ is large) and where very large concentration gradients of NO, NO₂ and O₃ exist.

The grid used to solve the diffusion equations had to be rather dense to describe the concentration gradients accurately, especially those near the stack. The number of grid points in the model needed to calculate the concentration profile of the plume was restricted to fifty in order not to use too much computer time. The number stayed the same during plume growth. The starting grid length was twice the stack diameter, i.e. 20 m and the distance between two grid points at $t=0$ was therefore 40 cm. To model plume growth, the grid was enlarged by increasing the distance between grid points as the width of the plume increased during dispersion in the atmosphere. The grid was enlarged by a factor of two when the concentrations at the edges of the grid became more than 1% of the concentrations at the plume axis.

NO₂, NO and O₃ block profiles, determined by the diameter of the stack, which was 10 m in all calculations, were assumed as starting conditions at $t=0$. The O₃ profile at $t=0$ is represented by a negative block, i.e. an ozone concentration of 0 ppb within the stack diameter and the O₃ background concentration as measured in the atmosphere outside the stack. NO and NO₂ concentrations within the stack diameter at $t=0$ in the model calculations correspond to the values measured during emission measurements by KEMA (Meij et al., 1986). The values found outside the stack proved to be negligible compared to the concentrations in the stack, i.e. 0 ppb.

Modelling daytime conditions

The computer program and its accuracy were tested by first solving the diffusion equation for SO₂, an inert gas. The results were compared with the exact analytical solution, i.e. the Gaussian plume model. Differences between the numerical results from the model and the exact analytical solution were 10% at most after about 100 s of plume travel. This accuracy was considered to be sufficient in view of the accuracy of the measurements which was somewhat less. Chemical reactions (22)-(24) were introduced next and calculations were carried out for the same daytime measuring flights (1-5) as used in the first model of Peters and Richards. The results from the diffusion model, together with the measured values, are shown in Figure 13. NO₂/NO_x ratios were calculated as averages over the plume width. If these results are compared with results obtained with the equilibrium model, it can be concluded that the NO-oxidation rate calculated with the diffusion model was lower than that calculated with the equilibrium model of Peters and Richards, especially for

flights 1 and 2, during which oxidation of NO was fast. This retardation was due to intrusion of O₃ into the plume. The results from the diffusion model agree with the measurements better than do results from the Peters and Richards model.

Figure 14 shows the NO₂/NO_x ratio as a function of distance from the plume axis for flight 1 after 25 s of plume travel, as calculated with the diffusion model. It shows that the NO₂/NO_x ratio is highest at the edges of the plume where the flue gases are in contact with background ozone. Ozone has to penetrate into the plume before the oxidation process starts.

Additional calculations were carried out with the diffusion model, in which the assumption of photostationary equilibrium is not needed, to investigate the assumption of photostationary equilibrium in the plume as used in the first model. Figure 15 shows that large deviations from photostationary equilibrium indeed occur in the first phase of plume dispersion at the edges of the plume, where the flue gas is in contact with intruding ambient air. These results are also in agreement with measurements and calculations carried out with a box model (Janssen, 1986).

These deviations from photostationary equilibrium arise because the process of dispersion and dilution is much faster in the first phase of plume dispersion than the chemical reaction rates and chemical equilibrium is therefore not established. (Janssen et al. 1987). On the basis of the diffusion model, photostationary equilibrium is reached after about 500 s of plume travel, which is also in accordance with previous calculations (Janssen, 1986). After this time has elapsed, i.e. in the second phase of plume dispersion, chemistry is faster than dispersion (Janssen & Elshout, 1987).

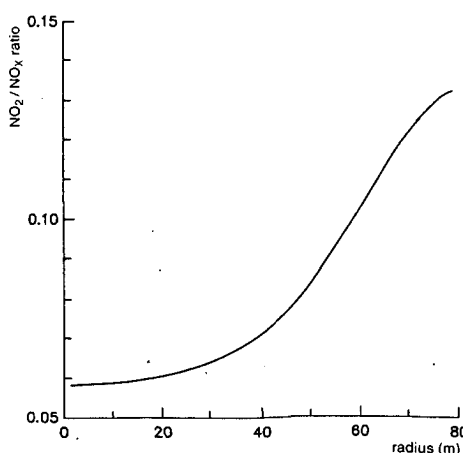


Fig. 14
The NO₂/NO_x ratio as a function of distance from the plume axis for flight 1 after 25 s of plume travel, as calculated with the diffusion model.

Modelling night-time conditions

There is no photostationary equilibrium at night because the photodissociation reaction of NO₂ (24) is absent. The model of Peters and Richards thus cannot be applied but the diffusion model can be used.

The results from the diffusion model were compared with those from five measuring flights in the plumes of the Amer power station near Geertruidenberg in The Netherlands. These results are shown in Figures 16A-16C. Measurements and model calculation generally agree fairly well.

The O₃ background concentrations to be used in the model depend on the measuring height and position of the plume with respect to the height of the temperature inversion (Table 6b). The O₃ concentration above the temperature inversion can be rather high (30-80 ppb) and can fall substantially (to about zero ppb) below the inversion (Fig. 8). During flight 6, the plume was entirely below the inversion in the nocturnal ground layer and O₃ concentrations were about 1 ppb. During flight 9, the plume was at about the same height as the inversion layer (400 m) and the O₃ concentrations at plume height were 25 ppb: between 50 ppb O₃ measured above the inversion and about zero ppb in the ground layer. During flights 7, 8 and 10, the plume was clearly above the inversion layer. The plumes stayed very narrow ($a_y \sim 200$ m at 30 km from the source) and O₃ became available for the oxidation reaction only very slowly. The NO-oxidation rate was therefore very low compared to that under daytime conditions. There was almost no oxidation of NO during flight 6 (plume in the ground layer) due to the very low O₃ concentration of about 1 ppb.

Richards (1983), Russell et al. (1985) and Platt et al. (1984) have discussed the night-time reactions of NO₂ involving the NO₃ radical, see Equations (35)-(40). HNO₃ may be formed after formation of NO₃ and N₂O₅ from homogeneous or heterogeneous reactions between N₂O₅ and H₂O. Platt (1984) even concluded that reactions at night involving the NO₃ radical could contribute more to the formation of HNO₃ than daytime processes involving the homogeneous OH

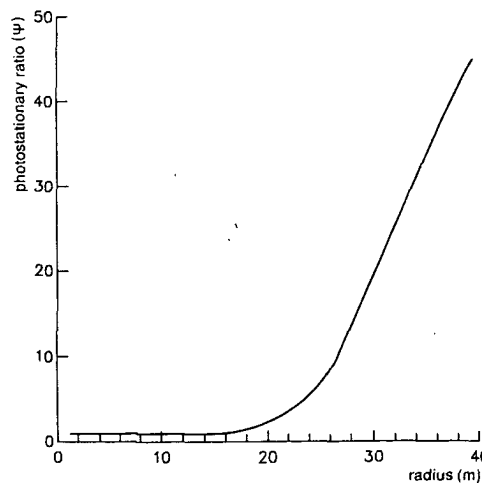


Fig. 15.
The photostationary ratio $\Psi = (k_1[NO] \cdot [O_3]) / (k_3[NO_2])$ as a function of distance from the plume axis for flight 1 after 10 s of plume travel, as calculated with the diffusion model.

radical reaction equation (34). The calculations for night-time conditions were therefore extended and the radical reaction (35) was incorporated in the diffusion model. Reactions (36) and (38) were so fast that including them in the model led to inaccuracies in the results calculated.

The maximal HNO₃ formation in the plume was calculated under the assumption that all NO₃ would lead to HNO₃ formation. When the diffusion model was used a maximal HNO₃ concentration of about 0.2 ppb HNO₃ was

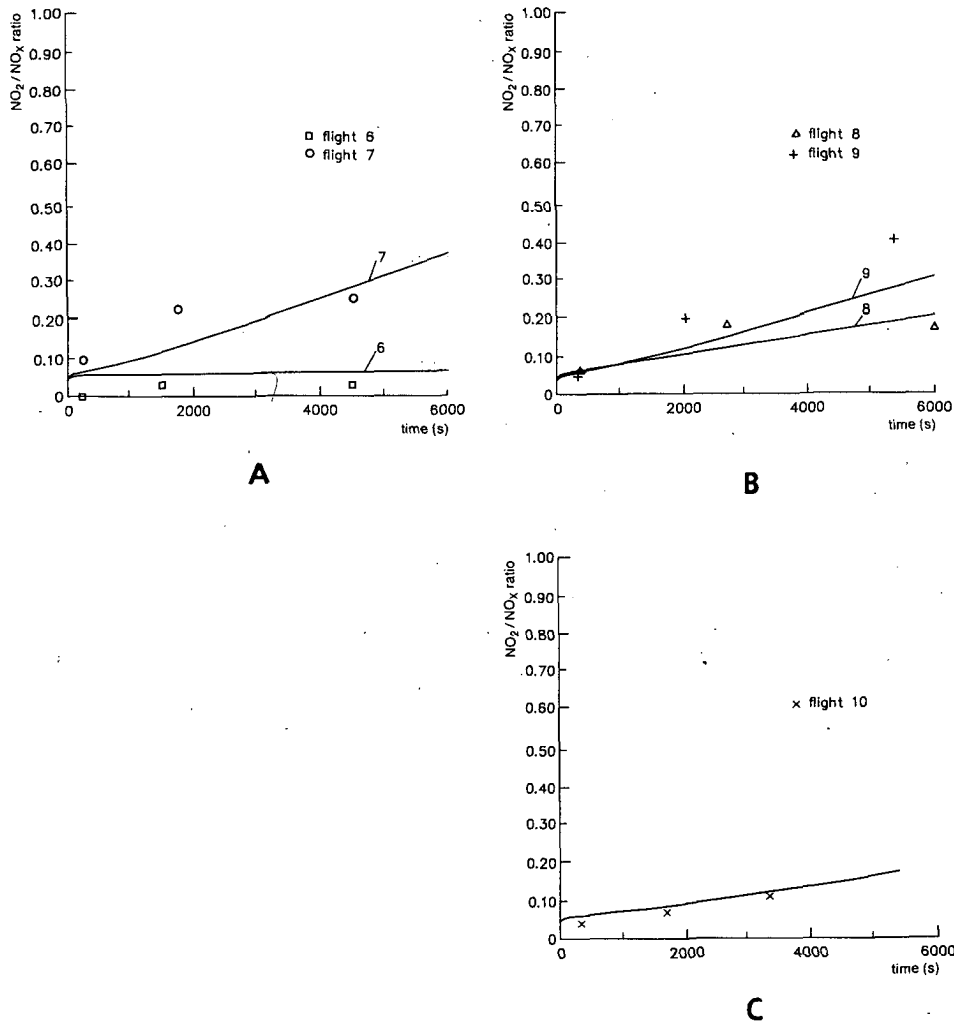


Fig. 16
NO-oxidation rates measured and calculated in the plumes of power plants at night, using the diffusion model.

A: flights 6 and 7.

B: flights 8 and 9.

C: flight 10.

calculated in the plume at a distance of 20 km from the source. Since it was questioned whether formation of HNO_3 could indeed take place in a power-plant plume, the aircraft was equipped with a filter packet to sample aerosols and nitric acid in the plume. SO_4 , NO_3 and HNO_3 concentrations of 0.4 ppb, 0.1 ppb and 0.4 ppb respectively were measured at 20 km from the stack. Another question to be answered was whether these components were emitted from the stack or were formed during transport of the plume in the atmosphere; this is currently under investigation.

Conclusions

Measurements of the oxidation rate of NO in the plumes of power plants showed that this conversion process differs for daytime and night-time conditions. During the daytime the plume is entirely in the mixing layer most of the time and reaches the ground at some distance from the stack. Ozone in the ground layer oxidizes NO in the plume, resulting in NO_2 concentrations at ground level. During the night, the plume is located either above the temperature inversion in the transport layer or below the temperature inversion in the nocturnal ground layer.

If the plume is in the transport layer, NO can be oxidized to NO_2 by O_3 in the transport layer but the plume will not reach the ground under these conditions so that there will be no NO_2 concentrations at ground level. If the plume is in the ground layer below the inversion it will reach the ground, resulting in NO ground level concentrations. However, because O_3 concentrations in the ground layer are very low at night, the oxidation rate of NO is very slow and little NO_2 will be formed in the ground layer. It could be concluded from the results of measuring flights in the plumes of power plants that, at night, power plants will not contribute greatly to NO_2 concentrations at ground level. This conclusion is based on a rather limited number of night-time measuring flights. The current measuring programme is therefore also aimed at increasing the number of measuring flights in power-plant plumes at night.

Carrying out successful measuring flights at night appeared to be rather difficult because of the small dimensions of the plume, which could be located either above or below the temperature inversion. An E-field meter installed in the aircraft and by which the plume could be detected remotely was very helpful.

The results of measuring flights during the daytime were compared with the results obtained from two reactive-plume models. The first model, described by Peters & Richards (1977), assumes photostationary equilibrium and instantaneous and homogeneous mixing of O_3 into the plume. Calculations with the diffusion model showed that large deviations from photostationary equilibrium occur in the plume near the stack and that the process of intrusion of O_3 into the plume causes retardation of formation of NO_2 , in agreement with the measurements. The results of calculations with the diffusion model agreed

fairly well with the results from five night-time measuring flights in the plumes of a large Dutch power station. Calculations of subsequent reactions of NO₂, e.g. the formation of HNO₃, made with the diffusion model, showed that only little HNO₃ can be formed in a power-plant plume. These results agree with KEMA measurements of HNO₃ in a power-plant plume at night. It is planned to carry out more measurements of sulphate, nitrate and nitric acid in power-plant plumes at night during the current measuring programme.

Chapter 6

Mixing of ambient air in a plume and its effects on the oxidation of NO

Abstract

NO_2 formation in the exhaust plumes of Dutch power plants was studied by both field measurement and modelling. It is argued that models that do not take inhomogeneous mixing into account cannot describe the results from measurements adequately since NO to NO_2 oxidation rates are determined by actual local concentrations. A simple way to introduce inhomogeneous mixing is described and incorporated in a simulation model roughly following that of Carmichael & Peters (1981).

Model calculations are applied to airborne and ground measurements which were carried out under widely varying atmospheric conditions. The results show that, at least at plume height (a few hundred metres), a significant part of the oxidation process occurs in an inhomogeneously mixed plume. NO_2/NO_x ratios are calculated. The contribution of oxygen to the oxidation of NO and the large deviations of photostationary equilibrium are analysed.

Deviations of photostationary equilibrium are explained by two factors: (1) the various time rates at which the physical processes of dispersion and mixing, and the chemical processes of molecular reactions in the atmosphere occur; (2) an extra contribution of ozone in unmixed ambient air parcels in the plume.

Introduction

Mixing of a plume is caused by turbulence in the atmosphere. Mixing takes time. So an inhomogeneous mixture exists as long as complete mixing is not achieved. This conditions the way in which conversion reactions continue. The reaction of NO with O_2 , for example, can contribute to the oxidation process only if, in the case of inhomogeneous mixing, locally high concentrations of NO are present.

The average concentration of gases which react slowly, e.g. SO_2 , can be calculated with the Gaussian plume model. The concentration of gases which

react rapidly, such as NO, however, is determined by conversion rates based on actual local concentrations. This was also discussed by Builijts (1981). Inhomogeneous mixing must therefore be taken into account in modelling. Model calculations are carried out here based on an adapted version of a model developed by Ghodsizadem (1978) and described by Carmichael & Peters (1981). The model is used as a diagnostic model, which means that - if the NO conversion processes measured can be described - it is assumed that the calculations also cover mixing processes occurring together with the conversion. This model has the advantage that the description of the mixing process is relatively simple compared with that from models developed by Peters et al. (1977), Kewley (1978), Melo (1978) and Shu et al. (1978). The advantage results that application of model calculations to oxidation rates measured in the atmosphere is facilitated.

The measurements were carried out in the plumes of Dutch power plants and one German power plant with an aircraft and a measuring van. Plume crossings were recorded within a few seconds. The plume image which then appeared was that of a momentary plume and only this type of image enables inhomogeneous mixing to be studied. It must, however, be kept in mind that measuring instruments that respond slowly observe an instantaneous plume in a distorted way, so that fast concentration fluctuations in the plume cannot be recorded. It will be shown that this distorts the measurement of the photo-stationary ratio in a plume mainly by influencing the O₃ concentration measured.

Model calculations and measurements show that, at least at plume height (some hundreds of metres), physical and chemical processes occur in an inhomogeneously mixed plume.

Representation of the plume

The image of the exhaust plume given by Carmichael & Peters (1981) is based on the mathematical formulation of the mixing process (Fig. 17A). This image is a formalised one which represents a time-averaged rather than a real or momentary plume.

A momentary plume model is needed to model NO-oxidation rates. It is assumed that the model presented in this chapter describes the mixing processes in a momentary plume. The flue gas, after emission from the stack, is considered to be broken up by turbulence into parcels. These parcels consist of undiluted exhaust-gas nuclei surrounded by plume parcels diluted with ambient air. If the dispersion of the plume continues, the mixed plume parcels increase at the expense of the unmixed ambient air which is found between the mixed plume parcels. A diagram of this plume model is given in Figure 17b. This representation agrees well with the findings from plume studies with photographic methods as carried out by Nappo (1984), and with daily visual observations.

Description of the model

Formation of NO_2 occurs when NO is emitted in an atmosphere that contains O_3 and O_2 . NO_2 is also formed by the reaction of NO with O_2 in the unmixed flue gases. Flue gases contain about 5% O_2 . Solar radiation causes the reduction of NO_2 to NO . The chemical reactions considered are:

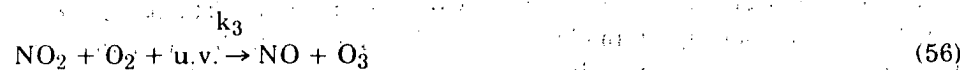


where $k_1 = 29 \text{ ppm}^{-1} \cdot \text{min}^{-1}$ (Becker & Schurath, 1975), and:



where $k_3 = 1.45 \cdot 10^{-9} \text{ ppm}^2 \cdot \text{min}^{-1}$ (Becker & Schurath, 1975).

Photodissociation of NO_2 by absorption of ultraviolet radiation leads during the daytime to the formation of NO and O_3 :



The value of k_3 depends on solar radiation and is between 0 in the dark and 0.4 min^{-1} in full sunlight (Becker & Schurath, 1975).

The mixing process in the model is described by two differential equations describing the decrease in volume of unmixed exhaust gases (f_u) and of unmixed

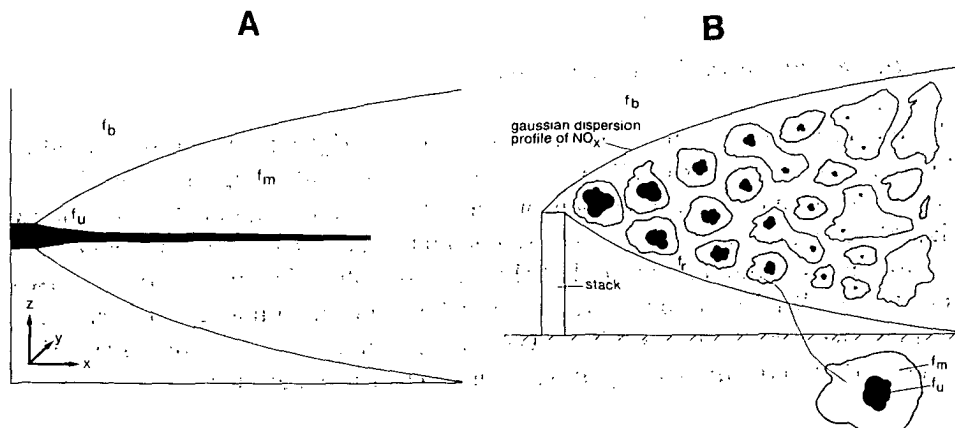


Fig. 17

Plume diagram

A: as used for model calculations by Carmichael & Peters (1981).

B: diagram of the momentary plume used to model NO-oxidation processes in an inhomogeneously mixed plume.

ambient air (f_b) during mixing in a fixed volume (mixing in a box), and by an equation describing the growth of the mixed volume (f_m).

The change in the fraction of 'unmixed flue gas' (f_u) is described by:

$$df_u/dt = -k_m f_u (1 - f_u) \quad (57)$$

The change in the fraction of 'unmixed ambient air' (f_b) is described by:

$$df_b/dt = -k_m f_b (1 - f_b) \quad (58)$$

in which k_m is a mixing parameter. The formulation of these mixing expressions was discussed by Ghodsizadem (1978) and Carmichael & Peters (1981).

The third mixing equation describing the growth of the mixed volume is:

$$f_u + f_b + f_m + f_r = 1 \quad (59)$$

In this model, the plume is not allowed to occupy the total mixing volume. After some time the value of f_m approximates the value $(1 - f_r)$ rather than 1. This value gives the fraction of total volume available for mixing. The parameter f_r determines the quantity of ambient air which is not available for mixing into the plume. This value is essential to model the rates at which NO is converted into NO_2 with the actual NO concentrations in the flue gas of power plants (some hundreds of ppm) as initial condition. These high NO concentrations will enhance the formation of NO_2 through the reaction of NO with O_2 . It will also be shown that, by using the fractions of unmixed ambient air f_b and f_r , the deviations of photostationary equilibrium measured in a plume can be explained.

Reaction equations in the exhaust plume

Chemical reactions in the 'unmixed plume' volume (f_u) are taken into account in this study. The reaction of NO with O_2 plays an especially important role in this part of the plume because no O_3 is present at the beginning but there are fairly high NO concentrations. It is also assumed for the description of the conversion process in the unmixed plume that the 'unmixed plume' volume only decreases and that no dilution occurs in the unmixed part of the plume (f_u). The changes in the concentration of NO, NO_2 , O_2 and O_3 formed by the photodissociation reaction (56) in the unmixed plume, are given by the equations:

$$d[\text{NO}]_u/dt = -k_1[\text{NO}]_u[\text{O}_3]_u - k_3[\text{NO}]_u^2[\text{O}_2]_u + k_3[\text{NO}_2]_u \quad (60)$$

$$d[\text{NO}_2]_u/dt = k_1[\text{NO}]_u[\text{O}_3]_u + k_3[\text{NO}]_u^2[\text{O}_2]_u - k_3[\text{NO}_2]_u \quad (61)$$

$$d[O_3]_u/dt = k_3[NO_2]_u - k_1[NO]_u[O_3]_u \quad (62)$$

$$d[O_2]_u/dt = -\frac{1}{2}k_2[NO]_u^2[O_2]_u \quad (63)$$

In these equations $[NO]_u$ is the initial concentration of NO which equals the NO concentration in the flue gas of the power plant. $[O_2]_u$ is the O_2 concentration in the exhaust gases of the power plant (5%).

The changes in concentration of NO, NO_2 and O_3 in the 'mixed plume' volume (f_m) are given by the equations:

$$\begin{aligned} d[NO]_m/dt = & - ([NO]_u/f_m) \cdot (df_u/dt) - ([NO]_m/f_m) \cdot (df_m/dt) + \\ & - k_1[NO]_m[O_3]_m - k_2[NO]_m^2[O_2]_m + k_3[NO_2]_m \end{aligned} \quad (64)$$

$$\begin{aligned} d[NO_2]_m/dt = & - ([NO_2]_u/f_m) \cdot (df_u/dt) - ([NO]_m/f_m) \cdot (df_m/dt) + \\ & + k_1[NO]_m[O_3]_m + k_2[NO]_m^2[O_2]_m - k_3[NO_2]_m \end{aligned} \quad (65)$$

$$\begin{aligned} d[O_3]_m/dt = & - ([O_3]_u/f_m) \cdot (df_u/dt) - ([O_3]_b/f_m) \cdot (df_b/dt) + \\ & - ([O_3]_m/f_m) \cdot (df_m/dt) - k_1[NO]_m[O_3]_m + k_3[NO_2]_m \end{aligned} \quad (66)$$

$$\begin{aligned} d[O_2]_m/dt = & - ([O_2]_u/f_m) \cdot (df_u/dt) - ([O_2]_b/f_m) \cdot (df_b/dt) + \\ & - ([O_2]_m/f_m) \cdot (df_m/dt) - \frac{1}{2}k_2[NO]_m^2[O_2]_m \end{aligned} \quad (67)$$

Equations (57)-(67) are solved by the numerical Euler forward method with step sizes of 0.001 s.

Results and analysis

This section concerns (1) the fitting procedure, (2) the atmospheric conditions, (3) deviations from photostationary equilibrium, (4) the width of the mixed plume, (5) the contribution of oxygen to the oxidation process, and (6) the measurements at ground level.

Fitting procedure

The model described is used to calculate the NO-oxidation rates for ten measuring flights and four measuring rides carried out by KEMA in the plumes of Dutch power plants and one German power plant (Elshout & Beilke, 1984). Emission data for the power plants are given, with the atmospheric conditions, in Table 8. The value for the photodissociation rate defined by k_3 was estimated from the atmospheric conditions and from the data of Becker et al. (1975). The

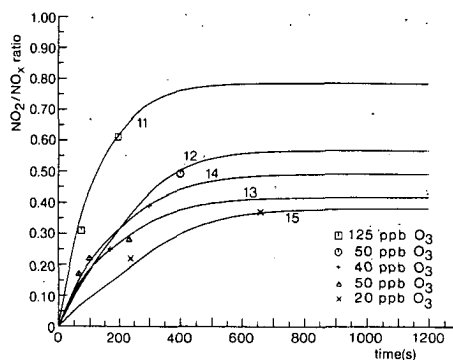
Table 8
Measuring conditions.

| <u>flight</u> | <u>date</u> | <u>unit</u> | <u>load</u> | <u>fuel</u> | <u>flue gas volume</u> ($10^{-3} \text{ m}_0^3 \cdot \text{h}^{-1}$) | <u>effective plume height</u> (m) | <u>NO_x</u> ($\text{kg} \cdot \text{h}^{-1}$) | <u>SO₂</u> ($\text{kg} \cdot \text{h}^{-1}$) | <u>stability class</u> (Pasquill) | <u>ozone</u> | <u>wind speed at plume height</u> ($\text{m} \cdot \text{s}^{-1}$) |
|---------------|-------------|---------------|-------------|-------------|---|--------------------------------------|--|--|--------------------------------------|--------------|---|
| <u>ride</u> | | | | | | | | | | | |
| 1 | 1981-03-19 | Waalhaven 4 | 320 | oil | 720 | 205 | 325 | 1245 | D | 35 | 15 |
| 2 | 1982-04-28 | Flevoland 1 | 150 | oil | 350 | 230 | 255 | 1200 | D | 50 | 10 |
| 3 | 1979-07-04 | Wilhelmshaven | 500 | coal | 1800-2500 | 515 | 1500-2000 | 1200-1700 | D | 40 | 10 |
| 4 | 1978-08-30 | Maasvlakte 1 | 450 | oil | 1100 | 335 | 615 | 1800 | D | 30 | 10 |
| 5 | 1975-11-04 | Maasvlakte 1 | 400 | gas | 1100 | 335 | 250 | D | 35 | 5 | |
| 6 | 1986-02-12 | Amer 8 | 625 | coal | 2000 | 575 | 1750 | 2300 | F | 1 | 4 |
| 7 | 1986-05-12 | Amer 8 | 625 | coal | 2000 | 510 | 1750 | 1900 | F | 70 | 4 |
| 8 | 1986-11-20 | Amer 8 | 625 | coal | 1950 | 552 | 1750 | 3000 | F | 35 | 3 |
| 9 | 1986-12-04 | Amer 8 | 625 | coal | 2050 | 475 | 1890 | 3000 | F | 25 | 6 |
| 10 | 1986-12-10 | Amer 8 | 625 | coal | 2000 | 602 | 1750 | 3000 | F | 30 | 3 |
| 11 | 1976-06-08 | Maasvlakte 1 | 500 | gas | 1150 | 365 | 400 | B | 125 | 8.5 | |
| 12 | 1980-04-23 | Flevoland 3 | 450 | oil | 1000 | 350 | 1000 | 3600 | C-D | 50 | 7.5 |
| 13 | 1976-08-17 | Maasvlakte 1 | 490 | gas | 1120 | 390 | 390 | B-C | 50 | 7.5 | |
| 14 | 1978-08-15 | Maasvlakte 2 | 500 | gas | 1150 | 285 | 400 | C | 40 | 15 | |
| 15 | 1978-11-29 | Maasvlakte 1 | 510 | gas | 1160 | 380 | 420 | B | 20 | 8 | |
| | | | | | | | | | | | |
| 1 | 1981-11-24 | Flevoland 3 | 450 | oil | 1000 | 235 | 1000 | 3600 | D | 26 | 17.5 |
| 2 | 1980-04-09 | Flevoland 3 | 450 | oil | 1000 | 250 | 1000 | 3600 | D | 40-45 | 15 |
| 3 | 1980-01-30 | Gelderland 11 | 123 | coal | 350 | 180 | 320 | 800 | D | 5-25 | 15 |
| 4 | 1981-04-22 | Flevoland 3 | 440 | oil | 1000 | 340 | 1000 | 3600 | D | 45 | 8 |

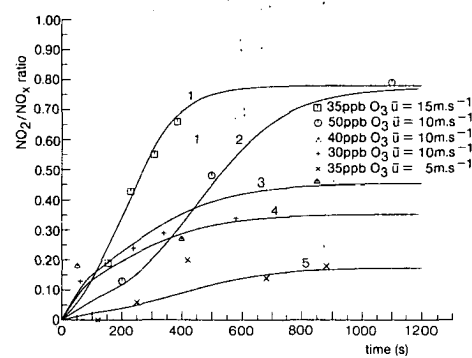
value of k_3 for Pasquill classes B and C was taken to be 0.3 min^{-1} . k_3 was estimated as 0.22 min^{-1} for a situation between Pasquill C and D and 0.15 min^{-1} for neutral conditions (Pasquill D).

The resulting parameters required for this model, the mixing rate parameter k_m and the volume fractions $f_u(t=0)$, $f_b(t=0)$, $f_m(t=0)$ and f_r , were chosen in such a way that the calculated NO_2/NO_x ratios would agree with the measured values. NO_2/NO_x ratios were calculated from Equations (64) and (65) as $[\text{NO}_2]_{\text{m}} / ([\text{NO}_2]_{\text{m}} + [\text{NO}]_{\text{m}})$.

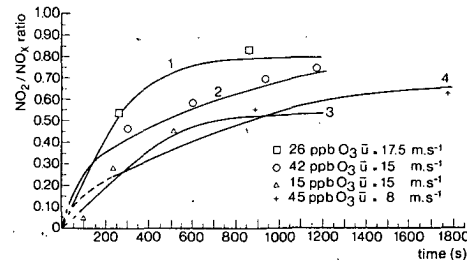
The results of the calculations are given in Figures 18a-c and in Table 9a. There is acceptable agreement of the measured and the calculated values with the values chosen here for the parameters. Table 9b shows the total quantities of NO and O₃ available for mixing in the plume.



A



B



C

Fig. 18

Measured and calculated oxidation rates in the plumes of Dutch power plants.

A: measured and calculated NO-oxidation rates in an unstable atmosphere (Pasquill B-C) at plume height.

B: measured and calculated NO-oxidation rates in a neutral atmosphere (Pasquill D) at plume height.

C: measured and calculated NO-oxidation rates in a neutral atmosphere (Pasquill D) at ground level.

Table 9a
Input parameters for model calculations.

| flight no. | [NO] _u (ppm) | [O ₃] _b (ppm) | k _m min ⁻¹ | k ₃ min ⁻¹ | f _u (t = 0) | f _b (t = 0) | f _m (t = 0) | f _r | L _{mix} |
|---------------|-------------------------|--------------------------------------|----------------------------------|----------------------------------|------------------------|------------------------|------------------------|----------------|------------------|
| flight | | | | | | | | | |
| 1 | 250 | 0.035 | 0.7 | 0.15 | 0.00008 | 0.962 | 0.01 | 0.028 | 0.45 |
| 2 | 350 | 0.050 | 0.4 | 0.15 | 0.00012 | 0.965 | 0.01 | 0.025 | 1.20 |
| 3 | 500 | 0.040 | 0.4 | 0.15 | 0.00012 | 0.78 | 0.05 | 0.17 | 2.8 |
| 4 | 300 | 0.030 | 0.4 | 0.15 | 0.00018 | 0.75 | 0.01 | 0.24 | 0.9 |
| 5 | 130 | 0.035 | 0.35 | 0.15 | 0.00013 | 0.92 | 0.04 | 0.04 | 0.8 |
| 11 | 170 | 0.125 | 0.6 | 0.3 | 0.00045 | 0.7 | 0.08 | 0.22 | |
| 12 | 450 | 0.050 | 0.55 | 0.22 | 0.00013 | 0.84 | 0.01 | 0.15 | |
| 13 | 170 | 0.050 | 0.3 | 0.3 | 0.00035 | 0.58 | 0.01 | 0.41 | |
| 14 | 170 | 0.040 | 0.5 | 0.3 | 0.00028 | 0.75 | 0.05 | 0.20 | |
| 15 | 150 | 0.020 | 0.6 | 0.3 | 0.00018 | 0.90 | 0.01 | 0.09 | |
| ride | | | | | | | | | |
| 1 | 450 | 0.026 | 0.30 | 0.15 | 0.00001 | 0.85 | 0.05 | 0.10 | |
| 2 | 450 | 0.042 | 0.10 | 0.15 | 0.00004 | 0.80 | 0.01 | 0.19 | |
| 3 | 450 | 0.017 | 0.45 | 0.15 | 0.00004 | 0.90 | 0.07 | 0.03 | |
| 4 | 450 | 0.045 | 0.15 | 0.15 | 0.00009 | 0.80 | 0.01 | 0.19 | |

Atmospheric conditions

The results of the model calculations show, on the average, a small difference between the values of k_m in presence of an unstable (Pasquill B-C) and a neutral atmosphere (Pasquill D). This difference is probably too small to be of any significance. The influence of ozone concentration and wind speed on the oxidation process is much clearer.

At the beginning of the oxidation process, there is only a minor concentration of O₃ compared with that of NO. The O₃ concentration therefore influences greatly both the initial rate of the oxidation process and the NO₂/NO_x ratio. Figures 18a and 18b show the relationship between ozone concentration and NO₂/NO_x ratio in situations with comparable wind speed.

This can be argued as follows:

Table 9b
Quantities of NO and O₃ present in the mixing volume.

| | [NO] _t = [NO] _u ·f _u (ppm) | [O ₃] _t = [O ₃] _b ·f _b (ppm) | [O ₃] _t /[NO] _t |
|---------------|--|--|---|
| <u>flight</u> | | | |
| 1 | 0.020 | 0.0337 | 1.685 |
| 2 | 0.042 | 0.0483 | 1.15 |
| 3 | 0.06 | 0.0312 | 0.52 |
| 4 | 0.054 | 0.0225 | 0.42 |
| 5 | 0.169 | 0.0332 | 0.19 |
| 11 | 0.0765 | 0.0875 | 1.14 |
| 12 | 0.0585 | 0.042 | 0.72 |
| 13 | 0.0595 | 0.029 | 0.49 |
| 14 | 0.0476 | 0.030 | 0.63 |
| 15 | 0.0306 | 0.018 | 0.58 |
| <u>ride</u> | | | |
| 1 | 0.0045 | 0.0221 | 4.9 |
| 2 | 0.0180 | 0.0336 | 1.9 |
| 3 | 0.018 | 0.0153 | 1.2 |
| 4 | 0.0405 | 0.036 | 0.9 |

$$\text{NO}_2/\text{NO}_x \sim \frac{[\text{NO}][\text{O}_3]}{[\text{NO}] + [\text{NO}_2]} \sim [\text{O}_3] \quad (68)$$

Figures 18b and 18c show the dependence of the oxidation rate on wind speed. The NO₂/NO_x ratio increases with increasing wind speed. The wind speed determines the quantity of ambient air which is blown into the plume and thereby the quantity of O₃ available for reaction (54). The values of k_m for flights 1-5 increase with increasing wind speed.

Deviation from photostationary equilibrium

Photostationary equilibrium is given by the equation:

$$\Psi = \frac{k_1 [NO] [O_3]}{k_3 [NO_2]} = 1 \quad (69)$$

The values of Ψ measured in the plume, however, are in general greater than 1 (Calvert, 1976; Hegg et al., 1976; White, 1977; Kewley et al., 1978). The photostationary ratio (Ψ) is therefore the preferred term. These deviations from photostationary equilibrium are generally related to inhomogeneous mixing of segregated packets of O_3 -rich and NO -rich air (Hegg et al., 1976).

Carmichael & Peters (1981) state that their results support this view, but their calculations assume homogeneous mixing in the mixed part (f_m) of the plume. The calculations of Ψ presented here, which are equivalent to the calculations of Ψ by Carmichael & Peters show, however, that the photostationary ratio deviates from 1 because the mixing rate - in this case determined by the mixing parameter k_m - is faster than the chemical reaction rates determined by k_1 , k_2 and k_3 . This is illustrated in Figure 19, where the values calculated for Ψ (without unmixed air) as $(k_1[NO]_m [O_3]_m)/(k_3[NO_2]_m)$ are shown as a function of distance from the source. The deviations from photostationary equilibrium are larger when mixing of the plume with ambient air, characterized by k_m , is faster. Examples of calculated values of Ψ without unmixed air for measuring flights 1 ($k_m = 0.7 \text{ min}^{-1}$) and 5 ($k_m = 0.35 \text{ min}^{-1}$) are shown in Figure 19. The calculated deviations from photostationary equilibrium may be caused in this case by the different time rates at which the physical processes of dispersion and mixing, and the chemical processes of molecular reactions proceed rather than by inhomogeneous mixing in the plume.

The model calculations of Ψ (without unmixed air) presented here show that photostationary equilibrium is approximated in the mixed plume parcels (f_m) at greater distances from the source ($> 6 \text{ km}$). However, the measured values of Ψ , which are plume averages, show much greater deviations from photostationary equilibrium than the calculated values. Because measured and calculated NO_2/NO_x ratios concur well, it is concluded that the differences between measured and calculated values of Ψ are caused by differences between measured and calculated O_3 concentrations in the plume. This can be explained as follows. The response time of the O_3 monitor is far too great to register the concentration fluctuations in the plume, especially when measurements are made at short distances from the source. The O_3 quantity in the parcels of unmixed air ($f_b + f_r$) and the O_3 quantity in the mixed plume (f_m) are therefore measured integratedly (Fig. 17b). This extra contribution of O_3 to the unmixed air will further enlarge the photostationary ratio Ψ .

This effect need not be taken into account when the measured NO and NO₂ concentrations in the background air ($f_b + f_r$) are considered because these are assumed to be negligible as compared with the concentrations in the plume (f_u and f_m). To test this hypothesis, supplementary calculations were carried out with a slightly altered model which takes unmixed air into account. The new O₃ concentration in the plume is then calculated with:

$$[O_3]_{cal} = [O_3]_m + [O_3]_b \cdot (f_b + f_r) \cdot L_{mix} \quad (70)$$

where $[O_3]_m$ is the calculated concentration in the mixed plume (Eq. 66), $[O_3]_b$ the O₃ background concentration and L_{mix} a mixing parameter which determines the quantity of unmixed ambient air in the plume.

The results of model calculations of the photostationary ratio given by $\Psi = (k_1[N\text{O}]_m[O_3]_{cal})/(k_3[N\text{O}_2]_m)$ are plotted in Figure 19 (calculated with unmixed air). This shows that large deviations from photostationary equilibrium can be explained by an extra contribution of unmixed ambient air. It is concluded, therefore, that deviations of photostationary equilibrium are caused by the different time rates at which physical and chemical processes occur and by an extra contribution of ozone in parcels of unmixed ambient air.

Representative traverse records which illustrate the influence of the response characteristics of the NO_x, SO₂ and O₃ monitors on the concentration profile observed are shown in Figures 20A and 20B together with the signal of the temperature sensor.

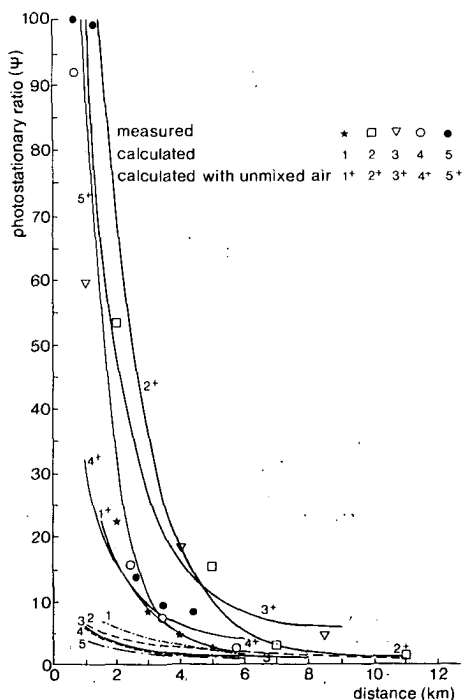


Fig. 19

Measured and calculated values of the photostationary ratio Ψ . Model calculations are presented with and without the contribution of unmixed ambient air.

Width of the mixed plume

Comparison of measurements with model calculations allows the average O₃ concentration in the plume to be divided into a contribution of O₃ in the mixed plume that also contains NO and NO₂, and a contribution of O₃ in the unmixed ambient air without NO and NO₂. Plume widths as measured by plume crossings can thus be interpreted in terms of a contribution of mixed plume (f_m) and unmixed ambient air ($f_b + f_r$) in the model calculations. Plume widths consisting of diluted exhaust gases only (f_m) can then be calculated from the equation:

$$W_{\text{cal}} = ([O_3]_b - [O_3]_{\text{meas}}) / ([O_3]_b - [O_3]_m) \cdot W_{\text{meas}} \quad (71)$$

where $[O_3]_m$ is calculated from Equation (66), $[O_3]_{\text{meas}}$ is the average O₃ concentration measured in the plume, $[O_3]_b$ is the O₃ background concentration, W_{cal} is the calculated part of the plume consisting of diluted exhaust gases

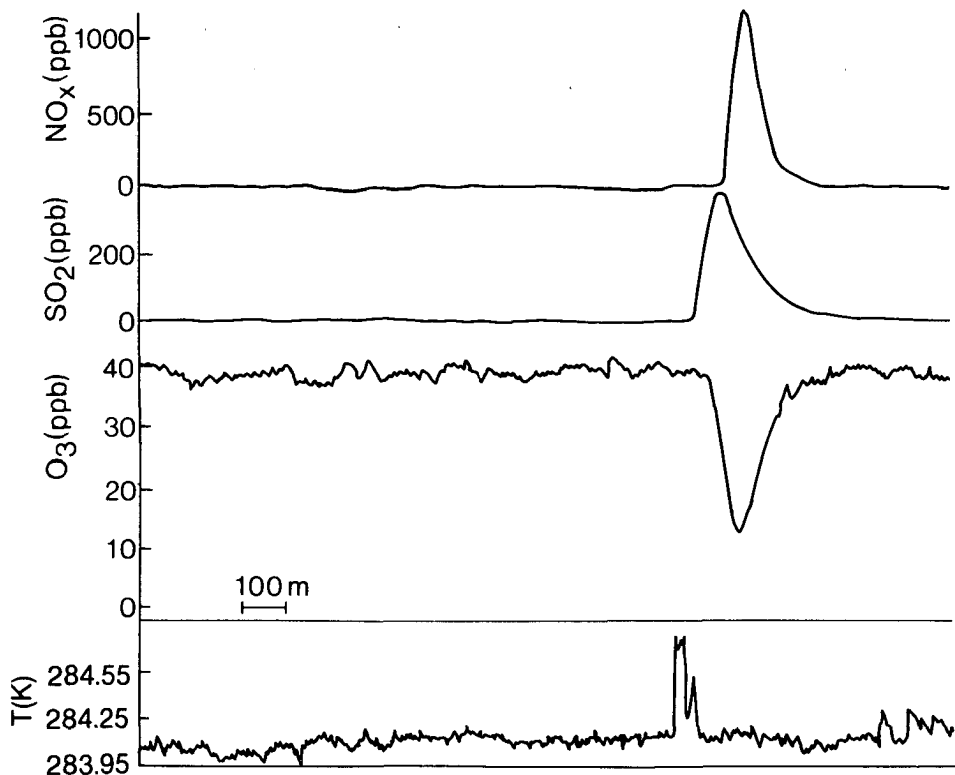


Fig. 20A

Characteristic traverse records for NO_x, SO₂, O₃ and temperature at a distance of 0.5 km from the source. The average value of Ψ in the plume was about 80. It can be seen from the signal of the relatively fast temperature sensor that there was more structure in the plume than the slower monitor signals revealed.

(f_m) only, and W_{meas} is the measured plume width consisting of diluted exhaust gases and unmixed ambient air ($f_m + f_b + f_r$).

Table 10 shows measured and 'corrected' plume widths together with measured and calculated values of O_3 for a few measuring flights. The calculated widths of the plume, given in Table 10, are not to be considered as directly measurable quantities. NO and O_3 have to be mixed on a molecular scale to form NO_2 . As can be seen from the $[O_3]_t/[NO]_t$ ratio in Table 9b, the quantity of O_3 which is introduced into the plume is insufficient for most flights to achieve complete oxidation of NO although the average O_3 concentration in the plume is high (see Table 10). It is therefore concluded that NO and O_3 are not mixed on a molecular scale and that the momentary plumes measured consist mainly of unmixed ambient air.

It is also clear that, when measured plume widths (W_{meas}) are transformed into corrected plume widths (W_{cal}) by means of Equation (71), the range of W_{cal} values obtained is much smaller than that of W_{meas} values. After transformation, very wide momentary plumes such as measured during flight number 2

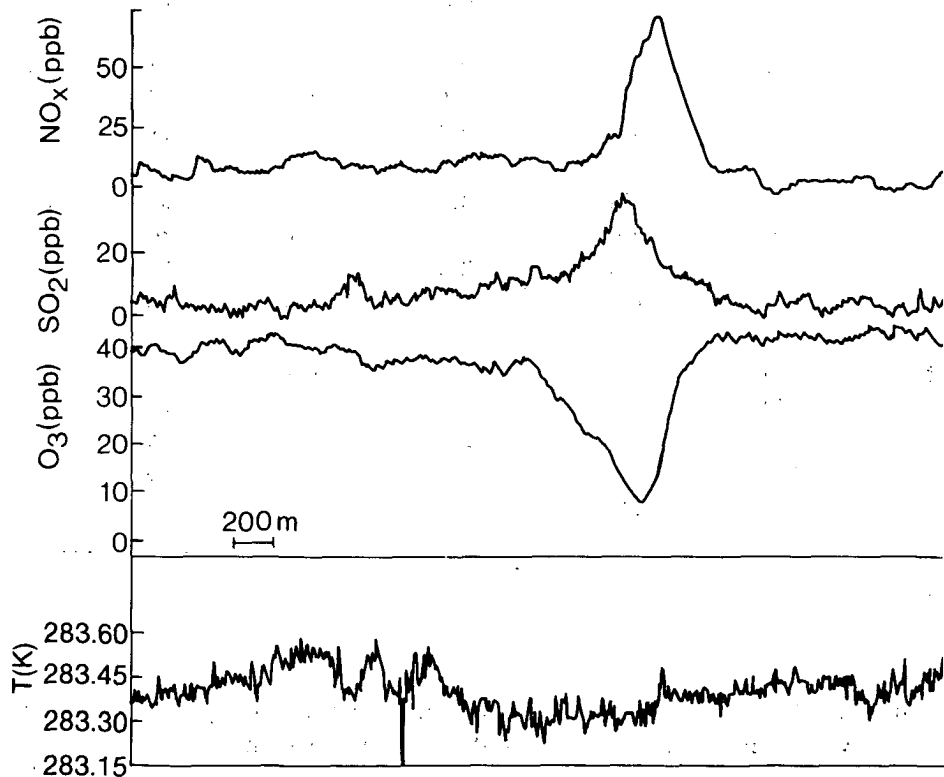


Fig. 20B

Characteristic traverse records for NO_x , SO_2 , O_3 and temperature at a distance of 8.5 km from the source. The average value of Ψ in the plume was about 5. No difference of temperature between the plume and the air was observed at this distance from the source.

Table 10
Measured and corrected plume widths (according to Eq. 71)

| flight no. | distance (m) | plume width measured (m) | plume width calculated (m) | [O ₃] _m (ppb) | [O ₃] _{meas} (ppb) | [O ₃] _b |
|------------|--------------|--------------------------|----------------------------|--------------------------------------|---|--------------------------------|
| 1 | 2000 | 600 | 65 | 7.3 | 32 | 35 |
| | 3000 | 760 | 213 | 10.0 | 28 | |
| | 4000 | 1140 | 256 | 12.7 | 30 | |
| | 5000 | 1720 | 426 | 14.8 | 30 | |
| 2 | 2000 | 595 | 63 | 2.8 | 45 | 50 |
| | 5000 | 1445 | 141 | 9.1 | 46 | |
| | 11000 | 8005 | 428 | 16.3 | 48 | |
| 3 | 500 | 580 | 183 | 2.0 | 28 | 40 |
| | 4000 | 1120 | 411 | 4.6 | 27 | |
| | 8500 | 1300 | 327 | 4.2 | 31 | |
| 4 | 650 | 470 | 82 | 7.2 | 26 | 30 |
| | 2400 | 360 | 139 | 4.1 | 20 | |
| | 3400 | 410 | 203 | 3.8 | 17 | |
| | 5750 | 925 | 244 | 3.5 | 23 | |
| 5 | 600 | 465 | - | 0.7 | 18 | 35 |
| | 1260 | 500 | 117 | 0.8 | 27 | |
| | 2600 | 870 | 434 | 0.9 | 18 | |
| | 3400 | 935 | 552 | 1.1 | 15 | |
| | 4400 | 1045 | 587 | 1.2 | 16 | |

(plume width > 8 km at 11 km distance from the source) appear to be comparable with other plume widths. The share of diluted exhaust gases in the total plume is roughly the same for most flights. An impression is thus obtained of the contribution of atmospheric turbulence to plume dispersion. The notion that the calculated plume widths, after transformation, are of the same order of magnitude is a necessary condition if the important influence of the O₃ background concentration on the oxidation rate is to be observed (see Fig. 18A-C).

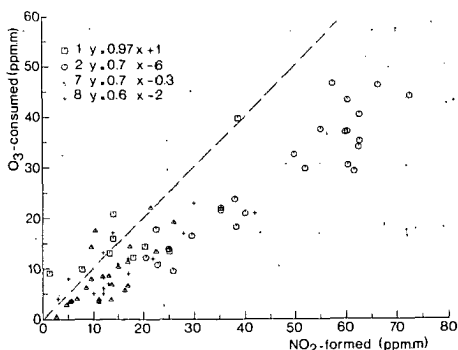


Fig. 21

Measured values of NO_2 formed and O_3 consumed for oxidation measurements at plume height. Deviations of the slope from 1 indicate a contribution of O_2 to the oxidation process.

Contribution of oxygen to the oxidation process

Figure 21 shows the NO_2 concentration integrated over the plume width ($\text{ppm}\cdot\text{m}$) and the integrated concentration of O_3 consumed ($\text{ppm}\cdot\text{m}$) by reaction (54) during daytime measuring flights. It appears that, for measuring flights, the quantity of NO_2 formed in these situations is always greater than that of O_3 consumed. It is assumed that this extra NO_2 is formed by the reaction with oxygen. The contribution of oxidation of NO by oxygen was discussed on the basis of measurements by Melo & Stevens (1977), Hov & Larssen (1984), Hegg and Hobbs (1985) and Richards (1985), and on the basis of model calculations by Varey et al. (1978). Lines through the data points were calculated for the separate flights using the least square method. It appears from Figure 21 that the slopes are between 0.6 and 0.97. These deviations from 1 indicate a contribution of oxygen of 3-40% to the formation of NO_2 .

Model calculations of the oxidation rates, for the same flights as shown in Figure 21, were done with Equations (60)-(67). This was done both with and without O_2 . The results of these calculations are shown in Figure 22. The calculated percentages of NO_2 formed in the oxidation reaction with oxygen are of the same order of magnitude as the measured values, although the calculated values are somewhat lower than the measured ones (compare Figs. 21 and 22).

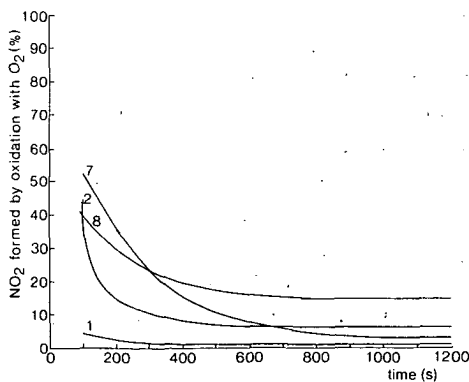


Fig. 22

Model calculations of NO_2 formed by the reaction with oxygen for the same measuring flights as in Figure 21.

The relationship between measured and calculated values for O₂ oxidation will be improved further if the NO₂ formed in the furnace (1-6%) is taken into account. The formation of NO₂ by O₂ originates almost completely from the reaction of NO with O₂ in the unmixed part of the plume. If mixing is very slow, there is a small contribution, ~ 1%, of O₂ oxidation in the mixed part of the plume.

These measurements and the model calculations confirm measurements by Hegg & Hobbs (1983, 1985) and also show that part of the NO₂ can be formed by O₂ in the atmosphere after emission of NO-containing flue gas from the stack.

The measurements show an approximately linear relation between NO₂ formed and O₃ consumed, even at a larger distance. This concurs well with the results of the model calculations, which also show a constant ratio between NO₂ formed by the reaction with O₂, and NO₂ formed by the reaction with O₃ at some distance from the source (Fig. 22). An important part of the oxidation process appears to occur at a relatively short distance (a few kilometres) from the source.

The concept of a plume divided into parcels of unmixed plume (f_u), mixed plume (f_m) and unmixed air ($f_b + f_r$), which is used to explain the measured large deviations from photostationary equilibrium, concurs well with the appearance of a locally high concentration of NO in unmixed plume nuclei (f_u).

Measurements at ground level

The course of the NO₂/NO_x ratio was also traced using a measuring van. It is interesting to compare measurements made on the ground with those at plume height because they give a different picture of the mixing process. Figure 18c shows the results of measurements and model calculations and Table 9a gives the parameter values of the fitted curves. It can be deduced from the [O₃]_t/[NO]_t ratio (Table 9b) that, compared with the results of measurements at plume height, more ambient air is usually mixed into the plume at ground level.

Oxidation of NO is therefore more advanced. It should be noted that mobile plume measurements at ground level are generally carried out at greater distances from the source than those during plume flights because the plumes originating from the relevant high point sources ($h > 150$ m) reach ground level under normal atmospheric conditions only at a much greater distance from the source. It must be added that the concentration profiles measured can easily be attributed to the power-plant plumes under investigation because the power plant is the only emission source of SO₂ in the neighbourhood. The conclusion that the plume is more diluted at ground level is also supported by the curve for the photostationary ratio (Fig. 23) and by the curve of the average SO₂ concentrations as a function of distance from the source (Fig. 24). As a consequence, it appears that formation of NO₂ by the reaction of NO with O₂ plays almost no part in the oxidation process for plume parcels which reach ground level, as shown in Figure 25.

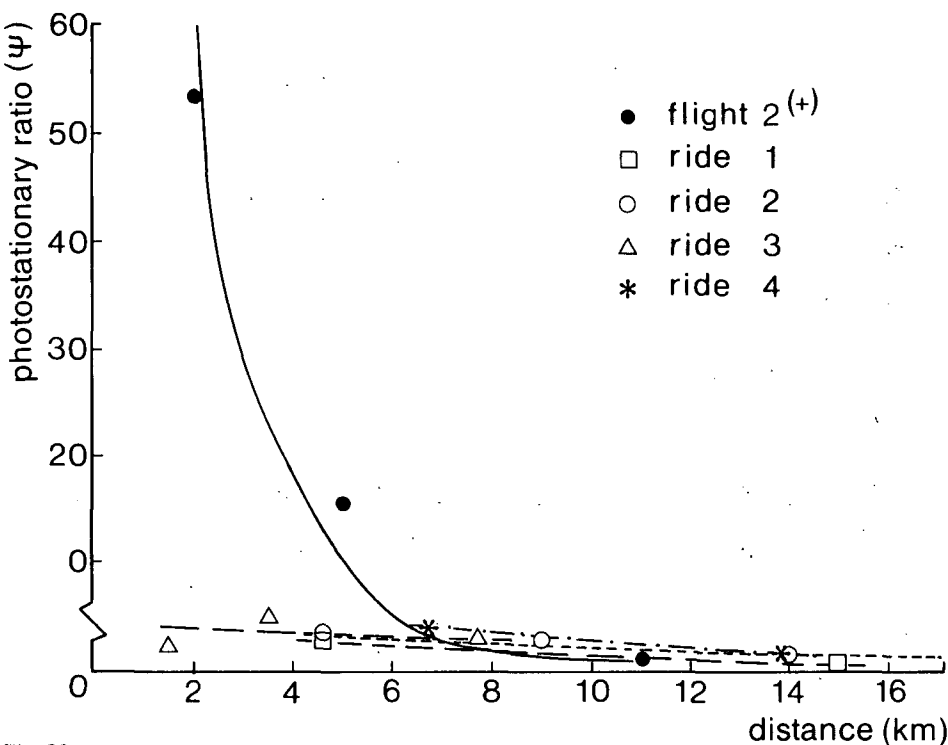


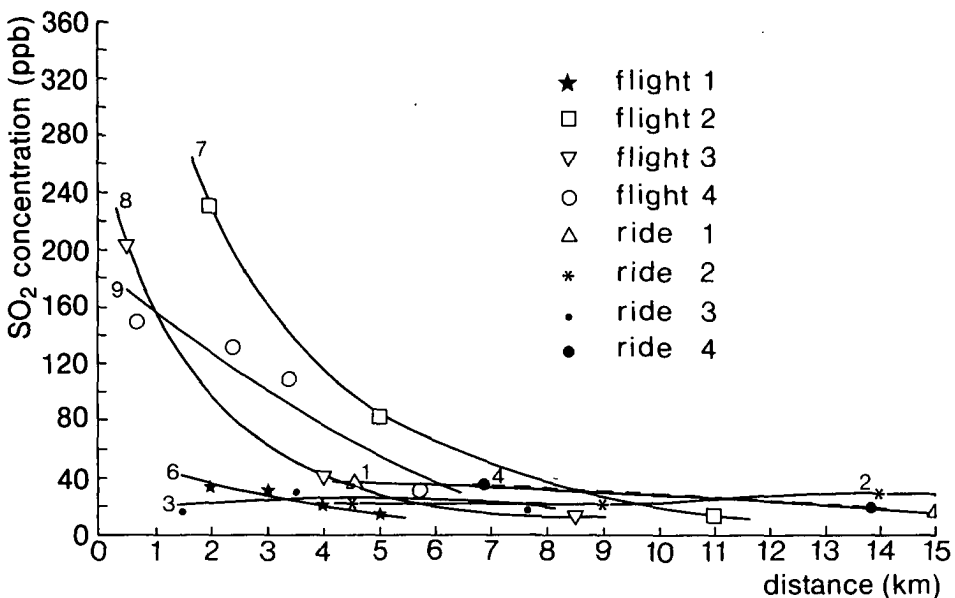
Fig. 23

Values of the photostationary ratio Ψ in the plume as measured at ground level. The curve of the photostationary ratio Ψ for measuring flight 7 was also drawn for comparison with measurements at plume height.

Conclusions

Measurements and model calculations were carried out in order to study oxidation processes of NO to NO_2 in the plumes of Dutch power plants and one German power plant. The rate of oxidation depends on atmospheric conditions such as ozone background concentration, solar radiation, wind speed and the interaction of physical and chemical reaction rates.

Application of the model described proved to be useful to unravel and quantify the varying contributions of the physical and chemical processes. The contribution of unmixed ambient air in a plume could be calculated by fitting calculated oxidation rates to measured ones and by using deviations of photostationary equilibrium. The results show that a plume at some distance from the source consists largely of unmixed ambient air. At plume height, the oxidation reaction of NO with O_2 must also be taken into account, as is shown by measurements and model calculations. The oxidation reactions appear to take place in an inhomogeneously mixed plume. A plume at ground level can be



considered to be diluted, well mixed and homogeneous. When a plume has reached such a state, O₂ oxidation no longer needs be taken into account.

Because measuring instruments which respond slowly cannot give a detailed view of an inhomogeneously mixed plume, fast monitoring instruments are needed to study the real momentary state of such a plume.

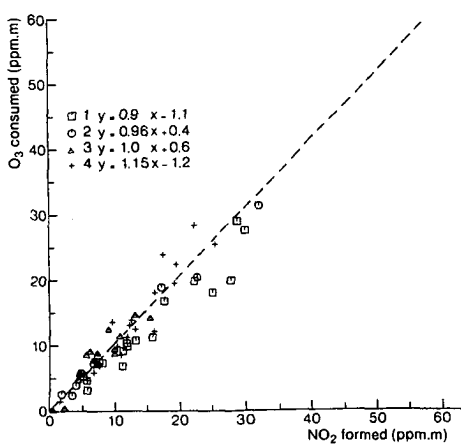


Fig. 25
Measured values of NO₂ formed and O₃ consumed for oxidation measurements at ground level.

Chapter 7

A classification of NO-oxidation rates in power-plant plumes based on atmospheric conditions

Abstract

The NO_2/NO_x ratio has been measured as a function of distance from the source in the plumes of Dutch power plants over a period of ten years (1975-1985). A large database was built up in this period, consisting of results from sixty measuring flights carried out under widely varying atmospheric conditions.

It is proposed that the total (cross-wind integrated) NO-oxidation rate in power-plant plumes can be described approximately by the phenomenological relation $\text{NO}_2/\text{NO}_x = A \cdot [1 - \exp(-ax)]$, x being the distance from the source. The database is used to classify the numerical values for A and a according to atmospheric conditions. Ozone concentration, wind speed and season of the year are the most important parameters for determining A and a . This classification can serve as a first approximation in the development of more accurate analytical models.

Variations in the NO_2/NO_x ratios measured are explained by natural variations of the ozone background concentration and the NO_2 photodissociation rate. The practical application of the classification is illustrated by calculation of the NO_2 ground-level concentrations for various atmospheric conditions, using Gaussian dispersion equations.

Introduction

The chemical and physical kinetics that determine the NO-oxidation rate in the atmosphere depend on meteorological conditions such as wind speed and solar radiation and on the concentration of the reactants. The interaction between chemical and physical kinetics has been discussed by Donaldson & Hilst (1972), Hegg et al. (1976), Elshout & Beilke (1984) and Janssen (1986).

Vermeulen (1983) made an inventory of well documented measurements published for NO conversion in stack plumes. These data were used to develop

and evaluate a reactive-plume model by Builtjes et al. (1985, 1986). Elaborate measurements of NO oxidation were carried out by Melo & Stevens (1981), Richards et al. (1981), Hegg & Hobbs (1983) and Elshout & Beilke (1984). These measurements were carried out as measuring campaigns and were related only to a limited number of meteorological conditions.

The classification of NO-oxidation rates presented in this chapter is based on a large database of NO and NO₂ concentration measurements in the plumes of power plants. The measurements were carried out under widely varying atmospheric conditions during winter, spring, summer and autumn. This classification can be used both to calculate NO₂ ground-level concentrations and as a guide for developing more accurate reactive-plume models.

Results and analysis

Three aspects are discussed in this section: (1) the NO₂/NO_x ratio as a function of distance from the source, (2) the selection of atmospheric parameters and (3) the classification of NO-oxidation rates.

The NO₂/NO_x ratio as a function of distance from the source

An important pathway for formation of NO₂ in the atmosphere is the second-order reaction of NO with O₃. This reaction in a homogeneous mixture can be written as:



It follows from the equation:



and the wind speed u:

$$u = dx/dt \quad (74)$$

that, if a constant ozone concentration is assumed, the NO₂/NO_x ratio becomes:

$$NO_2/NO_x = A(1 - e^{-\alpha x}) \quad (75)$$

and:

$$\alpha = (k_1[O_3])/u \quad (76)$$

Laboratory determination of the reaction rate constant k₁ gave a value of 29 ppm⁻¹·min⁻¹ (Becker & Schurath, 1975).

If this value for k_1 is substituted, with a wind speed of $0.01 \text{ km} \cdot \text{s}^{-1}$ and an ozone concentration of 35 ppb, a value of 1.7 km^{-1} is found for a . This value is not realistic since, in contrast to laboratory conditions, the plume is an inhomogeneous mixture of NO and O₃. The simplified scheme leading to Equation (75) implies a spatially constant ozone concentration (a flat profile) which can exist only if the 'replacement' of reacting O₃ through transport processes proceeds at a much faster rate than the chemical reaction. For the problem under consideration the time scales of the mixing and dispersion processes at some distance from the stack are greater than the chemistry time scales (Hegg et al., 1976). Therefore, Equation (75) must be regarded as a first approximation to handle NO-oxidation processes in the atmosphere.

Photodissociation of NO₂, in addition to the reaction of NO with ozone, influences the NO₂/NO_x ratio during the day:

$$\frac{d[NO_2]}{dt} = -k_3[NO_2] \quad (77)$$

The photodissociation rate k_3 depends on the intensity of solar radiation and lies between 0 in the dark and 0.55 min^{-1} in full sunlight (Parrish et al., 1983).

It was deduced from measurements of NO-oxidations rates in power-plant plumes reported by Janssen (1986) that photostationary equilibrium exists in the plume, during the daytime and at a larger distance from the source ($> 10 \text{ km}$), as determined by equating (72) and (77) according to:

$$\lim_{x \rightarrow \infty} \Psi = \frac{k_1 [NO][O_3]}{k_3 [NO_2]} = 1 \quad (78)$$

The constant A in Equation (75) can then be obtained by means of expressions (72), (73), (77) and (78). Equation (79) applies for the relation between NO and NO₂:

$$\lim_{x \rightarrow \infty} [NO] = \frac{k_3 [NO_2]}{k_1 [O_3]} \quad (79)$$

Using (73), (75) and (79), the following expression for A is found:

$$A = \left(\frac{k_3}{k_1 [O_3]} + 1 \right)^{-1} \quad (80)$$

After substitution in Equation (75), the description of NO₂ formation in the atmosphere is given by the equation:

$$\text{NO}_2/\text{NO}_x = \left(\frac{k_3}{k_1 [O_3]} + 1 \right)^{-1} \left(1 - e^{-ax} \right) \quad (81)$$

Formation of NO_2 takes place during mixing of a smoke plume with its surrounding air. Hegg et al. (1976) and Janssen (1986) discussed the NO_x -oxidation process in an inhomogeneously mixed plume in the atmosphere. It turns out that relations (72) and (75) are not exactly valid and that the value for a in expressions (76) and (81) cannot be derived directly from the ozone concentration and wind speed. Equation (81) should therefore be regarded as a phenomenological way to describe NO_2 formation in a plume. Values for a under varying meteorological conditions in different seasons are obtained from measurements of NO_2/NO_x ratios as a function of distance from the source. The value for A can be calculated using Equation (80), the value for the photodissociation rate k_3 , and the ozone concentration in the background air.

The power plants under investigation had an installed capacity between 500 and 1500 MWe and used oil, gas or coal as fuel. Variations in NO concentrations in the flue gases are due to the differences in fuels and to variations in load. The NO concentrations for these types of installations range from 150 to 450 ppm. The NO_2/NO_x ratio, however, is independent of this source of noise. The results show that Equation (81) can provide a fair description of the oxidation process.

Selection of atmospheric parameters

The value for the photodissociation rate, k_3 , must be known if Equation (81) is to be used. An estimate of this value can be obtained from concentration measurements of background NO, NO_2 and O_3 during the plume flights, assuming photostationary equilibrium in the background air (Van Egmond & Kesseboom, 1985). Application of Equation (78) makes it possible to calculate a value for k_3 :

$$k_3 = \frac{k_1 [NO] [O_3]}{[NO_2]} \quad (82)$$

Both the plume measurements and the background concentration measurements were carried out in the middle of the day, from about 11h00 to 16h00. The values for k_3 will therefore not differ greatly with variations of the solar angle (Parrish et al., 1983). The results of the background concentration measurements, solar radiation data and the calculated k_3 values are presented in Table 11. The values of k_3 were calculated for typical midday meteorological condi-

tions in The Netherlands, namely 0.15 min^{-1} , 0.25 min^{-1} and 0.35 min^{-1} in winter, spring/autumn and summer respectively.

It appears from previous research (Janssen, 1986) that ozone concentration and wind speed are important parameters in determining the NO-oxidation rate. A classification of NO-oxidation rates is therefore presented for each season - winter, spring/autumn and summer - with ozone concentration and wind speed as parameters.

The classification of NO-oxidation rates

The values for A and α were classified on the basis of the numerous measurements according to atmospheric conditions, i.e. season of the year, ozone background concentration and wind speed. This classification of A and α is presented in Figures 26, 27 and 28. The choice of class boundaries will be discussed in the next section.

Values were calculated for A from the average ozone concentrations in each class and the season-dependent values of the photodissociation rate k_3 (Table 11) by using Equation (80). The values for α were taken as the best values to describe the NO_2/NO_x ratios measured within one class, using Equation (81). These values for A and α in combination with Equation (81) can be used to calculate the NO_2/NO_x ratios as a function of distance from the source for a great number of meteorological conditions.

There is a lack of measuring data for some classes. The values for α are then obtained by inter- and extrapolation from values for α in adjacent classes. These values are shown between brackets in Figures 26-28. The values for α are 'normalized' in this procedure by multiplying each α by the factor $u \cdot ([\text{O}_3]k_1)^{-1}$ in its class. The values for A can always be calculated for each class by means of

Table 11

Values calculated for the photodissociation constant k_3 on the basis of average NO , NO_2 and O_3 background concentrations, assuming photostationary equilibrium. The final column shows the range of k_3 values used in the calculations of the uncertainty limits (Eq. 84b).

| season | solar radiation ($\text{W} \cdot \text{m}^{-2}$) | σ ($\text{W} \cdot \text{m}^{-2}$) | k_3 min^{-1} | range |
|---------------|---|--|----------------------------|-------|
| winter | 400 | 275 | 0.15 | 0.10 |
| spring/autumn | 1200 | 600 | 0.25 | 0.15 |
| summer | 1800 | 700 | 0.35 | 0.10 |

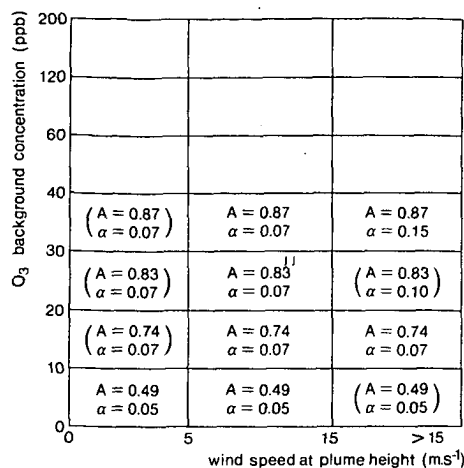


Fig. 26
Classification of the values for A and α in winter
(December - February).

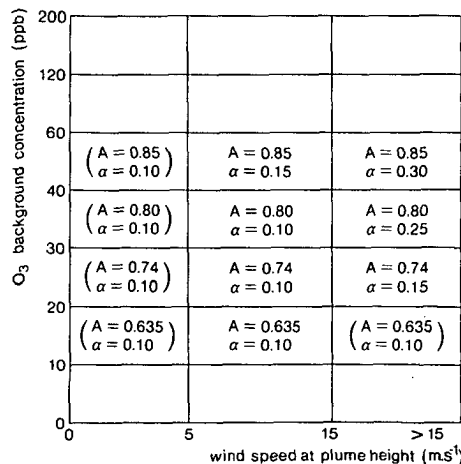


Fig. 27
Classification of the values for A and α in
spring/autumn (March - May and September -
November).

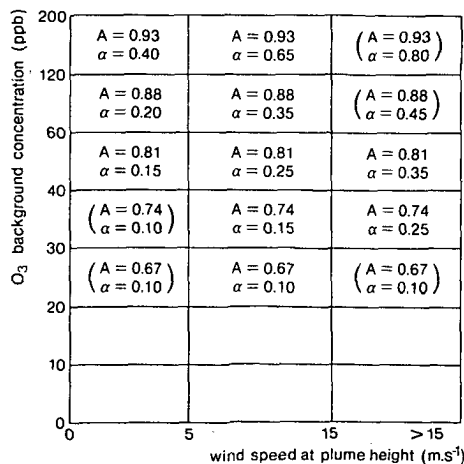


Fig. 28
Classification of the values for A and α in
summer (June - August).

Equation (80). These values for A and α are applied in model calculations using Equation (81), which results together with the values measured under corresponding conditions, are shown in Figures 30-35.

A good description of the measurements is obtained in most cases. Incidental deviations occur but their number is surprisingly small. The method presented here therefore proved to be highly suitable to predict NO_2/NO_x ratios in power-plant plumes under widely varying atmospheric conditions.

Uncertainty limits of measurements and model calculations

Adequate application of the various parameters requires knowledge of the uncertainty limits. Uncertainty concerning values obtained from measurements, uncertainty in model calculations and the uncertainties regarding parameters A and α are the topics in this section.

Measurements

Several (4-10) plume crossings were made at one distance from the source to determine the average NO_2/NO_x ratio in a plume. Each plume crossing is a record of a momentary plume. Figure 29 shows a typical traverse record for

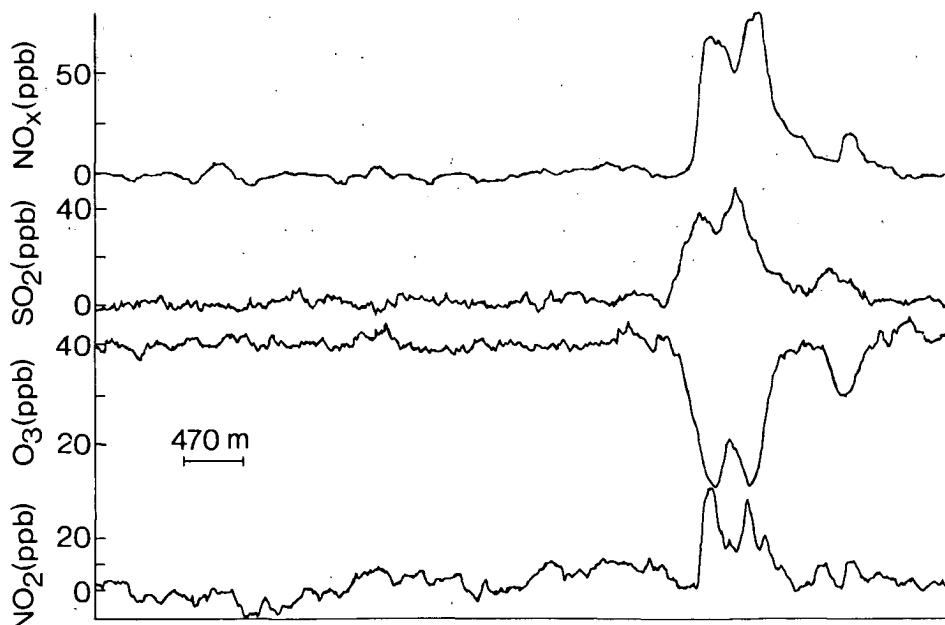


Fig. 29

Characteristic traverse record for NO_x , SO_2 , O_3 and NO_2 concentrations in a power-plant plume at a distance of 8.5 km from the source (flight 22). See also Figures 30 and 32.

NO_x , SO_2 , O_3 and NO_2 concentrations in a plume at a distance of 8.5 km from the source. The NO_2/NO_x ratio of this momentary plume was calculated by dividing the NO_x and NO_2 concentrations integrated over their plume profiles:

$$\left(\frac{\text{NO}_2}{\text{NO}_x} \right)_{\text{momentary plume}} = \frac{\int_{\text{plume width}} \text{NO}_2 dy}{\int_{\text{plume width}} \text{NO}_x dy} \quad (83)$$

This value for the momentary NO_2/NO_x ratio therefore represents a spatial average, i.e. a flat NO_2/NO_x profile over the plume width. This assumption was discussed by Cheng et al. (1986) on the basis of measurements. Each momentary plume is an element of the ensemble of momentary plumes belonging to a specific atmospheric condition. Variations in the parameters influencing the NO_2/NO_x ratio give rise to a distribution of momentary NO_2/NO_x values. This distribution is determined by the standard deviation σ if the distribution is Gaussian. The value for σ has been calculated for each series of four to ten plume crossings performed at one distance from the source.

Four to ten plume crossings can be completed in fifteen to thirty minutes. One crossing takes three to four minutes, during which the aircraft is actually in the plume for only ten to sixty seconds. By taking the average of the 4-10 momentary NO_2/NO_x ratios thus obtained, time averaging was carried out over a period of approximately twenty minutes. These spatially (flat NO_2/NO_x profiles in the plume) and temporally averaged (averaging period about twenty minutes) NO_2/NO_x ratios are shown in Figures 30-35.

Because the plumes studied are averaged, the standard errors σ/\sqrt{n} (n being the number of plume crossings) are also shown in Figures 30-35. The standard error of the mean will therefore be smaller than the standard deviation by a factor of about 2-3.

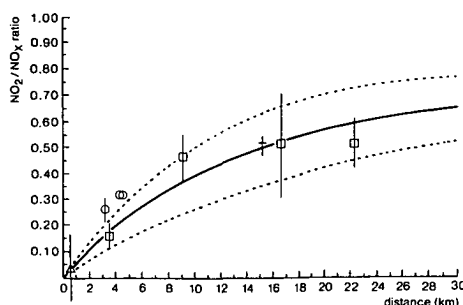


Fig. 30

NO_2/NO_x ratios measured and calculated with their uncertainty limits by using Equation (84b) for flights in winter. No effect of the wind speed on the oxidation rate was observed.

$10 \text{ ppb} < [\text{O}_3] \leq 20 \text{ ppb}; A = 0.74; \sigma = 0.07$.
 Flight 1 (squares): $5 \text{ m}\cdot\text{s}^{-1} \leq u \leq 15 \text{ m}\cdot\text{s}^{-1}$.
 Flights 2 (triangles), 3 (circles), 4 (dashes): $u > 15 \text{ m}\cdot\text{s}^{-1}$.

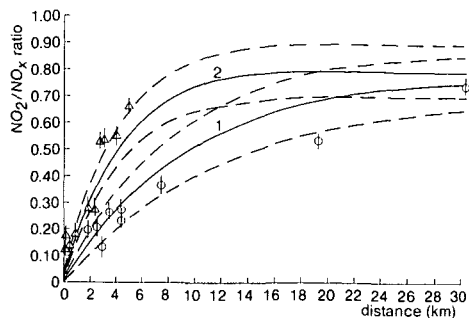


Fig. 31

NO_2/NO_x ratios measured and calculated with their uncertainty limits for measuring flights in spring/autumn. $30 \text{ ppb} < [\text{O}_3] \leq 40 \text{ ppb}$; $A = 0.8$. Increasing wind speed caused increasing NO_2 -rates.

Curve 1: flight 5, 6, 7, 8 (circles): $5 \text{ m}\cdot\text{s}^{-1} \leq u \leq 15 \text{ m}\cdot\text{s}^{-1}$; $a = 0.10$.

Curve 2: flight 9, 10, 11, 12 (triangles): $u > 15 \text{ m}\cdot\text{s}^{-1}$; $a = 0.25$.

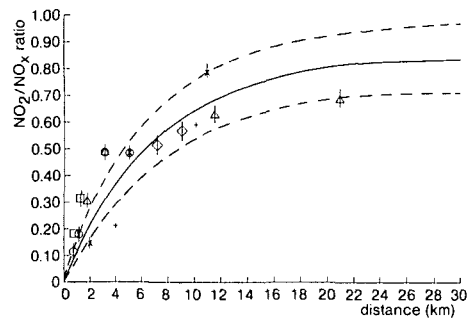


Fig. 32

NO_2/NO_x ratios measured and calculated with their uncertainty limits for measuring flights in spring/autumn. $40 \text{ ppb} < [\text{O}_3] \leq 60 \text{ ppb}$; $A = 0.85$; $a = 0.15$.

Flight 13 (squares), 14 (circles), 15 (triangles), 16 (crosses), 17 (dashes), 18 (diamonds): $5 \text{ m}\cdot\text{s}^{-1} \leq u \leq 15 \text{ m}\cdot\text{s}^{-1}$.

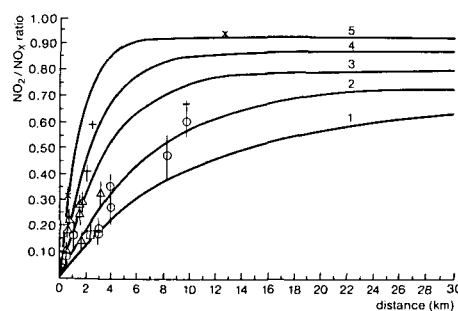


Fig. 33

NO_2/NO_x ratios measured and calculated for measuring flights in summer, showing the effect of the ozone concentration on the oxidation rate. $5 \text{ m}\cdot\text{s}^{-1} \leq u \leq 15 \text{ m}\cdot\text{s}^{-1}$.

Curve 1: flight 19 (squares): $20 \text{ ppb} < [\text{O}_3] \leq 30 \text{ ppb}$; $A = 0.67$; $a = 0.10$.

Curve 2: flight 20-22 (circles): $30 \text{ ppb} < [\text{O}_3] \leq 40 \text{ ppb}$; $A = 0.74$; $a = 0.15$.

Curve 3: flight 23-27 (triangles): $40 \text{ ppb} < [\text{O}_3] \leq 60 \text{ ppb}$; $A = 0.81$; $a = 0.25$.

Curve 4: flight 28-29 (dashes): $60 \text{ ppb} < [\text{O}_3] \leq 120 \text{ ppb}$; $A = 0.88$; $a = 0.35$.

Curve 5: flight 30-31 (crosses): $120 \text{ ppb} < [\text{O}_3] \leq 200 \text{ ppb}$; $A = 0.93$; $a = 0.65$.

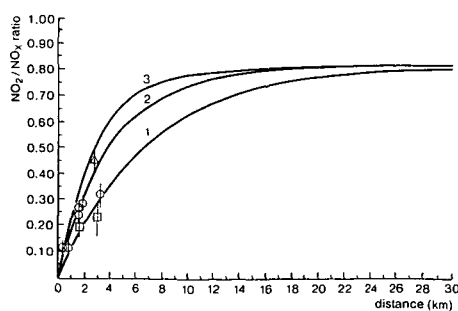


Fig. 34

NO_2/NO_x ratios measured and calculated for measuring flights in summer, showing the effect of wind speed on the oxidation rate. $40 \text{ ppb} < [\text{O}_3] \leq 60 \text{ ppb}$

Curve 1: flight 32-33 (squares): $0 \text{ m}\cdot\text{s}^{-1} \leq u < 5 \text{ m}\cdot\text{s}^{-1}$; $A = 0.81$; $a = 0.15$.

Curve 2: flight 23-28 (circles): $5 \text{ m}\cdot\text{s}^{-1} \leq u \leq 15 \text{ m}\cdot\text{s}^{-1}$; $A = 0.81$; $a = 0.25$.

Curve 3: flight 34 (triangles): $u > 15 \text{ m}\cdot\text{s}^{-1}$; $A = 0.81$; $a = 0.35$.

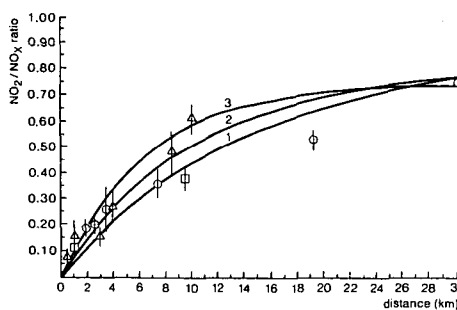


Fig. 35

NO_2/NO_x ratios measured and calculated for corresponding atmospheric conditions, e.g. ozone concentrations $30 \text{ ppb} < [\text{O}_3] \leq 40 \text{ ppb}$ and wind speed $5 \text{ m}\cdot\text{s}^{-1} \leq u \leq 15 \text{ m}\cdot\text{s}^{-1}$ at different times of the year.

Winter: curve 1: flight 35 (squares), $A = 0.87$; $a = 0.07$.

Spring/autumn: curve 2: flight 5-8 (circles), $A = 0.80$; $a = 0.10$.

Summer: curve 3: flights 20-22 (triangles), $A = 0.74$; $a = 0.15$.

Model calculations

Equation (81) implies a flat NO_2/NO_x profile over the plume width which corresponds with the NO_2/NO_x ratios calculated on the basis of measurements (see foregoing section). By fitting the best a for the spatially and temporally averaged NO_2/NO_x ratios measured, it is assumed that relation (81) describes spatially and temporally averaged NO_2/NO_x ratios.

It must be kept in mind that the scatter of the NO_2/NO_x ratios calculated on the basis of Equation (81) has to be related to the scatter of the mean and not to the instantaneous values of the parameters. Concentration fluctuations (micro-scale mixing) are not explicitly taken into account but are implicitly incorporated in the values for a if they would systematically influence the NO-oxidation rate.

The range of values for A , k_3 , O_3 and a to be discussed here therefore refers to the uncertainty in the estimation of the mean values, i.e. averaged over the plume and over time. A distinction is made between (1) variation in the values for A caused by taking the middle ozone concentration in each class and only one k_3 value per season, and (2) variation in the values for a caused by the distribution of NO_2/NO_x ratios measured in each class. These variations in a are thought to be chiefly caused by variations in wind speed.

The variation in the NO_2/NO_x ratios can be defined as:

$$\Delta^2 \overline{\left(\frac{\text{NO}_2}{\text{NO}_x} \right)} = \left(\frac{\delta \left(\overline{\frac{\text{NO}_2}{\text{NO}_x}} \right)}{\delta A} \right)^2 (\Delta A)^2 + \left(\frac{\delta \left(\overline{\frac{\text{NO}_2}{\text{NO}_x}} \right)}{\delta a} \right)^2 (\Delta a)^2 \quad (84a)$$

or, using Equation (81):

$$\Delta^2 \left(\frac{\text{NO}_2}{\text{NO}_x} \right) = (1 - e^{-ax})^2 (\Delta A)^2 + (x A e^{-ax})^2 (\Delta a)^2 \quad (84b)$$

Equation (84) would be valid if the variations in A and α were not correlated. However, this is not the case because A is a function of the ozone concentration and α is a function of not only the wind speed but also of the ozone concentration (Figs. 26-28). The differences in α caused by differences in wind speed are, however, of the same order or greater than the differences in α in the adjacent classes. The covariance of A and α will therefore be neglected and Equation (84) will serve as a reasonable approximation for explaining the variations of NO_2/NO_x ratios within one class.

The ozone parameter A

The distribution of values for A is obtained by establishing the discrete parameters of the meteorological conditions: one value for k_3 per season is selected for solar radiation and one value of the ozone concentration per class. The boundaries in the distribution of A (ΔA) must therefore be calculated by taking the difference between A minimum ($[O_3]$ minimal and k_3 maximum) and A maximum ($[O_3]$ maximum and k_3 minimum).

The values for ΔA are shown in Table 12. This table shows that ΔA increases when the ozone concentration decreases. A smaller division of ozone concentration classes was therefore chosen when background ozone concentrations were lower. Nevertheless, the values for ΔA are high when the ozone background concentrations are low. A further subdivision into still smaller classes of ozone concentrations would not be useful in view of the usual variations of ozone concentrations during measurements (about 10 ppb).

The wind parameter α

It is assumed that the parameter α represents the effect of wind speed on the oxidation rate in one ozone concentration class. Figures 26-28, however, show no significant effect of wind speed on the NO-oxidation rates at low ozone concentrations. This can be explained by taking into account the large variations in A caused by variations of ozone background concentrations at low levels. The effect of wind speed thus disappears because of the normal variation of about 10 ppb in the background ozone concentration. As these variations occur in outdoor air, more accurate measurements of the effect of wind speed on the oxidation rate at low ozone concentration levels are not a solution.

The values for α given in Figures 26-28 differ by discrete steps of at least 0.05 km^{-1} . This value proved useful for distinguishing between measurements under different meteorological conditions. A value of 0.03 km^{-1} was therefore chosen for $\Delta \alpha$ to represent variations of α within one class caused by variations in mean wind speed and other parameters which are not identified here.

The limits of uncertainty were calculated with Equation (84b), the values for ΔA shown in Table 12 and $\Delta \alpha = 0.03 \text{ km}^{-1}$.

Table 12

Variation in values for A caused by variations of the ozone concentration and the photodissociation rate k_3 . The distribution of A values was skewed and indicative values of ΔA as used in Equation 84b are shown in the final column.

| | [O ₃] (ppb) | A max (k ₃ = 0.10) | A mean (k ₃ = 0.15) | A min (k ₃ = 0.20) | ΔA |
|-----------------------|--|----------------------------------|-----------------------------------|----------------------------------|------------|
| winter ¹ | 1-10 | 0.74 | 0.49 | 0.13 | 0.25 |
| | 10-20 | 0.85 | 0.74 | 0.59 | 0.13 |
| | 20-30 | 0.90 | 0.83 | 0.74 | 0.10 |
| | 30-40 | 0.92 | 0.87 | 0.81 | 0.05 |
| | | | | | |
| | | | | | |
| | | | | | |
| | | | | | |
| | [O ₃] (k ₃ = 0.15) | A max (k ₃ = 0.25) | A mean (k ₃ = 0.40) | A min | ΔA |
| spring ² / | 10-20 | 0.74 | 0.635 | 0.42 | 0.15 |
| | 20-30 | 0.83 | 0.74 | 0.59 | 0.10 |
| | 30-40 | 0.87 | 0.80 | 0.685 | 0.10 |
| | 40-60 | 0.91 | 0.85 | 0.74 | 0.10 |
| | | | | | |
| | | | | | |
| | | | | | |
| | | | | | |
| | [O ₃] (k ₃ = 0.25) | A max (k ₃ = 0.35) | A mean (k ₃ = 0.45) | A min | ΔA |
| summer ⁴ | 20-30 | 0.78 | 0.67 | 0.56 | 0.10 |
| | 30-40 | 0.82 | 0.74 | 0.66 | 0.08 |
| | 40-60 | 0.87 | 0.805 | 0.72 | 0.08 |
| | 60-120 | 0.93 | 0.88 | 0.79 | 0.08 |
| | 120-200 | 0.96 | 0.93 | 0.89 | 0.04 |

¹ December to February.² March to May.³ September to November.⁴ June to August.

Measurements of a

When the phenomenological approach is used as described here, it is important to establish the best values for α under different meteorological conditions. When measurements are made it is therefore useful to know at what distances from the source the maximum variations of the NO_2/NO_x ratio caused by variations of α occur. This distance can be calculated as:

$$\frac{d \left[\Delta \left(\text{NO}_2 / \text{NO}_x \right) \right]_\alpha}{dx} = 0 \quad (85)$$

or, using Equation (84b), as:

$$\frac{d \left(x A e^{-\alpha x} \right)}{dx} = 0 \quad (86)$$

which leads to $\alpha x = 1$.

The maximum variations of the NO_2/NO_x ratio therefore occur at distances x of $1/\alpha$ km. This value is equivalent to distances between 1.5 and about 15 km from the source. This distance increases with decreasing wind velocity and ozone concentration, and obtains a minimum value in summer.

If the best values for α are to be found it is best to perform measurements close to the source where the oxidation is fast and the effect of the wind velocity can be measured, and at distances of about $1/\alpha$ km. It is found, however, that NO_2/NO_x measurements very close to the source ($500 \text{ m} < x < 1000 \text{ m}$) may be disturbed by the small dimensions of the plume and the large R-C times of the monitors with respect to flight speed ($\sim 70 \text{ m} \cdot \text{s}^{-1}$) (Janssen, 1986). A distance of 1-2 km appeared to be the most practical. The model used here assumes that photostationary equilibrium in the plume is established at a larger distance from the source ($x > 1/\alpha$ km). Measurements at distances between 15 and 30 km need to be carried out to check the errors due to this simplification.

The above considerations were taken into account in a current research programme which concentrates on measurements made during the night and at very high and very low wind speeds during daytime. NO_2/NO_x ratios are being measured at three distances from the source, e.g. 1-2 km, $\sim 1/\alpha$ km and 15-30 km.

Discussion

Three aspects need to be discussed here: (1) the seasonal dependence of the NO-oxidation rates, (2) homogeneous and inhomogeneous mixing and (3) the application of the classification in the calculation of ground-level NO_2 concentrations.

Seasonal dependence of the NO-oxidation rates

It appears from the results of measurements and of model calculations that the proposed classification of NO-oxidation rates can be a useful tool for predicting the NO_2/NO_x ratios in the plume of a power plant.

The values calculated for α , indicating the NO-oxidation rate, increase with rising O_3 concentrations. They also increase with wind speed at O_3 concentrations higher than 30 ppb. Figure 35 shows the NO_2/NO_x ratios calculated for the summer, winter and spring/autumn periods at the same range of ozone concentrations and wind speeds. It is obvious that NO_2 formation develops more rapidly in summer than in spring/autumn and is slowest in winter. This can be attributed to differences in turbulence in the atmosphere, considering the differences in solar radiation of the three periods (see Table 11).

More NO_2 will be formed at larger distances from the source in winter because of the lower photodissociation rate during this season; this is also shown in Figure 35.

Homogeneous and inhomogeneous mixing

The values for α based on measurements vary with atmospheric conditions. If the ozone concentration varies between 30 and 40 ppb, the wind speed between 5 and 15 $\text{m}\cdot\text{s}^{-1}$ then α ranges from 0.07 km^{-1} in winter to 0.15 km^{-1} in summer. These values for α can be compared with the value of 1.7 km^{-1} previously calculated for an ozone concentration of 35 ppb and a wind speed of $0.01 \text{ km}\cdot\text{s}^{-1}$, by using Equation (76) for a perfectly mixed plume. This 10- to 20-fold difference between measured and calculated values for α can be explained by inhomogeneous mixing of a plume with ambient air.

Inhomogeneous mixing of a plume can take place at two levels, i.e. the structure of the mean concentration fields, also termed 'macromixing', and the level of small-scale fluctuations that determines higher-order moments and correlations of these fields, also termed 'micromixing'.

Macromixing can be described as follows: parcels of NO-rich air (i.e. diluted flue gas) and O_3 -rich air (i.e. ambient air mixed into the plume) are spatially segregated in the atmosphere. The reaction of NO with O_3 occurs only within a relatively narrow reaction zone between the two regions. NO_2 formation is retarded because the bimolecular reaction of NO with O_3 occurs rapidly compared to the mixing times over the scale of the plume. This process of inhomogeneous mixing of a plume has been discussed by Hegg et al. (1976) and more recently by Janssen (1986).

Micromixing plays a role in the conversion of NO into NO_2 when the concentration fluctuations of NO and O_3 are correlated. If the correlation between the concentration fluctuations of NO and O_3 is negative, as is probably the case because NO and O_3 have different origins (i.e. flue gas and outdoor air

respectively), NO_2 formation in a plume may be retarded. This was discussed by Donaldson & Hilst (1972), Lamb & Shu (1978) and Builjtes (1981).

If these effects, i.e. macromixing and micromixing, play a role in the process of NO oxidation they both cause a retardation of the oxidation rate. This causes the values for α based on measurements in the plume to be smaller by a factor of 10-20 than the values for α calculated from Equation (76), where perfect mixing and zero correlation between concentration fluctuations of NO and O_3 are assumed.

Application of the classification to the calculation of ground-level NO_2 concentrations

The proposed classification of NO -oxidation rates can be used to calculate NO_2 concentrations at ground-level by means of a Gaussian dispersion model. It is assumed that the NO -oxidation rate averaged over the plume traverses also holds for the part of the plume that reaches the ground. The NO_2/NO_x ratio as a function of distance from the source can be added as a source depletion factor according to:

$$C(x,y,z;H) = Q \frac{\exp\left(-\frac{1}{2}\left(\frac{y}{\sigma_y}\right)^2\right)}{2\pi u \sigma_y \sigma_z} \left\{ \exp\left(-\frac{1}{2}\left(\frac{H-z}{\sigma_z}\right)^2\right) + \exp\left(-\frac{1}{2}\left(\frac{H+z}{\sigma_z}\right)^2\right) \right\} \quad (87)$$

with the source emission factor:

$$Q = A(1 - e^{-\alpha x}) \quad (88)$$

where Q is the NO_x emission calculated as NO_2 .

This is illustrated in Figure 36 which shows the NO_2 concentrations calculated in the centre of the plume at ground-level ($y = 0$ and $z = 0$) by means of:

$$C(x,0,0;H) = A(1 - e^{-\alpha x}) \frac{Q}{\pi u (\sigma_y \sigma_z)} \exp\left(-\frac{1}{2}\left(\frac{H}{\sigma_z}\right)^2\right) \quad (89)$$

The input data for the calculations are given in Table 13. The results show that the positions of the maximum NO_x and NO_2 concentrations are at most only a few hundred metres to two kilometres apart (case 2 in Fig. 36). This means that the position of the NO_x maximum can be considered to be the position of the NO_2 maximum for practical measuring conditions.

Table 13Emission and meteorological data for calculating ground-level NO₂ concentrations with Equation (89).

| flight | date | unit | fuel | load | H | NO _x | ozone | wind speed | A | α | stability class | σ_y | σ_z |
|--------|------------|------|------|------|-----|-----------------|-------|------------|-------|----------|-----------------------|-------------|----------------------|
| | | | | | | | | | (MWe) | (m) | (kg·h ⁻¹) | (ppb) | (m·s ⁻¹) |
| 1 | 1976-06-08 | MV1 | gas | 500 | 325 | 400 | 30 | 8 | 0.93 | 0.65 | A | 1.06 x 0.86 | 0.28 x 0.90 |
| 2 | 1978-03-20 | MV1 | gas | 512 | 385 | 400 | 30 | 6 | 0.80 | 0.10 | D | 0.26 x 0.90 | 0.20 x 0.76 |
| 3 | 1978-10-24 | MV1 | gas | 510 | 265 | 400 | 30 | 20 | 0.80 | 0.25 | D | 0.26 x 0.90 | 0.20 x 0.76 |

The values for σ_y and σ_z were calculated according to KNMI (1979).

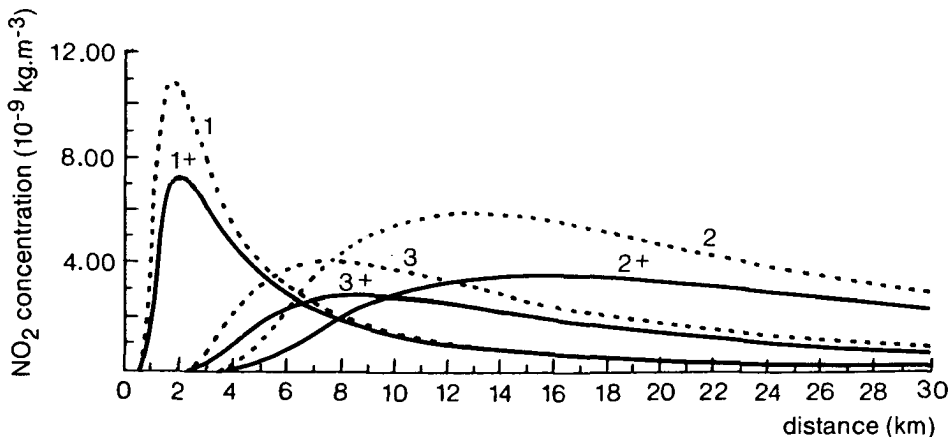


Fig. 36

NO_x and NO_2 ground-level concentrations calculated for different atmospheric conditions.

Unstable (Pasquill A), 1 and 1 + for NO_x and NO_2 ground-level concentrations respectively.

Neutral (Pasquill D) and moderate wind speed ($5 \text{ m}\cdot\text{s}^{-1} \leq u \leq 15 \text{ m}\cdot\text{s}^{-1}$), 2 and 2 + for NO_x and NO_2 ground-level concentrations, respectively.

Neutral and high wind speed ($u > 15 \text{ m}\cdot\text{s}^{-1}$), 3 and 3 + for NO_x and NO_2 ground-level concentrations, respectively.

Conclusions

A classification of NO-oxidation rates was made on the basis of sixty measuring flights in the plumes of power plants in The Netherlands. Ozone background concentration, wind speed and season of the year are the most important parameters determining the oxidation rate. NO-oxidation rates increase with rising ozone concentration, wind speed and solar radiation. Assuming that the oxidation reaction with ozone is the dominant process, the course of the NO_2/NO_x ratio as a function of distance from the source can be described in the classification system by a simple power of e. Much of the variation in NO_2/NO_x ratios measured can be accounted for with this model provided that allowances are made for naturally occurring variations (about 10 ppb) of the ozone background concentration and variations of the photodissociation rate k_3 .

It can also be concluded from the values for α that the formation of NO_2 in a plume in the atmosphere is delayed because of the rather slow process of mixing of the plume with its surrounding air.

This description of NO_2/NO_x ratios, in which Gaussian dispersion was also used, can be applied to the calculation of ground-level concentrations of NO_2 . It is concluded that the locations of the maximum NO_x and NO_2 concentrations are nearly the same under the conditions used for measuring.

Chapter 8

Summary and conclusions

Introduction

Traffic is the most important source of nitrogen oxides (> 50%) in The Netherlands. Generation of electricity in power plants fired with fossil fuel is another important source: it contributes about 15% to the NO_x emission in The Netherlands and about 2% to the average immission. The nitrogen oxides formed during the combustion process in power plants are emitted into the atmosphere together with the flue gases via a tall stack.

Nitrogen oxides contribute to the concentrations of nitrogen dioxide in outdoor air. In higher concentrations, nitrogen dioxide can harm human health. The concentrations of nitrogen dioxide measured in The Netherlands often exceed the guide values. Emission of nitrogen oxides also contributes to acidification and fertilization of water and soil and to photochemical air pollution.

Reactive-plume models

Measurements can be carried out to investigate the local influence of a power plant on air quality. Such measurements often have the limitation that they are restricted to a certain location and/or period or to a certain power plant, and therefore have no generally applicable validity. It is therefore attractive to have a model available which allows the influence on the air quality to be determined for any location, period or power plant. A model of this type is available for a slowly reacting gas such as SO₂, which is emitted from a point source such as the stack of a power plant; this model is the Gaussian plume model. No such model exists, however, for rapidly reacting gases such as nitrogen oxides.

Power plants fired with fossil fuel emit nitrogen oxides mostly (> 95%) as nitrogen monoxide (NO). NO is rapidly converted in the atmosphere into the much more poisonous nitrogen dioxide (NO₂). The rate of this conversion process is determined by both the rate of the physical processes of dispersion and mixing of the plume and the chemical reaction rates (Chapters 1 and 2).

The research reported in this thesis was mainly directed to investigations into the competition between the processes of dispersion and mixing (τ_p) and chemical reactions (τ_c) as it affects the conversion rate of NO in the plumes of power plants. The measurements of concentrations of NO and NO₂ were compared with calculations made with various dispersion models all of which incorporate chemical reactions (Chapters 5-7).

Results from four models compared with results from measurements

Some results and figures presented in previous chapters are repeated in this section to illustrate the mutual differences between the various models.

- (1) Comparison of the results of calculations with the first model, in which Gaussian dispersion of the plume and chemical equilibrium were assumed, with results from measurements showed that the calculated NO₂ concentrations were generally higher than the measured values (Fig. 37 and Chapter 4).
- (2) These differences were partly explained by means of the results from a second model in which Gaussian dispersion of the plume was assumed but chemical equilibrium was not (Chapter 5). It appeared that the processes of dispersion and mixing near the source are faster than the chemical reactions ($t_p/t_c < 1$), and that the assumption of chemical equilibrium ($t_p/t_c > 1$), as used in the first model, is incorrect. Calculations with the second model gave better results for NO₂ concentrations near the source. When greater distances from the stack (> 5 km) were considered the NO₂ concentrations calculated with the second model were nevertheless often higher than the results of measurements (Fig. 38).
- (3) These differences between measurements and model calculations for larger distances from the source were investigated with a third model in which neither Gaussian dispersion of the plume nor chemical equilibrium was assumed (Fig. 39 and Chapter 6). It appeared from calculations with this model that, even at larger distances from the source, chemical equilibrium is not measured in the plume because the momentary plume is inhomogeneously mixed and consists of parcels of flue gas and parcels of ambient air. The general conclusion may therefore be drawn that the oxidation rate of NO at smaller distances from the source is determined by the chemical reaction rates ($t_p/t_c < 1$), whereas the oxidation rate at greater distances from the source (> 5 km) is determined by the mixing rate of the plume with its ambient air ($t_p/t_c > 1$).
- (4) A fourth empirical model is presented that allows the oxidation rate of NO to be predicted for very different atmospheric conditions. This model is based on a statistical analysis of a large database of measurements (Chapter 7) carried out by means of an aircraft in the plumes of Dutch power plants. The ozone concentration in the air, wind velocity and season appeared the most important factors in parameterizing the oxidation rate of NO. The NO₂ concentration at ground level, caused by the NO_x emission of a power plant, can be calculated for almost all weather conditions on the basis of a classification of the NO-oxidation rate as a function of atmospheric conditions and assuming Gaussian dispersion of the plume. The NO₂/NO_x ratios calculated with this model from the same database as in the previous models are shown in Figure 40.

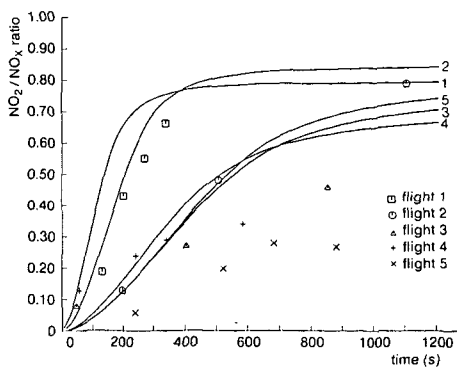


Fig. 37
 NO_2/NO_x ratios measured and calculated by the first reactive-plume model.

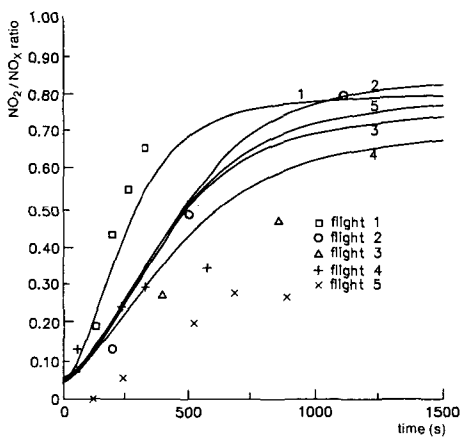


Fig. 38
 NO_2/NO_x ratios measured and calculated by the second reactive-plume model.

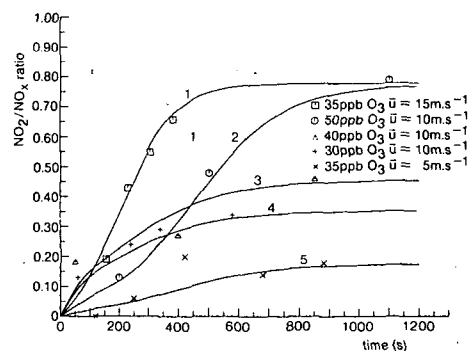


Fig. 39
 NO_2/NO_x ratios measured and calculated by the third reactive-plume model.

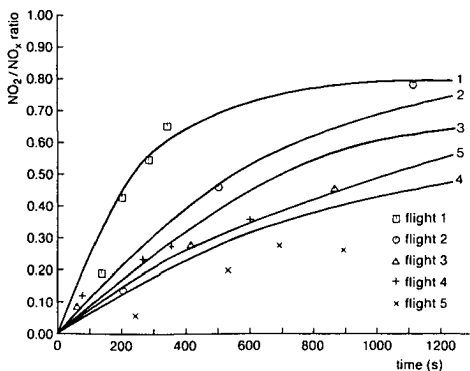


Fig. 40

NO_2/NO_x ratios measured and calculated by the fourth reactive-plume model.

Plume profiles

The differences between the four reactive-plume models with respect to calculated plume profiles are illustrated in Figure 41. This figure shows the calculated NO-concentration profiles at the height of the plume axis for measuring flight 2 at a distance of 5 km from the stack. The differences between these profiles can be explained by the differences between the models.

Model one uses a time-averaged dispersion parameter ($4\sigma_y = 1700$ m) and the NO concentration calculated will be much lower than the values measured in the momentary plume (plume width about 500 m).

Model two uses the same time-averaged dispersion equations as model one but chemical equilibrium is not assumed. The NO concentration in the plume will be higher than in the first model, but still too low with respect to the observation because the measurements concern a momentary plume.

Model three is a momentary plume model. The plume width calculated (141 m; Table 11) was much smaller than the plume widths calculated with the preceding models. As a result, the NO concentration calculated was much higher than those calculated with the preceding models and agrees better with the measured values. This model has the disadvantage, however, that it is a diagnostic model only and cannot be used to forecast concentrations in a plume.

The NO concentrations calculated with the fourth model were higher than those calculated with the first model. The fact that the plume is not completely mixed at this distance is taken into account in this empirical model. Because averaged dispersion equations were used, the concentrations calculated were lower than the values measured in a momentary plume.

Conclusions

When NO_2/NO_x ratios calculated with the various models are compared, it appears that the NO_2/NO_x ratios calculated with the first model are generally too high compared with measurements. The results of the second model for a

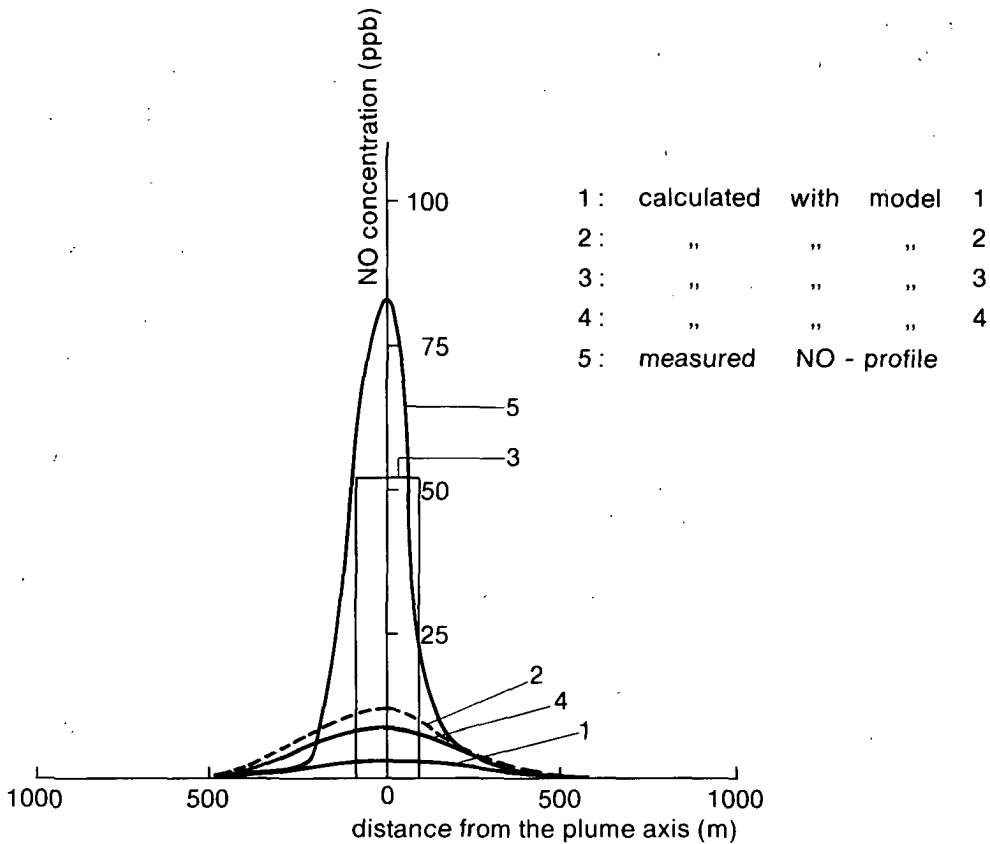


Fig. 41
NO concentration profiles measured and calculated by the four reactive plume models.

mean plume agree reasonably well for distances up to about 5 km from the stack. At larger distances from the stack (> 5 km), the NO_2/NO_x ratios calculated with the third and fourth model are lower than the values calculated with the first two models and in better agreement with observations. The conclusions are:

- (1) Comparison of measurements of the oxidation rate of NO in a plume in the atmosphere with calculated values for an ideal, homogeneously mixed gas shows that NO_2 formation in the plume is retarded by a factor of 10-20, due to the mixing process. If the oxidation rate is described by the empirical relation $\text{NO}_2/\text{NO}_x = A(1-e^{-\alpha x})$, the measured values for α vary between 0.07 km^{-1} in winter to 0.15 km^{-1} in summer ($30 \text{ ppb} < \text{O}_3 < 40 \text{ ppb}; 5 \text{ m}\cdot\text{s}^{-1} < u < 15 \text{ m}\cdot\text{s}^{-1}$). This is in an order of magnitude less than the value for α of 1.7 km^{-1} for an ideal, mixed gas. Correct modelling of the mixing process is

therefore essential in models which deal with formation of NO₂ in a plume in the atmosphere.

- (2) Dispersion and mixing are fast in the first phase of the dispersion of the plume in the atmosphere, faster at least than the chemical reactions. The formation of NO₂ in a mean plume at distances up to about 5 km from the stack can be calculated reasonably well with model two which uses Gaussian plume-dispersion equations.
- (3) Reactive-plume models which use the ordinary Gaussian profiles to describe the dispersion of the plume will overestimate NO₂ formation in the second phase at distances larger than 5 km from the stack. The Gaussian profiles are time averages and the contribution of meandering of the plume is thus also incorporated in the values of σ_y and σ_z . Formation of NO₂ is, however, a non-linear process so that the concentrations of reactants in a momentary plume must be incorporated in the reactive-plume model. Because the plume widths of a time-averaged plume, which includes the meandering component, are much larger than the plume widths of a momentary plume, formation of NO₂ will be overestimated in models that use ordinary Gaussian dispersion profiles, e.g. model two. The effect of meandering will be more important at greater distances and at lower wind speeds, so that the differences between measured and calculated values were greatest for measuring flight 5 where these conditions occur (Figs. 37 and 38).
- (4) The effect of meandering will probably be less at night when the plume is situated in the stable layer. Formation of NO₂ in a plume can then be described by a model which uses the ordinary Gaussian dispersion equations for a stable atmosphere, e.g. model two (Fig. 42).

The next step in theoretical model building might be an analysis of the measured concentration fluctuations of the existing data set which, in this study, largely have been averaged out.

Further development of analytical models is certainly desirable. However, given the limited time resolution of existing measuring instruments, more refined models cannot be tested with the required accuracy.

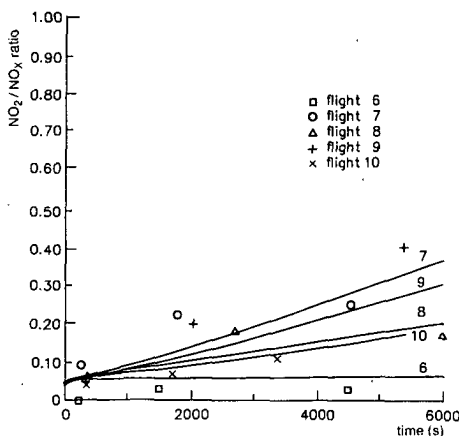


Fig. 42
 NO_2/NO_x ratios measured and calculated by the second reactive-plume model for plumes at night.

References

- Ames, W.F. 1965 New linear partial differential equations in engineering — Academic Press (New York - London).
- Anonymous 1980 Toekomstige energiesituatie in Nederland — Vereniging van Directeuren van Elektriciteitsbedrijven in Nederland (Arnhem): 379 pp.
- Anonymous 1983 Indicatief Meerjaren Plan Lucht 1984-1988 — Staatsuitgeverij ('s-Gravenhage).
- Anonymous 1984 Indicatief Meerjaren Plan Lucht 1985-1989 — Staatsuitgeverij ('s-Gravenhage).
- Anonymous 1987 Besluit Luchtkwaliteit Stikstofdioxide — Staatsblad van het Koninkrijk der Nederlanden, Staatsuitgeverij ('s-Gravenhage).
- Becker, K.H. & U. Schurath 1975 Der Einfluss von Stickstofoxiden auf atmosphärische Oxidationsprozesse — Staub 35: 156-161.
- Briggs, G. 1975 Plume rise predictions — Paper presented at the AMS Workshop on Meteorological and Environmental Assessment (Boston, 1975).
- Brodzinsky, R., B.K. Cantrell, R.M. Endlich & C.M. Bhumsalkan 1984 A long-range air pollution transport model for eastern North-America - Nitrogen oxides — Atmospheric Environment 18: 2361-2366.
- Brubaker, K.L. & D.M. Rose 1978 Dispersion models for sulfur oxides in urban environments. In: J.O. Nriagu (ed.): Sulphur in the environment, Part I: The atmospheric cycle — John Wiley & Sons (New York).
- Buitjes, P.J.H. 1981 A comparison between chemically reacting plumes and wind tunnel experiments — Paper presented at the 12th International Technical Meeting on Air Pollution Modelling and its Applications (Palo Alto, 1981).
- Buitjes, P.J.H., G.L.H. Beugeling & J. Vijge 1985 Plume dispersion models of coal fired power plants with respect to chemical transformation and dry deposition — TNO report 85-01234 (in Dutch).
- Buitjes, P.J.H., L.H.J.M. Janssen, G.L.H. Beugeling & A.J. Elshout 1986 Chemical reactive plumes; field experiments and modelling — Paper presented at the 7th World Clean Air Conference (Sydney, 1986).
- Buitjes, P.J.H. & A.M. Talmon 1987 Macro- and microscale mixing in chemical reactive plumes — Boundary Layer Meteorology 41: 417-426.
- Calvert, J.C. 1976 Test of the theory of ozone generation in Los Angeles atmosphere — Environmental Science and Technology 10: 248-256.
- Carmichael, C.R. & L.K. Peters 1981 Application of the mixing reaction in series model to NO_x-O₃ plume chemistry — Atmospheric Environment 15: 1069-1074.
- Cheng, L., E. Peake, D. Rogers & A. Davis 1986 Oxidation of nitric oxide controlled by turbulent mixing in plumes from oil sands extraction plants — Atmospheric Environment 20: 1697-1703.
- Demerjian, K.R., J.A. Kerr & J.G. Calvert 1974 The mechanism of photochemical smog formation. In: J.N. Pitts & R.L. Metcalf (eds.): Advances in environmental science and technology, volume 4 — John Wiley (New York).
- Donaldson, C. & G.R. Hilst 1972 Effect of inhomogeneous mixing on atmospheric photo-chemical reactions — Environmental Science and Technology 6: 812-816.
- Elshout, A.J. & S. Beilke 1984 Die Oxidation von NO zu NO₂ in Abgasfahnen von Kraftwerken — VGB Kraftwerkstechnik 7: 64, 648-654.

- Eschenroeder, A.Q. & J.R. Martinez 1972 Concepts and applications of photochemical smog models — Advances in Chemistry, Series 113: 101-167.
- Finlayson-Pitts, B.J. & J.H. Pitts 1986 Atmospheric chemistry - fundamentals and experimental techniques — John Wiley & Sons (New York).
- Forney, L.J. & Z.G. Giz 1980 Slow chemical reactions in power plant plumes: application to sulphates — Atmospheric Environment 14: 533-541.
- Forney L.J. & Z.G. Giz 1981 Fast reversible reactions in power plant plumes: application to the nitrogen dioxide photolytic cycle — Atmospheric Environment 15: 345-352.
- Georgopoulos, P.G. & J.H. Seinfeld 1986a Mathematical modelling of turbulent reacting plumes I. General theory and model formulation — Atmospheric Environment 20: 1791-1807.
- Georgopoulos, P.G. & J.H. Seinfeld 1986b Mathematical modelling of turbulent reacting plumes II. Application at the NO-NO₂-O₃ system — Atmospheric Environment 20: 1809-1818.
- Ghodsizadem, Y. 1978 Simultaneous mixing and chemical reaction — Ph.D. thesis, Department of Chemical Engineering, Case Western Reserve University.
- Hanna, S.R. 1984 Concentration fluctuations in a smoke plume — Atmospheric Environment 18: 1091-1106
- Harrington, W. & A.J. Krupnick 1985 Short term nitrogen dioxide exposure and acute respiratory disease in children — Journal of the Air Pollution Control Association 35: 1061-1067.
- Hecht, T.A. & J.H. Seinfeld 1972 Development and validation of a generalized mechanism for photochemical smog — Environmental Science and Technology 6: 47-57.
- Hecht, T.A., J.H. Seinfeld & M.C. Dodge 1974 Further development of generalized kinetic mechanism for photochemical smog — Environmental Science and Technology 8: 327-339.
- Hegg, D.A. & P.V. Hobbs 1983 Particles and trace gases in the plume from a modern coal-fired power plant in the western United States and their effects on light extinction — Atmospheric Environment 17: 357-368.
- Hegg, D.A. & P.V. Hobbs 1985 Nitrogen dioxide from a coal fired power plant - authors' reply — Atmospheric Environment 19: 206.
- Hegg, D.A., P.V. Hobbs, L.F. Radke & H. Harrison 1976 Reactions of ozone and nitrogen oxide in power plant plumes — Atmospheric Environment 11: 521-526.
- Högström, U. 1978 Sulfur in the environment: Part 1 — John Wiley and Sons (New York).
- Horst, T.W. 1982 A correction to the Gaussian source depletion model — Proceedings of the 4th Conference on Scavenging, Dry Deposition and Resuspension (Los Angeles, 1982).
- Hov, O. & S. Larssen 1984 Street canyon concentrations of nitrogen dioxide in Oslo - measurements and model calculations — Environmental Science and Technology 18: 82-87.
- Isakson, I.S.A., E. Hesstvedt & O. Hov 1978 A chemical model for urban planning: test for ozone and particulate sulfur formation in St. Louis urban plume — Atmospheric Environment 12: 599-604.
- Janssen, L.H.J.M. 1986 Mixing of ambient air in a plume and its effects on the oxidation of NO — Atmospheric Environment 20: 2347-2357.
- Janssen, L.H.J.M. & A.J. Elshout 1987 Formation of NO₂ in power plant plumes field experiments and modelling — KEMA Scientific and Technical Reports 5: 259-279.
- Janssen, L.H.J.M., A.J. Elshout, H. van Duuren & F. van Haren 1987 Modelling reactions of nitrogen oxides in power plant plumes. In: Proceedings of the Conference on Acid Rain. Scientific and Technical Advances (Lisbon, 1987) — Publication Division, Selper Ltd. (London): 137-143.
- Janssen, L.H.J.M., J.H.A. van Wakeren, H. van Duuren & A.J. Elshout 1988 A classification of NO-oxidation rates in power plant plumes based on atmospheric conditions — Atmospheric Environment 22: 43-53.
- Kewley, D.J. 1978 Atmospheric dispersion of a chemically reacting plume — Atmospheric Environment 12: 1895-1900.
- Kewley, D.J. & K. Post 1978 Photo-chemical ozone formation in the Sydney airshed — Atmospheric Environment 12: 2179-2184.
- KNMI (Royal Dutch Meteorological Institute) 1979 Air pollution and weather — Staatsuitgeverij ('s-Gravenhage) (in Dutch).

- Lamb, R.G. & W.R. Shu 1978 A model of second order chemical reactions in turbulent fluid part I. Formulation and valuation — Atmospheric Environment 12: 1695-1704.
- Lanting, R.W. 1983 De aantasting van materialen door NO_x — Publikatiereeks Lucht, Ministerie van Volkshuisvesting, Ruimtelijke Ordening en Milieubeheer ('s-Gravenhage) 12.
- Liu, M.K. 1977 Numerical simulation of reactive plumes — Paper presented at the 4th International Clean Air Congress (Tokyo, 1977).
- Llewelyn, R.P. 1983 An analytical model for the transport, dispersion and elimination of air pollutants emitted from a point source — Atmospheric Environment 17: 249-256.
- Lusis, M.A. 1976 Mathematical modelling of chemical reactions in a plume — Proceedings of the 7th International NATO/CCMS Technical Meeting on Air Pollution Modelling and its Applications (Airlie, 1976): 831-855.
- Meij, R., L.H.J.M. Janssen & J. van der Kooij 1986 Air pollutant emissions from coal-fired power stations — Kema Scientific and Technical Reports 4: 51-69.
- Melo, O.T., M.A. Lusis & R.D.S. Stevens 1978 Mathematical modelling of dispersion and chemical reactions in a plume; oxidation of NO to NO₂ in the plume of a power plant — Atmospheric Environment 12: 1231-1234.
- Melo, O.T. & R.D.S. Stevens 1981 The occurrence and nature of brown plumes in Ontario — Atmospheric Environment 15: 2521-2529.
- Nappo, C.J. 1984 Turbulence and dispersion parameters derived from smoke plume photo-analysis — Atmospheric Environment 18: 299-306.
- Parrish, D.D., P.C. Murphy, D.L. Albritton & F.C. Fehsenfeld 1983 The measurement of the photodissociation rate of NO₂ in the atmosphere — Atmospheric Environment 17: 1365-1379.
- Pasquill, F. 1974 Atmospheric diffusion — John Wiley & Sons (Chichester).
- Persson, C. 1986 Local scale plume model for nitrogen oxides. Model verification — Swedish Meteorological and Hydrological Institute Reports Meteorology and Climatology RMK 50 0347-2116.
- Persson, C. & L. Funkquist 1984 Local scale plume model for nitrogen oxides - model description — Swedish Meteorological and Hydrological Institute Reports Meteorology and Climatology RMK 41 0347-2116.
- Peters, L.K. & L.W. Richards 1977 Extension of atmospheric dispersion models to incorporate fast reversible reactions — Atmospheric Environment 11: 101-108.
- Richard, H.G., F. Schneider & J. Janicca 1985 Ausbreitung und reaction von Stickoxiden in Abgasfahnen von Punktquellen — Staub 45 (2).
- Richards, L.W. 1983 Comments on the oxidation of NO₂ to nitrate - day and night — Atmospheric Environment 17: 397-402.
- Richards, L.W. 1985 Nitrogen dioxide from a coal fired power plant — Atmospheric Environment 19: 205-206.
- Richards, L.W., J.A. Anderson, D.L. Blumenthal, A.A. Brandt, J.A. McDonald, N. Waters, E.S. Macias & P.S. Bhardwaja 1981 The chemistry, aerosol physics, and optical properties of a Western coal-fired power plant plume — Atmospheric Environment 15: 2111-2134.
- Russel, A.G., G.J. Mc Rae & S.R. Cass 1985 The dynamics of nitric acid production and the fate of nitrogen oxides. Atmospheric Environment 19, 893-903.
- Schneider, A.T. & A. Bresser 1987 Tussentijdse rapportage van het Additionele Programma Verzuringsonderzoek — Rijksinstituut voor Volksgezondheid en Milieuhygiëne (Bilthoven).
- Schurath, U. & K. Ruffing 1981 Die oxidation von NO durch Sauerstoff und Ozon in Abgasfahnen — Staub 41: 277-281.
- Shu, W.R., R.G. Lamb & J.H. Seinfeld 1978 A model of second-order chemical reactions in turbulent fluid - part 11. Application to atmospheric plumes — Atmospheric Environment 20: 1695-1704.
- Singer, J.A. & H.E. Smith 1966 Atmospheric dispersion at Brookhaven National Laboratory — International Journal on Air and Water Pollution 10: 125-135.
- Tennekes, H. & J.L. Lumley 1972 A first course in turbulence — MIT Press.

- Vaessen, R.J. 1985 NO-oxidation in stack plumes of power stations. Description of a classification of NO conversion based on O₃ background concentrations and wind speed — KEMA report 60652-MOL, 86-3026 (in Dutch).
- Van der Kooij, J. & A.J. Elshout 1975 NO_x-messungen in den niederländischen Kraftwerken — Elektrotechniek 53: 314-319.
- Van Egmond, N.D. & H. Kesseboom 1985 A numerical mesoscale model for long term average NO_x and NO₂-concentration — Atmospheric Environment 19: 587-595.
- Van Wakeren, J.H.A., A.J. Elshout & L.H.J.M. Janssen 1984 Measuring the electric field in the atmosphere in connection with investigations on the dispersion of air pollution — KEMA Scientific and Technical Reports 2: 91-99.
- Varey, R.H., S. Sutton & A.R.W. March 1978 The oxidation of nitric oxide in power station plumes - a numerical model — CERL Laboratory Note RD/LIN 184/78.
- Varey, R.H., S. Sutton & A.R.W. Marsh 1984 A numerical model for the production of nitrogen dioxide in power station plumes — Environmental Pollution B 7: 107-127.
- Vermeulen, P.E.I. 1983 Inventory of measurements of oxidation of nitrogen monoxide in stackplumes — TNO report 83-01620 (in Dutch).
- White, H.W. 1977 NO_x-O₃ photochemistry in power plant plumes: comparison of theory with observation — Environmental Science and Technology 11: 995-1000.
- Wilson, D.J., A.G. Robins & J.E. Fackrell 1985 Intermittency and conditionally averaged-concentration fluctuation statistics in plumes — Atmospheric Environment 19: 1053-1064.

Appendix: nomenclature

| | |
|-----------------------------------|--|
| A | ozone parameter |
| D _r | turbulent diffusion coefficient |
| f _b | fraction of ambient air volume, available for mixing into the plume |
| f _m | fraction of mixed plume volume |
| f _r | fraction of unmixed ambient air volume, not available for mixing into the plume |
| f _u | fraction of unmixed exhaust gas volume |
| k ₁ | reaction-rate constant (ppm ⁻¹ ·min ⁻¹) of the reaction between NO and O ₃ |
| k ₂ | reaction-rate constant (ppm ⁻² ·min ⁻¹) of the reaction between NO and O ₂ |
| k ₃ | photodissociation rate (min ⁻¹) of NO ₂ by solar radiation |
| k _m | mixing-rate parameter (min ⁻¹) |
| L _{mix} | parameter determining the quantity of unmixed ambient air in the plume |
| [NO] _m | NO concentration in f _m |
| [NO] _t | total available NO in the mixing volume ([NO] _u (t = 0)·f _u (t = 0)) |
| [NO] _u | NO concentration in f _u |
| [NO ₂] _m | NO ₂ concentration in f _m |
| [NO ₂] _u | NO ₂ concentration in f _u |
| [NO _x] | [NO] + [NO ₂] |
| [O ₂] _b | O ₂ concentration in f _b (2·10 ⁵ ppm) |
| [O ₂] _m | O ₂ concentration in f _m |
| [O ₂] _u | O ₂ concentration in f _u |
| [O ₃] _b | O ₃ concentration in f _b |
| [O ₃] _{cal} | calculated average O ₃ concentration in the plume which consists of parcels of unmixed ambient air and of mixed plume parcels |
| [O ₃] _m | O ₃ concentration in f _m |
| [O ₃] _{meas} | measured average O ₃ concentration in the plume |
| [O ₃] _t | total available O ₃ in the mixing volume ([O ₃] _b (t = 0)·f(t = 0)) |
| [O ₃] _u | O ₃ concentration in f _u |
| [O _x] | oxidation concentration [O ₃] + [NO ₂] |
| Q | NO _x emission calculated as NO ₂ (kg·h ⁻¹) |
| u | mean plume velocity (m·s ⁻¹) |
| W _{cal} | calculated plume width using the photostationary ratio |
| W _{meas} | measured plume width |
| x | distance from the source |

| | |
|------------|---|
| α | wind parameter |
| σ_y | cross-wind standard deviation of mean concentration profile (m) |
| σ_z | vertical standard deviation of mean concentration profile (m) |
| t_c | chemical time scale |
| t_p | physical time scale |
| Ψ | photostationary ratio $k_1[NO][O_3]/(k_3[NO_2])$ |

Samenvatting

Bij de opwekking van elektriciteit in met fossiele brandstoffen gestookte elektriciteitscentrales worden tijdens het verbrandingsproces aanzienlijke hoeveelheden stikstofoxiden (NO_x) gevormd. Deze worden met de rookgassen via de schoorsteen geloosd in de buitenlucht. Zij dragen daarbij aan de concentratie van stikstofdioxide, dat in hogere concentratie directe schade kan toebrengen aan de gezondheid van de mens. Emissies van stikstofoxiden dragen verder bij aan de verzuring en verusting van bodem en water en aan fotochemische luchtverontreiniging.

De belangrijkste bron van NO_x -emissie is het verkeer, maar elektriciteitsproductie draagt ongeveer 15% bij aan de NO_x -emissie in Nederland en ongeveer 2% aan de landelijk gemiddelde immissie. Om de lokale invloed van een elektriciteitscentrale op de luchtkwaliteit na te gaan, kunnen metingen worden uitgevoerd in de omgeving van een centrale. Metingen hebben echter vaak het nadeel dat ze beperkt zijn tot een bepaalde plaats en/of periode en een bepaalde centrale. Het is daarom aantrekkelijk om een rekenmodel beschikbaar te hebben waarmee voor een willekeurige plaats, een willekeurige periode en een willekeurige centrale de invloed van die centrale op de luchtkwaliteit kan worden nagegaan.

Een dergelijk model, namelijk het Gaussisch pluimmodel, bestaat voor een langzaam reagerend gas als SO_2 dat geëmitteerd wordt vanuit een puntbron, zoals bijvoorbeeld de schoorsteen van een elektriciteitscentrale. Zo'n model bestaat echter niet voor snel reagerende gassen als stikstofoxiden. Elektriciteitscentrales die fossiele brandstoffen verstoken, emitteren stikstofoxiden voornamelijk in de vorm van stikstofmonoxide (NO). In de atmosfeer wordt NO echter snel omgezet in het veel giftiger NO_2 . De snelheid van dit omzettingsproces wordt bepaald door zowel de snelheid van de fysische processen van verspreiding en menging van de pluim, als door de snelheid van de chemische reacties (Hoofdstuk 1 en 2).

Het onderzoek dat in dit proefschrift is beschreven, heeft zich in hoofdzaak gericht op studie van de competitie tussen de processen van verspreiding en menging (gekarakteriseerd door tijdschaal τ_p) en van chemische reacties (gekarakteriseerd door tijdschaal τ_c) bij de omzettingssnelheid van NO in de rookpluimen van elektriciteitscentrales. Hierbij zijn metingen aan concentraties van NO_2 en NO_x in een pluim vergeleken met berekeningen met behulp van verschillende modellen (Hoofdstuk 4-7).

Uit een vergelijking van metingen met berekeningen waarbij in het eerste model de aanname van gaussische verspreiding en chemisch evenwicht in de pluim was aangenomen, bleek dat voor afstanden tot ongeveer 5 km van de bron de berekende concentraties van NO₂ hoger waren dan de gemeten waarden (Hoofdstuk 4). Dit werd verklaard met behulp van de resultaten van een tweede model waarin wel gaussische verspreiding was aangenomen maar de hypothese van chemisch evenwicht niet nodig was (Hoofdstuk 5). Uit deze tweede modelstudie bleek dat dichtbij de bron de processen van verspreiding en menging sneller waren dan de chemische reacties ($t_p/t_c < 1$) en dat de hypothese van chemisch evenwicht ($t_p/t_c > 1$) zoals gebruikt in het eerste model onjuist was. Berekeningen met het tweede model gaven dichtbij de bron dan ook betere resultaten. Verder weg van de bron (> 5 km) gaven berekeningen met het tweede model daarentegen vaak een overschatting ten opzichte van gemeten NO₂ concentraties. Dit is onderzocht in een derde model waarin geen gaussische verspreiding van de pluim werd verondersteld (Hoofdstuk 6). Uit berekeningen met dit model bleek dat ook op grotere afstand van de bron locaal wel chemisch evenwicht mogelijk is omdat $t_p/t_c > 1$, maar gemiddeld over de pluim is er geen chemisch evenwicht. De reden is dat de pluim inhomogeen gemengd is en beschouwd kan worden als opgedeeld in delen pluim en delen lucht. Dit betekent dat op grotere afstand van de bron de oxidatiesnelheid van NO dan ook bepaald wordt door de mengsnelheid van de pluim met de lucht.

Om de oxidatiesnelheid van NO onder zeer verschillende atmosferische omstandigheden te kunnen voorspellen, wordt tenslotte een empirisch model gepresenteerd dat gebaseerd is op een groot bestand van meetgegevens (Hoofdstuk 7). Deze metingen zijn met behulp van een vliegtuig uitgevoerd in de rookpluimen van een aantal elektriciteitscentrales in Nederland. Aan de hand van een classificatie van de NO-oxidatiesnelheid als functie van meteorologische condities kan, onder de aanname van gaussische verspreiding van NO_x, voor de meeste weersituaties de NO₂-concentratie op leefniveau ten gevolge van de emissie door de centrale worden berekend.

De volgende conclusies kunnen worden getrokken (Hoofdstuk 8). De vorming van NO₂ in een gemiddelde rookpluim niet te ver van de bron kan worden berekend met model twee, beschreven in Hoofdstuk 5, dat de gebruikelijke vergelijkingen voor een gaussische pluimverspreiding gebruikt. Op afstanden groter dan 5 km van de bron zal dit model de vorming van NO₂ vaak overschatte. Dit wordt veroorzaakt doordat de vergelijkingen voor de pluimverspreiding gelden voor een over een bepaalde periode (10 minuten) gemiddelde pluim.

In een gemiddelde pluim dragen langzame variaties van de pluimas, het zogenaamde meanderen van de pluim, extra bij in de groei van de gemiddelde pluimbreedte. De pluimbreedte van een gemiddelde pluim is dus groter dan die van een momentane pluim. Daardoor zullen concentraties van NO in een gemiddelde pluim lager en die van O₃ hoger zijn dan die in een momentane

pluim. Omdat de vorming van NO_2 een niet-lineair proces is, moeten in het model van een reactieve pluim de momentane concentraties worden meegenomen. In modellen die een over de tijd gemiddelde pluim beschrijven, wordt de beschikbaarheid van O_3 voor de oxidatiereactie van NO te hoog ingeschat en dus wordt de vorming van NO_2 overschat. Uit eerste metingen van de vorming van NO_2 in de nacht bleek dat het meanderen van de pluim 's nachts, wanneer de pluim zich in de stabiele atmosferische laag bevindt, minder was; de vorming van NO_2 in een gemiddelde pluim kan dan beschreven worden door een model dat de gebruikelijke vergelijkingen voor gaussische pluimverspreiding in een stabiele laag gebruikt, zoals model 2.

Stellingen

behorende bij het proefschrift

Reactions of nitrogen oxides in power-plant plumes

- models and measurements -

Reacties van stikstofoxiden
in de rookpluimen van elektriciteitscentrales

van

Léon Janssen

1

De door Carmichael en Peters berekende afwijkingen van fotostationair evenwicht in een rookpluim kunnen beter verklaard worden door de verschillende tijdschalen van de fysische processen van verspreiding en menging enerzijds en die van de chemische processen van moleculaire reacties anderzijds dan door de aannname van inhomogene menging in de rookpluim.
G.R. Carmichael & L.K. Peters, Atmospheric Environment 15 (1981) 1072.
Dit proefschrift.

2

De aannname van Forney en Giz dat de oxidatiereactie van stikstofmonoxide in een rookpluim snel is ten opzichte van de verspreiding van de pluim geldt alleen voor afstanden groter dan enkele kilometers van de schoorsteen.

L.J. Forney & Z.G. Giz, Atmospheric Environment 15 (1981) 346.
Dit proefschrift.

Natuurlijke variaties in de achtergrondconcentratie van ozon en in de fotodissociatiesnelheid van stikstofdioxide moeten betrokken worden bij vergelijking van de uitkomsten van modelberekeningen met die van metingen met betrekking tot de vorming van stikstofdioxide in een rookpluim.

Dit proefschrift.

Om het door Cheng et al. gerapporteerde ruimtelijk oplossend vermogen van een chemoluminescentie NO_x-monitor te bepalen moet naast de monstername-frequentie ook de RC-tijd van de monitor meegenomen worden.

L. Cheng, E. Peake, D. Rogers & A. Davis, Atmospheric Environment 20 (1986) 1698.

Bij onderzoek naar de ruimtelijke correlatie van luchtverontreinigende stoffen moet eerst de correlatie in de tijd bepaald worden.

Bij het relateren van de SO₄/SO₂-verhouding aan de omzettingssnelheid van SO₂ in de atmosfeer moet niet alleen rekening worden gehouden met meteorologische omstandigheden, maar ook met de herkomst van de luchtverontreiniging.

S. Kadawaki, Environmental Science and Technology 20 (1986) 1252.

Het effect van snelle meteorologische veranderingen op de waterstroom-snelheid in bomen overtreft verre de invloed van luchtverontreiniging.

Alvorens men met metingen aan dauw op vegetatie begint, is het aan te raden om eerst de depositie van dauw op een kunstmatig oppervlak met goed bekende eigenschappen te onderzoeken.

De schijnbare verrijking van chroom in poederkool-as is het gevolg van contaminatie door roestvaststalen monsternama-apparatuur.

R.M. Mann, R.A. Magee, R.V. Collins, M.R. Fuchs & F.G. Mesich, EPA report no: 908/4- 78-008.

C. Huygen, C. Veldt, L.H.J.M. Janssen, J. van der Kooij & R. Mey, PEO-rapport 2070-012.40 Utrecht (1986).

Het selecteren van variabelen, alsook het schatten van de daarbij behorende parameters in een multiple regressiemodel, wordt problematisch wanneer verklarende variabelen onderling hoog gecorreleerd zijn. Het gebruik van transformatie vooraf met behulp van hoofdcomponent-analyse dient echter afgeraden te worden.

De hypothese dat volgens de theorie van N. Chodorov de overdracht van de ongelijke arbeidsverdeling tussen mannen en vrouwen - vrouwen als moeder en mannen als kostwinner - kan worden beïnvloed door mannen van het begin af aan ook de kinderen te laten verzorgen is niet in de praktijk getoetst.

N. Chodorov, The reproduction of mothering. Psychoanalysis and the Society of Gender, University of California Press (1978).

Het geven van de voorkeur aan een vrouw bij het vervullen van vacatures voor functies waarin zij nu ondervertegenwoordigd zijn, is onvoldoende om deze onevenredige verdeling te veranderen. Dit beleid dient daarvoor aangevuld te worden met betere mogelijkheden voor het in deeltijd werken van mannen.

Delft, 17 mei 1988